17700

NATIONAL LIBRARY
OTTAWA

CANADA

BIBLIOTHÈQUE NATIONALE
OTTAWA

NAME OF AUTHOR...GERALD...W...STOCKTON.....

TITLE OF THESIS..HYDROGEN.AND.CARBON.NUCLEAR.....
MAGNETIC.RESONANCE..STUDIES.OF....
IONIC.SOLVATION.IN.WATER.&.ALCOHOLS

UNIVERSITY.OF..ALBERTA.....

DEGREE FOR WHICH THESIS WAS PRESENTED...Ph.D.....

YEAR THIS DEGREE GRANTED....1973.....

Permission is hereby granted to THE NATIONAL LIBRARY OF CANADA to microfilm this thesis and to lend or sell copies of the film.

The author reserves other publication rights, and neither the thesis nor extensive extracts from it may be printed or otherwise reproduced without the author's written permission.

(Signed)..G.W. Stockton.....

PERMANENT ADDRESS:

#703-10250-133.ST.
..EDMONTON.....
..ALBERTA.....

DATED..23..July.....1973

NL-91 (10-68)

THE UNIVERSITY OF ALBERTA

HYDROGEN AND CARBON NUCLEAR MAGNETIC RESONANCE STUDIES OF IONIC SOLVATION IN WATER AND ALCOHOLS

BY

© GERALD WILLIAM STOCKTON

A THESIS

SUBMITTED TO THE FACULTY OF GRADUATE STUDIES AND RESEARCH

IN PARTIAL FULFILMENT OF THE REQUIREMENTS FOR THE DEGREE

OF

DOCTOR OF PHILOSOPHY

DEPARTMENT OF CHEMISTRY

EDMONTON, ALBERTA

FALL 1973

THE UNIVERSITY OF ALBERTA

FACULTY OF GRADUATE STUDIES AND RESEARCH

The undersigned certify that they have read, and recommend to the Faculty of Graduate Studies and Research for acceptance, a thesis entitled

"HYDROGEN AND CARBON NUCLEAR MAGNETIC RESONANCE STUDIES OF IONIC SOLVATION IN WATER AND ALCOHOLS"

submitted by GERALD WILLIAM STOCKTON in partial fulfilment of the requirements for the degree of Doctor of Philosophy.

J. S. Martin
Supervisor

R. E. Wasylishen

A. E. Mather

J. B. Hyne

D. J. Robinson

Melvin W. Hanna
External Examiner

17 July 1973
Date

TO

MY WIFE, CYNTHIA,

AND

MY PARENTS

A B S T R A C T

Association constants and hydroxyl proton NMR shifts have been measured for 1:1 complexes in acetonitrile of six diamagnetic cations and eight hydroxylic substrates (water, alcohols and diols). Their values follow the trend appropriate to a simple electrostatic association of the cation with the oxygen of the substrate. Molal shifts Δ_m of small cations in water and methanol may be adequately accounted for by a solvation model which takes explicit account of nearest neighbour interactions only. It leads to an equation of the form $\Delta_m = (nM/1000)(\Delta_c + \Delta_h)$, where n is the solvation number, M the molecular weight of the solvent, Δ_c the cation complex shift, and Δ_h a shift which characterises the disruption of hydrogen bonding in the solvent. n appears to have a value close to six for small and/or polyvalent cations. Δ_h has a value of about 1.5 ppm for cations in water at +25° and methanol at -69°, and about 6 ppm for anions in methanol at -69°. It decreases with increasing temperature and presumably reflects the amount of hydrogen bonding in the solvent. It appears to be possible to interpret Δ_h in terms of structure-making by small cations and structure-breaking by the larger anions. Deviations from predicted behaviour by Rb^+ and Cs^+, and the molal shifts of the larger halide ions, are most plausibly interpreted in terms of a disordered solvation shell, such that the effective solvation number of these ions is less than the number of nearest-neighbour

molecules.

The carbon-13 NMR spectra of solvent molecules coordinated to the cation in ethanol solutions of $Mg(ClO_4)_2$ and $AlCl_3$, and in n-propanol solutions of $AlCl_3$, have been observed over a wide range of temperatures. Separate resonances were observed for solvation shell carbon nuclei as many as three bonds removed from the site attachment of the ion. Their multiplicity and coalescence phenomena are consistent with the ^1H NMR observations. The shielding changes relative to the bulk solvent are negative at C_1 and positive at C_2; they resemble the β and γ carbon shifts induced in an alkane by an electronegative α substituent. The ^1H and ^{13}C spectra of ethanolic $AlCl_3$ solutions show the presence of at least three solvated species. The signal multiplicity is largely removed when the chloride ion is replaced by perchlorate. This could be explained by postulating the presence of solvent separated ion-pairs or ion-clusters involving Al^{3+}, Cl^- and solvent molecules.

A C K N O W L E D G E M E N T S

The author wishes to express his appreciation and gratitude to:

Dr. John S. Martin, for his guidance throughout the course of this work;

Dr. B. Kratochvil and Mr. F. Fujiwara, for stimulating conversations about many aspects of this work;

Dr. R. E. D. McClung and Dr. D. L. Rabenstein, for carefully reading earlier drafts of this thesis and for many helpful comments;

Mon Pon and Jack Pannekoek (summer research assistants), for their help with the preparation of more than 1000 NMR samples;

Mrs. Mary Waters, for her excellent typing of this manuscript.

CONTENTS

Chapter 1. INTRODUCTION 1

1.1 The structure of associated liquids 1

1.1.1 Mixture models 2

1.1.2 Uniformist models 4

1.1.3 Interstitial models 5

1.1.4 The model adopted for this thesis 6

1.2 Solvation of electrolytes in associated liquids 7

1.2.1 Coulombic solvation 8

1.2.2 Solvation number 9

1.2.3 Structural solvation 10

1.3 Use of NMR in solvation studies 13

1.3.1 Electrolytes in single solvents 19

1.3.1.1 Experiment I. Ionic molal shifts 21

1.3.1.2 Experiment II. Separate solvation shell resonances 22

1.3.2 Electrolytes in mixed solvents 23

1.3.2.1 Experiment III. 1:1 ion-molecule association 25

1.3.3 NMR and structural solvation 26

1.4 Scope of this thesis 29

Chapter 2. EXPERIMENTAL 32

2.1 Materials 32

2.2 Preparation of samples for NMR 34
2.3 NMR spectroscopy 35

Chapter 3. 1:1 ION-MOLECULE ASSOCIATION IN ACETONITRILE. 37
3.1 Analysis of the equilibrium 39
3.2 Accuracy of the parameters Δ_c and K 43
3.3 1:1 cation complexes of water and the alcohols . . 45
3.3.1 Association constants 49
3.3.2 Complex shifts 54
3.3.3 Effect of the counterion 54
3.3.4 Effect of the solvent 55
3.4 Cation complexes of bidentate substrates 57
3.5 Cation complexes of nitrogen bases 62

Chapter 4. ELECTROSTATIC MODELS FOR THE 1:1 ION-MOLECULE ASSOCIATION 67
4.1 The equilibrium constants 67
4.2 The complex shieldings 74
4.2.1 The solvent-substrate interaction 80

Chapter 5. TYPE I AND II SOLVATION SPECTRA 82
5.1 TYPE II spectra of Mg(II) in methanol 83
5.2 TYPE II spectra of Mg(II) in ethanol 86
5.3 The molal shift of Ba(II) in methanol 92

Chapter 6. CORRELATION OF THE NMR SOLVATION EXPERIMENTS 94
6.1 A solvation model 95
6.2 Solvation of small cations in water 97
6.3 Solvation of small cations in methanol 100
6.4 Solvation of large monovalent cations 108
6.5 Solvation of anions 113
6.6 Solvation in ethanol 114

Chapter 7. CARBON-13 SOLVATION SPECTRA 115
7.1 TYPE II solvation spectra 115
7.1.1 ^{13}C spectra of ethanolic $Mg(ClO_4)_2$ solutions 117
7.1.2 ^{13}C and ^{1}H spectra of Al(III) solvation shells 122
7.2 TYPE III carbon-13 solvation spectra 133
7.3 The ^{13}C shieldings in coordinated molecules . . . 135
7.4 The selective broadening of the C_1 resonance . . . 138

Chapter 8. CONCLUSIONS 142
8.1 Cation complexes in acetonitrile 142
8.2 The solvation model 143
8.3 Carbon-13 solvation spectra 145
8.4 Aluminum(III) solvation shells 147
8.5 Suggestions for future work 148

REFERENCES 151

Appendix A. CHEMICAL EXCHANGE AND SOLVATION SPECTRA . . 159

A-1 Two-site exchange 159

A-2 TYPE II ^{1}H solvation spectra 161

A-3 TYPE II ^{13}C solvation spectra 163

TABLES

1.1 Solvation numbers of diamagnetic cations determined from NMR intensities 24

3.1 Equilibrium constants of cation-substrate complexes in acetonitrile at 35° 46

3.2 Saturation range ΔS of the 1:1 complex equilibria 47

3.3 Limiting shifts Δ_c of the cation-substrate complexes in acetonitrile at 35° 48

3.4 Shieldings of substrates in acetonitrile 50

3.5 Temperature dependence of shifts, shieldings and equilibrium constants of the methanol-cation complexes 51

3.6 Limiting hydroxyl proton shifts and equilibrium constants of the cation complexes of bidentate substrates 61

3.7 Limiting CH_2 and CH_3O proton shifts and equilibrium constants of the cation complexes of bidentate substrates 63

4.1 Quantities used in the calculation of the ion-molecule electrostatic potential energy for methanol complexes of the cations 71

6.1 Prediction of the cation molal shifts in methanol at -69° 107

6.2 Prediction of cation complex shifts and molal shifts 109
7.1 ^{13}C solvation shell shifts for ethanolic $AlCl_3$ titrated with $AgClO_4$ 129
7.2 Hydroxyl proton shifts for ethanolic $AlCl_3$ titrated with $AlClO_4$ 132
7.3 The carbon-13 shieldings of coordinated molecules 136

FIGURES

1.1 Summary of the NMR solvation experiments 17

1.2 Schematic NMR spectra of the TYPE I, II and III experiments 18

3.1 Simulations of the dependence of the hydroxyl proton shielding on the concentration of added salt for varius equilibrium constants 40

3.2 Dependence of the alkyl proton shieldings on $Mg(ClO_4)_2$ concentration for ethanol and diethylamine in acetonitrile 65

4.1 Interaction of the cation with bond dipole and polarisability 72

4.2 Relationship between the observed cation-molecule association constant and the calculated electrostatic potential energy 73

4.3 Planar cation-methanol complex 76

4.4 Derivation of the Buckingham-Musher A coefficient for cation complexes of water, methanol and ethanol 77

5.1 Deduction of Δ_s for Mg(II) in methanol 85

5.2 Effect of temperature on the separation of the bulk and bound solvent hydroxyl proton signals for $Mg(ClO_4)_2$ in ethanol 87

5.3 The dependence of the hydroxyl proton shielding of ethanol coordinated to Mg(II) on the salt concentration 89

5.4 The dependence of the hydroxyl proton shielding of the residual solvent on salt concentration for ethanolic $Mg(ClO_4)_2$ at -70° 91
6.1 Correlation of the molal shifts Δ_m and the 1:1 complex shifts Δ_c for water at 25° 99
6.2 Correlation of the molal shifts Δ_m and the 1:1 complex shifts Δ_c for methanol at -69° 101
6.3 Primary cation solvation shells 112
7.1 Carbon-13 NMR spectra of ethanolic $Mg(ClO_4)_2$. . . . 118
7.2 Temperature dependence of the CH_2 and CH_3 carbon-13 bulk-bound chemical shift for ethanolic $Mg(ClO_4)_2$ 120
7.3 Temperature dependence of the ^{13}C CH_2 and CH_3 bulk solvent linewidths for ethanolic $Mg(ClO_4)_2$ . . 121
7.4 The effect of temperature on the hydroxyl proton signals of ethanol coordinated to Al(III). . 123
7.5 Hydrogen-bonded solvated-cation dimer in alcoholic $AlCl_3$ solutions 124
7.6 Carbon-13 spectra of ethanolic $AlCl_3$ at several temperatures 126
7.7 22.63 MHz NMR spectra of the solvation shell carbon-13 nuclei of ethanolic $AlCl_3$, as the chloride ion is replaced by perchlorate 128
7.8 100 Mhz NMR spectra of the solvation shell hydroxyl proton of ethanolic $AlCl_3$, as the chloride ion is replaced by perchlorate 131

7.9 Selective broadening of the C_1 resonance at low temperatures 139

GLOSSARY OF COMMONLY-USED SYMBOLS

A	Coefficient of the linear term of the Buckingham-Musher equation.
b	Moles of solvent per 1000 g.
C, [ ]	Concentration, moles litre^{-1}.
E	Electric field strength.
H	Magnetic field strength.
J	Spin-spin coupling constant.
K	Molar equilibrium constant.
K_{th}	Thermodynamic molar equilibrium constant.
k	Boltzmann constant; reaction rate constant.
M	Moles litre^{-1} (molarity).
m	Moles kg^{-1}. (molality).
M	Molecular weight.
n	Any integer.
n	Solvation number.
q	Electric charge.
R	C_nH_{2n+1}; ideal-gas constant.
r	Ionic radius; internuclear distance.
T	Temperature in degrees Celsius.
T_1	Longitudinal nuclear magnetic relaxation time.
T_2	Transverse nuclear magnetic relaxation time.
U	Potential energy.
Ze	Ionic charge.

α	Polarisability.
γ	Activity coefficient.
δ	Increment.
ε	Dielectric constant.
μ	Dipole moment.
σ	Nuclear magnetic shielding constant relative to that of an internal reference.
Δ	Chemical shift (difference of two σ's).
τ	Lifetime.
τ_c	Correlation time.
ω	Angular frequency (radians $sec.^{-1}$)
$^\circ$	Degrees Celsius.

Defined shieldings σ, and chemical shifts Δ.

σ_s	Free substrate shielding.
σ_c	1:1 complex shielding.
σ_p	Pure bulk solvent shielding.
σ_b	Coordinated (bound) solvent shielding.
σ_r	Residual solvent shielding.
Δ_m	Ionic molal shift, $(d\sigma/dm)_{m\to 0}$
Δ_s	Solvation shell shift, $(\sigma_b - \sigma_p)_{m\to 0}$
Δ_r	Residual solvent shift, $(d\sigma_r/dm)_{m\to 0}$
Δ_c	1:1 complex shift, $\sigma_c - \sigma_s$
Δ_h	Desolvation shift for the hydroxyl group.
Δ_h^p	Desolvation shift for the hydroxyl proton.
Δ_h^o	Desolvation shift for the hydroxyl oxygen.

CHAPTER 1

I N T R O D U C T I O N

1.1. The Structure of Associated Liquids.

The present work is concerned primarily with the solvation of electrolytes, for the most part in hydroxylic solvents such as water and the alcohols. It is appropriate to introduce the modern concepts concerning the physical structure of the associated liquids. In this respect, water has been most extensively studied, but its actual structure is still unknown.

There exists an embarrassment of partially successful models for the structure of water. Each of the proposed models is able to account for some of the properties of water, and sometimes several models describe a particular property equally well. However, no single model is presently able to account for all of the known facts. It is likely that the ultimate model will contain some of the features of all the current alternatives.

The most important properties of water which must be described by this model are the X-ray and neutron scattering correlation functions, thermodynamic functions, maximum density at 4°, dielectric and structural relaxation, and the spectroscopic parameters from infrared, Raman and NMR spectra. Furthermore, the model should account for the differences in the properties of normal water and those of heavy water, the alcohols and ice. The results of

some of these studies and the features which must be incorporated in models to explain the results are discussed below.

The structure of ice I is well understood. The X-ray radial distribution function shows that each water molecule is tetrahedrally coordinated to four others.[1] The interaction is one of hydrogen bonding.[2] All of the models for liquid water are based upon the consideration of changes in the ice I crystal lattice upon melting of the solid and the models differ with regard to the number, distribution, strength, and geometry of hydrogen bonds in the liquid. A brief survey of the alternative models will now be given. For a more complete account, the reader is referred to the books by Franks [3] and Eisenberg and Kauzmann.[2]

1.1.1. Mixture Models. The first class of models proposed that water could be viewed as a mixture of different molecular aggregates. When ice melts, some but not all of the hydrogen bonds are thought to be broken, giving rise to a mixture of single molecules (the monomers) and regions of short range order in which the hydrogen bonds persist. The first model of this kind is probably Röntgen's [4] suggestion that normal cold water is a "solution of ice in a classical liquid". This means that some water is 4-coordinate and some is uncoordinated. The hydrogen-bonded ice-like regions were later called clusters.[5] Estimates in the literature

of the proportion of broken hydrogen bonds in liquid water near its freezing point have varied between 2.5 and 70%.[6] The equilibrium between free molecules and the clusters would qualitatively account for many properties of water, for example the maximum density at 4°, the heat capacity (anomalous C_v/R and temperature dependence), and the viscosity (anomalous pressure dependence).

The most direct evidence for the existence of two (or more) molecular states in water is found in the vibrational spectra. The Raman spectrum of a dilute solution of D_2O in H_2O shows, in the O-D stretching region, a broad band due to the O-D oscillators and a distinct higher frequency shoulder.[7,8] Walrafen [7] has proposed that the former peak is due to hydrogen-bonded molecules and the latter to non-bonded molecules. The intensity of the shoulder increases as expected with rising temperature. Very careful infrared spectroscopy and the application of advanced curve fitting techniques have demonstrated a definite substructure to the O-H and O-D stretching regions of H_2O and D_2O.[9] At least four components are indicated and the decomposition of the infrared spectrum has been shown to be consistent with a similar decomposition of the Raman spectrum of water.[10] Thus, liquid water appears to contain a finite number of distinct species, rather than a continuum, and this evidence favours a mixture model.

1.1.2 Uniformist Models. The evidence in favour of the two-state model (or other mixture models involving a finite number of polymeric species) is by no means complete. Water exhibits a single dielectric dispersion region, representing a small spread of relaxation times (*ca* 10^{-11} sec.),[11] compared with three dispersion regions (*ca* 10^{-9}, 10^{-10}, and 10^{-11} sec.) for the primary alcohols.[12] This was offered as evidence in favour of a continuous distribution of molecular states in liquid water and an equilibrium between monomers and polymeric species in the alcohols. Neutron scattering experiments show no evidence of large molecular aggregates in water.[13]

A number of "uniformist" models have evolved in order to account for those experiments which show evidence of a continuous distribution of molecular states in liquid water. Bernal and Fowler,[14] and Pople,[15] have pictured water as the ice I crystal lattice in which the hydrogen bonds have become "bent" but not broken. Every molecule remains hydrogen bonded but the neighbours to a reference molecule adopt "distorted" orientations. The average degree of bond bending is the parameter which is assumed to be sensitive to changes in temperature and pressure. This class of models appears to be incompatible with the vibrational spectra since a continuum model would predict simple, unstructured bandshapes. A bent-hydrogen-bond model would only explain the vibrational spectra if there existed a finite

number of preferred orientations, or favoured bent-bond angles, in which case the model would not strictly represent a continuum. A continuum model does not easily explain the maximum density at 4° or the anomalously high heat capacity of water. The question also arises of how far a hydrogen bond must be bent before it can be regarded as broken, and the distinction between the uniformist and mixture models may be a matter of semantics.

1.1.3 Interstitial Models. Samoilov [16] and others [17,18] have proposed models for the structure of water which can be regarded as being intermediate between uniformist and mixture models. The notion is one of a water molecule leaving its position in the ice I lattice in order to occupy an interstitial position in the open lattice, which then "heals" itself. The extended ice-like lattice remains and the non-bonded interstitial water molecules serve to increase the density of the liquid. The lattice is distorted and the long range order is destroyed, thus giving rise to the fluidity of the liquid. Pauling's [19] clathrate model is similar: the hydrogen-bonded regions are described as polyhedral cages of water molecules and the non-bonded molecules are enclosed by the cages.

The interstitial models, with the exception of Pauling's clathrate model, are more in accordance with the X-ray radial distribution function than the mixture models [18]

and they can account for the maximum density at 4°. They are apparently unable to account for the anomalously high heat capacity of water, in contrast to the mixture models. The single dielectric dispersion region is difficult to interpret because the interstitial water molecules may not be completely free rotators.

The absorption spectrum of ultrasound by a medium may be interpreted in terms of relaxation processes associated with density fluctuations. The pressure dependence of the absorption of ultrasound by water indicates the presence of at least two distinguishable species whose mechanism of rearrangement is the "uncorrelated jumping of molecules between quasicrystalline sites".[20] However, the single structural relaxation time (the time for the structure of the liquid to change) argues against the existence of large ice-like clusters and this evidence appears to favour the interstitial models.

1.1.4 The Model Adopted for this Thesis. The results of the nuclear magnetic resonance experiments presented in later chapters of this thesis are most easily interpreted in terms of a two state model for water in which some of the *hydrogen atoms* in water are involved in hydrogen bonds and some are not. Proton NMR monitors only the state of the hydrogen atoms and, for this reason, consideration of the structural arrangement of the *water molecules* is deliber-

ately avoided. The assumption of hydrogen bonded and non-hydrogen-bonded hydrogen atoms is in accordance with most of the data presented in the previous sections of this chapter. The important consequences of adopting a two-state model for the present purposes are that the equilibrium between the hydrogen-bonded and non-hydrogen-bonded hydrogen atoms in the water molecules may be altered by changing the temperature or by adding a solute, and that the equilibrium may be treated by simple chemical thermodynamics.

The structure of liquid alcohols is well understood.[21] Coordination to an alcohol is known to be limited to a maximum of two hydrogen bonds per molecule (2-coordinate) and it is not possible for an open three dimensional network of hydrogen bonds to form in a liquid (or solid) alcohol.[22,23] Association in liquid alcohols is believed to be restricted to linear polymers of only a few hydrogen-bonded molecules.[21] However, the important consideration is again that the degree of hydrogen bonding may be altered by changing the temperature or by adding a solute.

1.2 Solvation of Electrolytes in Associated Liquids.

Water, and to a lesser extent the alcohols, are the media in which ionic chemistry and solvation processes have been most extensively studied. The historical development of the concept of solvation began with the study of electro-

lyte solutions by electrochemists. The physical description of these solutions was at that time conceptually simple and rather unsatisfactory. The solvent was regarded as a continuous dielectric medium in the electric field of the ionic solute. The solvation energy (or hydration energy in the case of water) was evaluated by Born [24] as the Gibbs free energy ΔG of transfer of a gas phase ion of radius r and charge Ze to a medium of dielectric constant ε.

$$\Delta G = \frac{(Ze)^2}{2r}\left(\frac{1 - \varepsilon}{\varepsilon}\right) \qquad (1.1)$$

This process is not accessible to direct observation but an "observed" value can be estimated from a suitable thermodynamic cycle. On comparison with the "observed" energies, the solvation energies given by the Born equation were found to be too large. Many attempts were made to obtain agreement of experimental and calculated energies, usually by adjusting the ionic radius [25] or dielectric constant [26] until agreement was achieved.

1.2.1 Coulombic Solvation. The suggestion was later made that the ion should be regarded as interacting strongly with only a small number of nearest neighbour molecules, the primary solvation shell, and perhaps only weakly with more distant molecules. The orientation of the molecules in the primary solvation shell by the electric field of the ion is

designated *coulombic solvation.* If other factors, such as the change in ionic radius upon dissolution of the gas phase ion, are taken into account, then excellent agreement is obtained between experimental hydration energies and entropies and those calculated using this model.[27]

1.2.2. Solvation Number. A model of this kind requires a knowledge, preferably an experimental evaluation, of the number of nearest neighbour molecules: the primary solvation number. Close packing requirements would limit this number to four or six, depending on the radii of the ion and solvent molecule.

Numerous experimental methods have been used to determine solvation numbers and it is essential to understand that the different experiments do not always provide solvation numbers with the same significance. For example, NMR studies measure the number of highly polarised nearest neighbour molecules, whereas electrolytic transference measurements determine the number of molecules moving with the ion in an applied d.c. electric field. The latter quantity may be an order of magnitude greater than the primary solvation number.[28]

The lifetimes of the solvation shells of most diamagnetic ions are short compared with the NMR time scale[29] and the definition of the primary solvation number n adopted and used throughout the remainder of this thesis is the

"time average statistical excess of nearest neighbour molecules in the lowest energy orientation". This definition adequately allows for the exchange of the solvation shell and bulk solvent molecules.

1.2.3 Structural Solvation. The discussion so far has been concerned with the restriction of the motion of solvent molecules in the immediate vicinity of dissolved ions. There is also the possibility of a profound effect of the solvated ions on the hydrogen-bonded structure of the residual bulk solvent (i.e. solvent not coordinated to an ion). This was first suggested by Frank and Evans [30] in their classic paper on the entropies of ion hydration. They found that the entropy decrease for the hydration of two argon atoms is greater than that for the hydration of a potassium ion and a chloride ion.

$$2Ar(gas) \longrightarrow 2Ar(aq) \qquad \Delta S = -60.4 \text{ cal. deg.}^{-1} \text{ mol.}^{-1} \qquad (1.2)$$

$$K^+(gas) + Cl^-(gas) \longrightarrow K^+(aq) + Cl^-(aq) \qquad \Delta S = -51.9 \text{ cal. deg.}^{-1} \text{ mol.}^{-1} \qquad (1.3)$$

Coulombic solvation of the ions is expected to lead to increased order and a large entropy decrease, which should be larger than for the hydration of two argon atoms. They

explained the anomalous entropy of hydration of potassium chloride by postulating breakdown of the residual solvent hydrogen-bonded network due to the presence of the hydrated ions. The disruption of the solvent-solvent interactions would result in decreased order and a net entropy of hydration of the salt that is less negative than expected when compared with the value for two argon atoms. The effect of the solvated ions on the residual solvent hydrogen-bonded structure is now called *structural solvation*.

Many other physical properties of aqueous electrolyte solutions show anomalies which indicate structural solvation. The thermodynamic aspects have been reviewed recently by Desnoyers.[31] More direct evidence of structural solvation is supplied by the recent work of Walrafen [32] on the Raman spectra of aqueous solutions. The intensities of bands attributed to non-bonded water molecules increase in the presence of salts which are expected to decrease the water-water interactions.

The phenomenon of structural solvation is not restricted to the decrease of water-water interactions; the structural order may be increased by certain salts. The consensus appears to be that the divalent cations and lithium increase the structural order in the residual solvent: they are "structure-makers". The large monovalent ions and all anions decrease the structural order and are called "structure breakers".

Very little is known about structural solvation by ions dissolved in alcohols. Krishnan and Friedman [33] have compared the entropies of solvation of potassium chloride and argon in methanol and find that they are in the order to be expected if the ion-solvent interactions dominate any structural solvation.

$$2Ar(gas) \longrightarrow 2Ar(MeOH) \quad \Delta S = -32 \text{ cal. deg.}^{-1} \text{ mol.}^{-1} \tag{1.4}$$

$$K^+(gas) + Cl^-(gas) \longrightarrow K^+(MeOH) + Cl^-(MeOH) \quad \Delta S = -80 \text{ cal. deg.}^{-1} \text{ mol.}^{-1} \tag{1.5}$$

They conclude that structural solvation is a phenomenon which is unique to water and can be attributed to the unparalleled ability of water to form a three dimensional hydrogen-bonded network.

In view of the contrary conclusions which will be presented in later chapters of this thesis, it must be pointed out that the above comparison of water and methanol was made in terms of the solvents in their thermodynamic standard states, i.e. 25° and 1 atm. The freezing points of water and methanol are 0° and -97° respectively. A more valid comparison might be drawn if both of the solvents were close to their freezing points, where the states of hydrogen bonding are likely to be more similar.

1.3 Use of NMR in Solvation Studies

The magnetic parameters which characterise the nuclear magnetic resonance spectra of liquids are the nuclear shielding constants, the spin-spin coupling constants, and the magnetic relaxation times. In principle, all of these parameters may be used to probe solvation processes.

When a molecule is placed in an applied magnetic field H_o, the molecular electronic currents induced by H_o generate a net secondary magnetic field σH_o at the particular "observed" nucleus, and the effective magnetic field H_{eff} at that nucleus becomes

$$H_{eff} = H_o - \sigma H_o \qquad (1.6)$$

Any perturbation of the molecular electronic cloud will alter σ and consequently the measurement of the nuclear shielding constant is a sensitive means of monitoring changes in the electronic environment of the nucleus.

It is necessary to measure nuclear shielding relative to that of a reference nucleus, since magnetic field strengths cannot be measured accurately. Thus, σ may be redefined

$$\sigma = 10^6 \times (\sigma_{abs} - \sigma_{ref}) \qquad (1.7)$$

where σ_{abs} is the absolute shielding of the nucleus, (the σ

in equation (1.6)), σ_{ref} is the absolute shielding of the reference nucleus, in which case the relative shielding σ has the (conventional) units of parts per million (ppm).

Nuclear magnetic shieldings have been widely used in solution chemistry to study solute-solvent and solvent-solvent interactions. In a hydroxylic solvent such as water, the hydroxyl proton shielding is sensitive to such associations as hydrogen bonding and interaction with solute molecules.[39] It is desirable to formulate the response of the shielding to intermolecular associations and to use the formulation to gain further understanding of the solvation processes. For ionic solutes, a great deal of effort has been expended towards this goal in recent years.[29]

Both the longitudinal and transverse nuclear relaxation times, T_1 and T_2, may be used to study electrolyte solvation. If a solvent molecule exchanges between a cation solvation shell and the bulk solvent, the transverse relaxation time T_2 of each site will vary in a manner determined by the lifetime of each environment.[35] Thus, T_2 measurements may be used to study cation solvation shell exchange kinetics, within a limited range of exchange rates (the limits are controlled by the time scale of the NMR experiment as described in appendix A). The exchange rates for solvent molecules exchanging between the solvation spheres of all anions and many cations and the bulk solvent, lie outside the range accessible to the NMR experiment. The lifetimes of the

solvation shells of a few highly polarising cations in certain solvents (e.g. Mg(II) in MeOH) are sufficiently long to allow measurement of their exchange with the bulk solvent molecules.[36,37]

The longitudinal relaxation time T_1 has been used to probe structural hydration in aqueous electrolyte solutions.[38,39] A clear distinction is found between the values of T_1 of the water protons for solutions containing structure making and structure breaking salts. Structure breaking salts increase the water mobility, decrease the correlation time τ_c of the bulk solvent molecules compared with pure water, and hence increase the relaxation rate T_1. The structure making salts have the reverse effect. There is an extremely close correlation between the entropies of hydration (which reflect structural solvation) and the T_1 values of the alkali halides, for low salt concentrations.

The magnitude of the spin-spin coupling between nuclei in a solvent molecule could, in principle, be altered by coordination to an ion or through changes in hydrogen bonding. However, changes in J of more than a few percent have rarely been observed[40-42] and no solvation studies have been based upon observations of small changes in spin-spin interactions.

The observation of coupling between the hydroxyl proton and alkyl group protons in alcohols coordinated to cations has served to prove the persistence of bonding of the hydroxyl proton and to establish the mechanism of

exchange between the coordinated and bulk solvent molecules.[36]

There have been several excellent review articles [29,43-45] dealing with the use of NMR spectroscopy in the study of ion solvation. Therefore, only a brief summary of the different kinds of NMR solvation experiment will be attempted here. Distinction between the types of experiment is somewhat arbitrary, but will be made according to the scheme shown diagramatically in Figure 1.1.

The breakdown is made according to the nature of the solvent (single or mixed), observed nucleus (solvent or ion), and the rate of exchange of molecules between the solvation shell and the bulk solvent. Figure 1.1 includes an indication of the property studied (e.g. mixed solvation shells) by each method and the parameter measured: n is the primary solvation number and the Δ's are characteristic NMR shifts which will be discussed more fully in later chapters. Three of the experiments are of particular relevance to the present work and are labeled TYPE I, II, and III experiments. They will be defined in detail in the following sections and will be referred to by the labels throughout the remainder of this thesis.

Figure 1.2 shows diagramatically the kinds of spectra to be expected from the three experiments and also specifies the NMR shieldings which characterise them. The hydroxyl

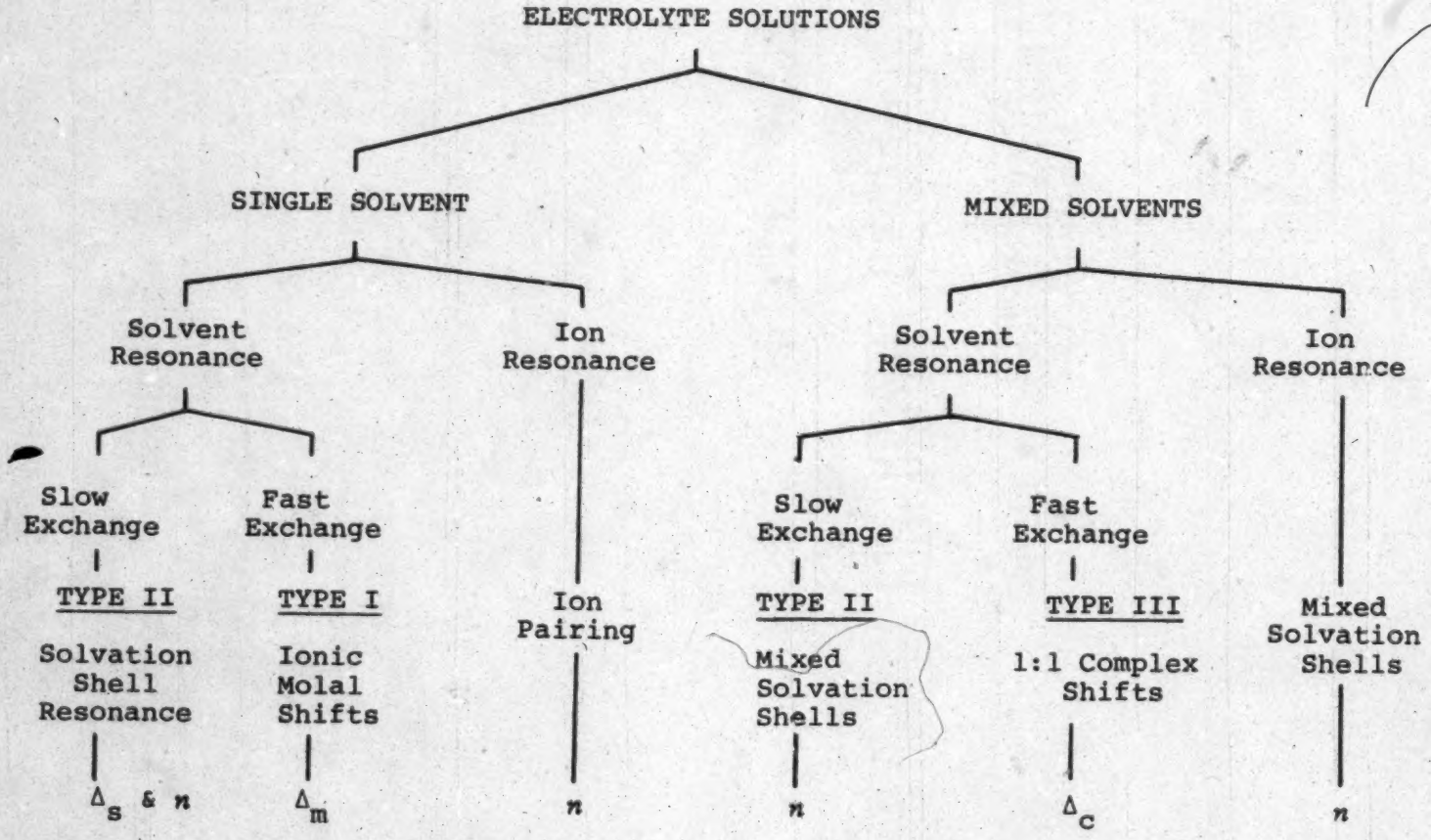

FIGURE 1.1 Summary of the NMR Solvation Experiments

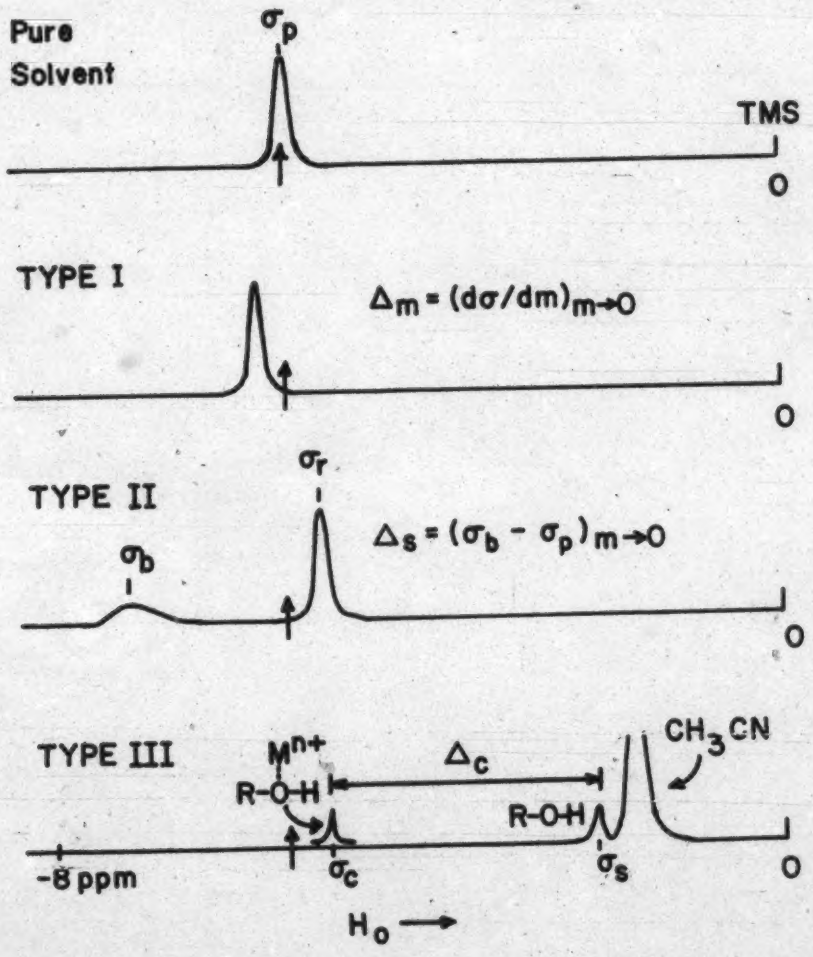

FIGURE 1.2. Schematic NMR spectra of the TYPE I, II and III experiments.

proton shieldings σ are labeled by subscripts as follows: p represents the pure solvent, b the solvent in the solvation shell (bound solvent) of an ion, r the residual bulk solvent in the solution, s the free substrate and c the 1:1 complex in the TYPE III experiment. Only the solvent (or substrate) hydroxyl proton signal is shown for simplicity and the four "spectra" are drawn to the same shielding scale. They will be referred to in the appropriate sections below.

1.3.1. Electrolytes in Single Solvents.

The NMR spectra of the solvent in solutions containing diamagnetic electrolytes in single hydroxylic solvents are of two kinds, depending upon the nature of the ions. If a particular ion has a low surface potential (small charge to radius ratio) then the lifetime of the primary solvation shell will be short compared with the time scale of the NMR experiment.[29] The coordinated molecules exchange rapidly with the bulk solvent molecules and only a single NMR absorption will be observed at the population average of the shieldings of the free and bound molecules.* Most of the cations and all of the anions have rapidly exchanging solvation shells and give fully coalesced solvent spectra,

---

* The effects of chemical exchange on NMR spectra are described more fully in Appendix A.

which are designated TYPE I spectra.

Cations with high surface potentials, such as Be(II), Mg(II), Al(III), Ga(III), have relatively long lived solvation shells,[44] especially at low temperatures, and it is possible to observe separate NMR signals for the solvation shell and bulk solvent molecules under favourable circumstances. These spectra are designated TYPE II.

It is sometimes possible to monitor the resonance of the ion nucleus. Most heavy atoms have high nuclear spin (greater than 1/2) and large electric quadrupole moments. The motional modulation of the interaction between the quadrupole moment and the electric field gradient at the nucleus provides an additional mechanism for nuclear magnetic relaxation.[46] The relaxation is enhanced when the electronic environment is asymmetric. If one solvent molecule in a symmetrical octahedral solvation shell is replaced by the counterion, then extensive quadrupole broadening of the central ion resonance will occur. Thus, direct contact ion-pairing can be studied by this technique.[47,48]

Because of their special relevance to the present work, the TYPE I and II experiments will now be described in detail.

1.3.1.1 Experiment I. Ionic Molal Shifts.

The hydroxyl proton NMR shieldings of pure water [49-56] and methanol [52,57-59] have been studied as a function of the concentration of added diamagnetic salt. The time-averaged resonance moves to lower or higher fields, depending upon the salt, as shown in figure 1.2. The parameter which characterises this experiment is the salt molal shift Δ_m, which is defined as the limiting slope of the exchange-averaged shielding σ *vs.* salt concentration curve.

$$\Delta_m = (d\sigma/dm)_{m\to 0} \qquad (1.8)$$

where m is the salt molality.

The salt shifts have been shown to be additive in individual ion contributions [55,59]

$$\Delta_m(\text{salt}) = \sum \Delta_m(\text{ions}). \qquad (1.9)$$

It should be noted that absolute individual ion shifts cannot be obtained from the salt shifts alone. Arbitrary scales have been devised by assigning a convenient value (such as zero) to one ion and calculating values for the other ions by least-squares methods. Taken alone, the ionic molal shifts are of little value and Butler and Symons [55,59] have pointed out that separations [50,58] of the molal shifts into contributions due to the effects of coulombic and structural solvation are in principle erroneous because of

the arbitrary origin of the shifts. Scales of absolute individual ion shifts based upon the results of independent TYPE II experiments have been reported recently [55,59] and they are interpreted quantitatively in the present work.

1.3.1.2 Experiment II. Separate Solvation Shell Resonances.

For certain highly polarising cations in hydroxylic solvents, the lifetime of the solvation shell may be long enough to allow observation of separate bulk and bound solvent resonances.[36,37,60-63] as shown in figure 1.2. The solvation shell hydroxyl proton signal occurs at lower field than that of the bulk solvent in all cases. The shieldings of both signals depend upon the total salt concentration [60] and two characteristic NMR shifts may be defined in the limit of infinite dilution. If σ_p, σ_b, and σ_r are the shieldings of the pure solvent, cation solvation shell, and residual bulk solvent in the solution respectively, as shown in figure 1.2, then it is convenient to define the shifts

$$\Delta_s = (\sigma_b - \sigma_p)_{m\to 0} \qquad (1.10)$$

$$\Delta_r = (d\sigma_r/dm)_{m\to 0} \qquad (1.11)$$

Δ_s is designated the "solvation shell shift", and Δ_r the "residual shift".

The primary solvation number n may be obtained directly

from this experiment by analysis of the relative intensities of the bulk and bound signals.[36] The accumulated experimental errors usually lead to an uncertainty of about ± 0.5 in the measured solvation number. The solvation numbers found in this way for several pairs of cations and hydroxylic solvents are given in table I. The values are consistent with the requirements of close packing.

1.3.2 Electrolytes in Mixed Solvents.

The TYPE I and II experiments above may be repeated with the gradual addition of a second solvent. This has several advantages, as described below.

Fratiello *et al* [64] have shown that the addition of acetone to aqueous electrolyte solutions has the effect of lowering the freezing point of the solution and slowing down the rate of exchange of coordinated and bulk solvent molecules. This allows the observation of separate bulk solvent and solvation shell resonances at low temperatures, which would not otherwise be possible for aqueous solutions. The addition of the co-solvent also affects the water hydrogen-bonded structure. The presence of a large excess of an "inert" co-solvent should completely disrupt the water (or alcohol) hydrogen bonded structure and allow the study of the ion-solvent interaction in the absence of the solvent-solvent interactions. In this way, the effects of coulombic

TABLE 1.1

Solvation Numbers* of Diamagnetic Cations Determined from NMR Intensities

	H_2O	MeOH	EtOH	Pr^nOH
Be^{++}	4			
Mg^{++}	6	6	6	
Al^{3+}	6	6	4	4
Ga^{3+}	6			
In^{3+}	6			

* Taken from reference 29 and rounded to the nearest digit. The experimental uncertainties are about $\pm$ 0.5.

solvation might be studied in the absence of those of structural solvation.

Several workers [65-69] have used binary solvent systems to study mixed solvation shells, for example dimethylsulphoxide and water coordinated to Al(III), by the observation of separate resonances for each bound solvent. The quadrupole broadening of the resonance of the ion has also been used to study mixed solvation shells.[70]

1.3.2.1 Experiment III. 1:1 Ion-Molecule Association.

If the second solvent is inert (i.e. weakly solvating) and present in large excess, and one ion is also inert (weakly polarising), it is possible to form a specific 1:1 complex between the minor solvent (called the substrate in this experiment) and the other ion.[71] The characteristic shift Δ_c is the difference between the hydroxyl proton shielding in the complex σ_c and that in the free substrate σ_s, in the inert solvent.

$$\Delta_c = \sigma_c - \sigma_s \qquad (1.12)$$

The complex shift Δ_c is obtained in the absence of the structural effects which accompany studies in pure hydroxylic solvents. If the solvent in the TYPE III experiment is truly inert, then Δ_c represents the shift due to the direct polarisation of the substrate molecule by the ion.[71]

Previous to the present study, the results of experiments of this type have been published only for complexes between the halide anions and a few highly polar substrates in carbon tetrachloride solution,[71-72] and for the sodium and lithium cation complexes of water in propylene carbonate solution.[74]

1.3.3 NMR and Structural Solvation

In 1955, Shoolery and Alder [49] published the first extensive tabulation of molal shifts for aqueous electrolyte solutions. The spectra were obtained on a 30 MHz instrument monitored with an oscilloscope. The added salts were found to shift the water resonance to both higher and lower fields. It was expected that both cations and anions should polarise water molecules in such a way as to deshield the protons.* Since both positive and negative molal shifts occur, Shoolery and Alder concluded that changes in hydrogen bonding must be responsible for an upfield shift which counteracts the downfield polarisation shift. The relative magnitudes determine the sign of the observed molal shift.

Shoolery and Alder derived a scale of individual ion molal shifts by choosing a value for the molal shift of one

---

* This has been confirmed for both cations and anions in this and other work.[41]

particular reference ion (they chose Δ_m of ClO_4^- to be +0.85 ppm. kg. $mole^{-1}$ in order to make the scale fit their arguments). They concluded that large monovalent ions mainly break up the solvent structure whilst small and multivalent ions predominantly polarise the solvent.

Since the work of Shoolery and Alder, there have been numerous improved tabulations of individual ion shifts.[50-54] The improvements were concerned largely with the choice of (internal or external) NMR reference material and with the choice of the arbitrary reference ion. The tabulations were accompanied by interpretations of varying complexity. The work of J. C. Hindman [50] is outstanding in this respect. He interpreted the molal ionic shift in terms of four contributions: a) a shift due to direct polarisation of molecules in the first solvation shell; b) a shift due to hydrogen bond breaking when some molecules are reoriented to take up position in the primary solvation shell; c) a shift due to additional structural changes because the solvated ion cannot fit into the normal water structure (structure making/breaking); d) a shift due to non-electrostatic interaction between the ion and solvent.

Although none of the four proposed contributions had been measured separately, Hindman attempted to estimate them. The structural effects b) and c) were regarded in terms of the number of hydrogen bonds broken per mole of water and he assumed a value for the percentage of hydrogen bonding in pure

water. Despite the gross approximations involved, Hindman concluded that, of the alkali metal and halide ions, Li^+ and F^- are structure makers (effect c) and that the larger ions are structure breakers.

Butler and Symons [35,59] have criticised this early work because of the arbitrary separations of cation and anion effects. On the basis of independent TYPE II experiments, they have proposed a scale of "absolute" individual ion shifts for both water [55] and methanol.[59] They state that their results do not require the concept of structure making/breaking (effect c) and that their molal shift data may be accounted for in terms of the relative effects of hydrogen bonding to the solvent (effect b) and bonding to the ions (effect a). They made no attempt to quantitatively separate the effects of coulombic solvation (a and b) from that of structural solvation (c) and their conclusions are not supported by the measurement of any quantity which is characteristic of structural solvation.

At this point, it seems fair to say that no previous NMR experiments have been directed towards the determination of a parameter which is characteristic of structural solvation, nor has anyone determined independently the several components of the ionic molal shift.

1.4 Scope of this Thesis

Of the three major kinds of solvation experiments (TYPE I, II and III) involving the magnetic resonance of solvent nuclei, the TYPE I and II results have appeared most frequently in the literature. A systematic study of the TYPE III 1:1 ion-molecule association experiments for diamagnetic cations and hydroxylic substrates has not yet been reported. A study of this kind represents a major portion of this thesis, and these results turn out to be the key to the interpretation of the TYPE I and II characteristic ^{1}H NMR shifts.

The association equilibria for 1:1 complexes between six cations and eight hydroxylic substrates (water, alcohols and diols) were studied in dilute acetonitrile solution. The association constants and complex shifts are reported in Chapter 3 and they are interpreted by means of simple electrostatic models in Chapter 4. A single cation-amine complex was also investigated and its properties are compared with those of the hydroxylic complexes.

Chapter 5 deals with miscellaneous TYPE I and II experiments which are required for the correlation of the three types of experiments in Chapter 6. The various components of the ionic molal shift are evaluated, using the results of the TYPE II and III experiments and a simple solvation model, which incorporates the effects of both coulombic and structural solvation. The basis of the model

is explained in detail, and the characteristic NMR shifts from the three different experiments involving small or multivalent cations in water and methanol are fitted to its defining equations. The solvation properties of large monovalent cations and anions are also discussed in terms of this model, utilising values of the NMR shifts taken from the literature.

In previous work with the NMR spectra of hydroxylic solvents in electrolyte solutions, attention has been focussed almost exclusively on the hydroxyl group ^{1}H resonance. Since the advent of the Fourier transform method has allowed the observation of carbon 13 NMR spectra of natural abundance samples, a series of experiments was performed which should be regarded as a preliminary study of the application of ^{13}C NMR to solvation chemistry. Chapter 7 deals with the TYPE II and III carbon-13 NMR spectra of solutions of Mg(II) and Al(III) in bulk alcohols. The features of the spectra and ^{13}C shieldings in the solvent molecules coordinated to the cations are discussed. The effect of the cation on the shielding of nuclei in the coordinated molecules is compared with that of an electronegative substitutent in an α-substituted alkane. The unusual effects on the anion in ethanolic solutions of aluminum chloride were investigated by comparison of the ^{1}H and ^{13}C spectra with those of ethanolic alumium perchlorate solutions.

The conclusions inferred from the results of all of the experiments are summarised in Chapter 8. A list of suggestions for future work is included, since several interesting phenomena were observed which were not rigorously investigated.

CHAPTER 2.

E X P E R I M E N T A L

2.1 Materials.

Perdeuterioacetonitrile (CD_3CN), from Stohler Isotopic Chemicals, was distilled from freshly opened phosphorus pentoxide, then from calcium hydride, collecting the middle 90% from each distillation. The product was stored over 4A molecular sieve. Tetramethylsilane (TMS) was added before sample preparation to serve as an NMR internal reference.

Acetonitrile (CH_3CN), Baker reagent grade, was distilled twice from phosphorus pentoxide and then from calcium hydride, the middle 60% being collected and stored over 4A molecular sieve.

Tetramethylsilane, from NMR Specialties, was refrigerated over 4A molecular sieve before use.

The sample of purified water was supplied by Dr. H. B. Dunford. It had been passed over cation and anion exchange resins, distilled three times from alkaline permanganate and finally distilled normally.

Reagent grade methanol, n-propanol, iso-propanol, n-butanol and t-butanol, all from Fisher Chemicals, were soxhlet extracted with 4A molecular sieve for 24 hours and then distilled, the middle 60% being collected over 4A molecular sieve

Ethanol containing impurities (including water) at the level of a few parts per million was obtained from the U. S.

Industrial Chemical Co. The NMR spectrum of the neat liquid at 20° contained a well resolved hydroxyl proton multiplet, indicating very low concentrations of acidic or basic impurities.

1,2-Ethanediol and 2-methoxyethanol, from Eastman Chemicals, were distilled under reduced pressure, collecting the middle 60% over 4A molecular sieve.

Diethylamine, from Eastman Chemicals, was refluxed with fresh sodium hydroxide and then distilled, collecting the middle 60% over 4A molecular sieve.

All of the perchlorate salts were supplied by the G. F. Smith Chemical Co. The calcium and strontium perchlorates were obtained as hexahydrates and the barium salt as the trihydrate; they were dehydrated by heating at 100° under vacuum, gradually increasing the temperature during several days to 200°. The lithium, sodium and magnesium salts were obtained labeled "anhydrous". They were dried by heating at 200° under vacuum.

All of the perchlorate salts were then dissolved in a minimum of acetonitrile. The heat of solution in most cases caused the solvent to boil and the hot solutions were filtered through previously dried Whatman's No. 1 papers to remove slight residues. The solutions were cooled and the crystals separated by filtration. Occluded solvent was removed under vacuum and the salts were dried by heating at 200° for several days.

Aluminum and gallium trichlorides were obtained from Alfa Inorganic Chemicals in anhydrous form and were used without further purification.

All of the materials were stored in a drybox (a description of the drybox is given below). 100 MHz ^{1}H NMR spectra of the solvents and concentrated acetonitrile solutions of the perchlorate salts were used to confirm the absence of significant residual water. The perchlorate salts contained no chloride detectable by the silver nitrate test and aqueous solutions of them were neutral.

2.2 Preparation of Samples for NMR.

All materials except water were handled in a specially equipped glove box. The nitrogen atmosphere was constantly exposed to fresh phosphorus pentoxide and was cycled using a small gas pump, which bubbled it through sulphuric acid and over sodium hydroxide pellets. The glove box was kept slightly above atmospheric pressure.

All weighings were done inside the glove box on a Cahn DTL millibalance. A radioactive source was used to eliminate static charge accumulation, which would otherwise have caused large weighing errors.

In the TYPE III 1:1 association experiment, solid was weighed directly into a 1 ml. volumetric tube. Solvent was added to dissolve the solid and the liquid substrate was

added from a 10 μl. syringe. Solvent was then added to make the solution up to the calibrated volume. The solutions were mixed and transferred to 5 mm. o.d. medium wall NMR tubes fitted with auxilliary stopcocks to exclude air. The tubes were connected to a vacuum rack, the solutions degassed by freezing and pumping (two cycles), and the tubes were sealed.

Samples for the low temperature TYPE II solvation shell spectra were prepared in a similar manner with the exception that the hydroxylic solvents were added from calibrated pipettes to ensure a known molar ratio of salt to solvent. 5 mm. o.d. tubes were used for the proton spectra and 10 mm. for the carbon-13 studies. The 10 mm. tubes were sealed with plastic stoppers and the solutions for carbon-13 spectroscopy were not degassed.

2.3 NMR Spectroscopy

Most of the proton spectra were obtained on a Varian HA-100 spectrometer and the rest on a HA-60. Unless otherwise stated, the spectra were recorded at ambient probe temperature: 35 $\pm$ 1° on both spectrometers. Lower temperatures were obtained with the use of the Varian V-4540 temperature controller and nitrogen coolant gas. Temperatures were measured with the use of a copper-constantan thermocouple inserted in an NMR tube containing methanol. Line positions were measured to 0.1 Hz (for narrow lines) by setting the frequency sweep at resonance, adjusting the radio-

frequency field to avoid saturation, and measuring the frequency difference between the sweep and lock oscillators.

All chemical shifts are reported as shieldings; that is, a positive shift is upfield and represents increased nuclear shielding. In some cases, overlap of strongly coupled multiplets required computer simulation in order to obtain accurate chemical shifts. The computer program LAME[75] was used to calculate spectra.

The natural abundance carbon-13 NMR spectra were recorded on a Bruker HFX-10 pulse Fourier transform spectrometer at 22.63 MHz. using 10 mm. sample tubes and an external deuterium lock. The proton decoupled spectra required *ca* 500 accumulations, and the coupled spectra *ca* 3000 accumulations, for satisfactory signal to noise ratio. Since only the difference between the shieldings of the bulk and bound solvent molecules was required, a reference signal was not needed.

Peak areas in the proton spectra were measured by electronic integration; those in the carbon-13 spectra were measured with a planimeter. The accuracy of the solvation numbers derived from the peak areas is controlled by the reproducibility of the spectra, rather than that of the instruments used to measure the areas. The signal to noise ratio of the carbon-13 spectra also limits the accuracy of the solvation numbers. The uncertainty in the solvation number is usually $\pm$ 0.5.

CHAPTER 3

1:1 ION-MOLECULE ASSOCIATION IN ACETONITRILE

The present study is based upon the methods developed by Green and Martin [41,71] for the investigation of halide-ion complexes of polar molecules. They have reported the NMR spectra of 1:1 complexes between several kinds of proton donor molecules and the halide ions in carbon tetrachloride solution. The formation of the hydrogen-bonded complex was represented by

$$X—H + Y^- \rightleftharpoons X—H\cdots Y^- \qquad (3.1)$$

where X is an electronegative group such as Cl_3C- or R-O-, and Y^- is a halide ion supplied by a tetraalkylammonium salt. The association constants and NMR shifts on complex formation were reported for several ion-molecule combinations.

It was hoped that 1:1 complexes between diamagnetic cations and electron donor molecules could be studied in a similar way. The 1:1 complex polarisation shifts of water and the alcohols in an inert solvent were expected to be of significance in the understanding of the solvation mechanism of electrolytes in bulk hydroxylic solvents.

The choosing of a suitable "inert" solvent presented some difficulty. A truly inert solvent would not dissolve inorganic salts, and highly polar solvents such as dimethyl-sulphoxide solvate the cation and substrate so strongly that

no complex is formed. Of the three most suitable candidates, acetone, acetonitrile and propylene carbonate, acetonitrile was chosen because it is easily purified and is readily obtainable in fully deuterated form at reasonably low cost. The perdeuterated solvent has the advantage that it does not obscure regions of interest in the proton NMR spectra of the substrate. Perchlorate salts were used to minimise anion effects.

The experiment was performed as follows. To solutions containing small quantities (*ca* 0.1 M) of the substrate, increasing amounts of the perchlorate salt of a cation were added, up to *ca* 1 M. These conditions were chosen to favour 1:1 association.

(3.2)

It is found that the substrate hydroxyl proton signal shifts to lower field but remains sharp, which indicates rapid equilibration of the free and complexed substrate. The protons in the alkyl group are affected to a much smaller extent, the shift decreasing in magnitude with distance from the oxygen atom, consistent with attachment of the ion at the oxygen atom.

The NMR shift Δ_c which is characteristic of this experiment is defined as the difference between the shielding σ_s

of the hydroxyl proton in the free substrate and the shielding σ_c in the 1:1 complex with the cation. The 1:1 association constant is defined as K = [C]/[I][S], where C, I, and S represent the complex, the ion and the free substrate respectively. Figure 3.1 shows computer simulations (based upon the equations given in the next section) of several possible graphs of O-H shielding *vs.* salt concentration at constant substrate concentration. It is evident that for large association constants (K > 100) the shielding should become independent of salt concentration when the salt is in excess, and the complex shift Δ_c may be observed directly. This was observed in several cases. In these cases the observed shielding approached the stoichiometric line (curve a in figure 3.1), thus supporting the assumption that only 1:1 association is significant. In cases of smaller association constants, Δ_c and K were obtained from a suitable analysis of the equilibrium.

3.1 Analysis of the Equilibrium

We proceed for the present with the assumption that the association depicted in equation (3.1) for the case of an alcohol complex is the only one occurring in the systems studied. The thermodynamic equilibrium constant K_{th} appropriate to this interaction is given by

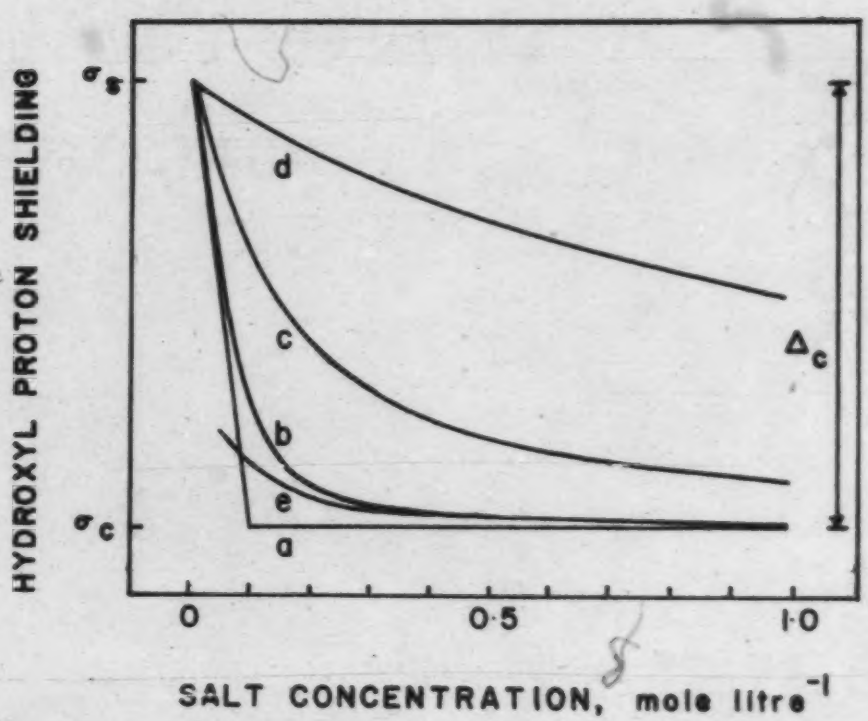

FIGURE 3.1. Simulations of the dependence of the hydroxyl proton shielding on the concentration of added salt for various equilibrium constants K, at a fixed substrate concentration (0.1M) and complex shift Δ_c. Curve (a) K = ∞; (b) K = 100; (c) K = 10; (d) K = 1. Curve (e) illustrates the occurrence of multiple equilibria at low salt concentrations.

$$K_{th} = \frac{\gamma_C}{\gamma_I \gamma_S} \cdot \frac{[C]}{[I][S]} \qquad (3.3)$$

Debye-Huckel theory [76] predicts that the substrate activity coefficient γ_S will be independent of ionic strength; γ_C and γ_I will both vary as the square root of ionic strength which is proportional to the salt concentration. Thus, the term $\gamma_C/\gamma_I\gamma_S$ appearing in equation (3.3) should be substantially independent of salt concentration. This would indeed be fortunate because the appropriate activity coefficients are not known, nor are they easily measured. It is thus convenient to define a new equilibrium constant

$$K = \frac{[C]}{[I][S]} \qquad (3.4)$$

related to K_{th} by an undetermined factor $\gamma_C/\gamma_I\gamma_S$, which is predicted by the Debye-Hückel limiting law to be 1.

Since the NMR signals of the free and complexed substrate are coalesced by rapid exchange, the experimental shielding σ will be the population average

$$\sigma = \frac{[S]}{C_s}\sigma_s + \frac{[C]}{C_s}\sigma_c \qquad (3.5)$$

where C_s is the total substrate concentration

$$C_s = [S] + [C] \qquad (3.6)$$

$$\Delta = \sigma - \sigma_s \tag{3.7}$$

$$\Delta_c = \sigma_c - \sigma_s \tag{3.8}$$

and note that

$$[I] = C_I - [C] \tag{3.9}$$

where C_I is the total salt concentration.
Equations (3.4) to (3.9) may be combined to yield the appropriate form of the Scott-Benesi-Hildebrand equation.[77,78]

$$\frac{[I]}{\Delta} = \frac{[I]}{\Delta_c} + \frac{1}{K\Delta_c} \tag{3.10}$$

Equation (3.10) is of the form $y = c_1 + c_2X$, where $y = [I]/\Delta$ and $x = [I]$. A least-squares fit of the observed shifts, for a series of samples with different C_I, to equation (3.10) yields $\Delta_c = 1/c_2$ and $K = c_2/c_1$. The standard deviations in the coefficients, and hence Δ_c and K, are obtained by methods which have been described before and they include estimates of error contributions arising from evaluable uncertainties in the observed quantities.[71]

The actual free ion concentration [I] used in equation (3.10) is unknown. It may be approximated by C_I and values of Δ_c and K are calculated by least-squares fit to equation (3.10). [I] can then be calculated using the deduced values of K and Δ_c. The calculation may be performed iteratively until K and Δ_c remain unchanged on successive iterations.

The n^{th} iteration value of [I] is

$$[I]_n = C_I - C_{s(\frac{\Delta}{\Delta_c})_{n-1}} \qquad (3.11)$$

where $(\Delta_c)_{n-1}$ is the deduced complex shift from the n-1 iteration.

The correct value of Δ_c will be obtained by this method provided that K is independent of salt concentration and σ_s and σ_c are not affected by changes in the concentration of the substrate or the complex. The NMR spectra of several solutions of water and methanol in acetonitrile were recorded and the substrate hydroxyl proton shielding σ_s was shown to be essentially independent of substrate concentration over the range 0.2 to 0.001 M. The hydroxyl proton in the complex is expected to respond similarly.

3.2 The Accuracy of the Parameters Δ_c amd K.

The question of the accuracy of the parameters Δ_c and K has been treated by Deranleau [79] in terms of the saturation fraction $S = [C]/C_s$, which is the fraction of the substrate actually complexed. The most accurate values of both parameters are obtained from equation (3.10) when the observed saturation range ΔS lies between 0.2 and 1. When ΔS is less than 0.2, both parameters are uncertain.

When the equilibrium constant is very large (greater than *ca* 100), Δ_c can be observed directly to within about 1%, but

the intercept of the least squares fit to equation (3.10) is very small and the equilibrium constant is very uncertain.

There remains the possibility that complexes with other than 1:1 stoichiometry may go undetected and influence the values of K and Δ_c. A straight line fit to equation (3.10) is not always proof of wholly 1:1 association. Deranleau [70] has discussed the consequences of multiple equilibria rather thoroughly. He concludes that at least 75% of the entire saturation curve ($\Delta S \geq ca\ 0.75$) must be observed in order to show correspondence between the equation for a given stoichiometric model and the equation fitting the data. In the systems studied here, it was possible to meet this requirement in most cases.

The error analysis is consistent with Deranleau's criteria: somewhat larger relative errors are given for cases of restricted saturation range. The computer program used for this analysis weights points inversely as the squares of their estimated error. Points at high salt concentration have the largest [I] and Δ, and thus least error. It is these points, for which multiple substrate-ion complexing is least likely (see Curve e, Fig. 3.1), which have greatest weight in the analysis. Consequently, even though multiple substrate complexes are not explicitly treated, the analysis minimises their effect on the deduced parameters. Further evidence that multiple equilibria are not significant in most cases, is the fact that no significant curvature

was observed in any linear regression according to equation (3.10).

The discussion of possible anion and solvent effects on the parameters is appropriately made in terms of the experimental results, which are presented in the next sections.

3.3 1:1 Cation Complexes of Water and the Alcohols

Table 3.1 gives the deduced substrate - cation molar association constants, in acetonitrile at 35°, of all systems studied. The value for the water-magnesium system is listed as "large" since it cannot be precisely determined from the concentration dependence of the shift. It is probably of the order of several thousand.

Table 3.2 lists the observed saturation ranges for all of the systems studied. It can be seen that Deranleau's criterion of a saturation range in excess of 75% is met in most cases, for which the equilibrium constants and complex shifts must be adequately represented. The condition is met for complexes of all ions except sodium and for all substrates with the remaining ions except for t-butanol.

Table 3.3 gives the deduced complex shifts, Δ_c of all of the systems studied. Where the association constant was large, the deduced shift was close to that observed at high salt concentrations. The shielding in the complex may be computed by adding the complex shift to the shielding of the free substrate in 0.1 M acetonitrile solution (see equation

TABLE 3.1

Equilibrium Constants, Litre Mole^{-1}, of Cation-Substrate Complexes, with the Substrate at 0.1 M in Acetonitrile at 35 ± 1°C

Substrate	Na^+	Li^+	Ba^{++}	Sr^{++}	Ca^{++}	Mg^{++}
H_2O	2.3 ± .1	14 ± 1	16 ± 2	45 ± 16	151 ± 69	Large
MeOH	1.5 ± .2	5.6 ± .1	8.3 ± .8	16 ± 2	37 ± 1	300 ± 100
EtOH	1.5 ± .1	5.7 ± .3	5.7 ± .4	10 ± 2	19 ± 4	140 ± 80
n-BuOH	1.6 ± .2	5.2 ± .3	4.2 ± .2	7.3 ± .6	22 ± 6	150 ± 70
i-PrOH	1.1 ± .2	4.2 ± .2	2.8 ± .1	3.8 ± .2	8.2 ± .7	66 ± 30
t-BuOH	0.7 ± .1	3.2 ± .2	1.2 ± .1	1.0 ± .1	1.7 ± .1	2.8 ± .2

TABLE 3.2

Saturation Range* ΔS of the 1:1 Complex Equilibria

Substrate	Na^+	Li^+	Ba^+	Sr^{++}	Ca^{++}	Mg^{++}
H_2O	0.66	0.92	0.94	0.98	0.99	1.00
MeOH	0.62	0.84	0.87	0.93	0.96	1.00
EtOH	0.56	0.84	0.78	0.88	0.94	0.99
n-BuOH	0.59	0.84	0.79	0.87	0.72	1.00
i-PrOH	0.56	0.81	0.64	0.75	0.87	0.98
t-BuOH	0.38	0.75	0.51	0.39	0.58	0.71

* The values given in the table are maximum observed saturation fractions. Since the minimum fraction is 0 in all cases, the values also represent the observed saturation ranges.

TABLE 3.3

Limiting Shifts Δ_c, ppm, of Cation-Substrate Complexes in Acetonitrile at 35 ± 1°C

Substrate	Na^+	Li^+	Ba^{++}	Sr^{++}	Ca^{++}	Mg^{++}
H_2O	-0.89 ± .03	-1.48 ± .02	-1.54 ± .03	-1.75 ± .03	-2.17 ± .02	-2.98 ± .02
MeOH	-0.78 ± .05	-1.57 ± .02	-1.45 ± .03	-1.65 ± .03	-2.09 ± .03	-2.99 ± .03
EtOH	-0.70 ± .03	-1.51 ± .02	-1.31 ± .04	-1.47 ± .06	-1.98 ± .03	-2.75 ± .04
n-BuOH	-0.63 ± .05	-1.47 ± .06	-1.36 ± .03	-1.53 ± .03	-1.94 ± .05	-2.70 ± .05
i-PrOH	0.70 ± .10	-1.48 ± .02	-1.17 ± .03	-1.35 ± .03	-1.79 ± .03	-2.45 ± .03
t-BuOH	-0.85 ± .12	-1.52 ± .04	-1.34 ± .06	-1.66 ± .02	-2.08 ± .07	-2.36 ± .07

(3.8)). The shieldings for the substrates are given in table 3.4.

The cation-methanol experiments were repeated at lower temperatures, using the sodium, lithium and magnesium perchlorates. These salts span the range of observed shifts and association constants, and thus should be representative of the temperature dependence to be expected of the cation-substrate association. Over the range +35° to -21°, the cation-methanol association constants increased with decreasing temperature, by a factor of two or three. As shown in table 3.5, the complex shifts changed only by amounts comparable to their standard errors. The substrate shielding, and thus the complex shieldings, decreased significantly as the temperature decreased.

At the two lowest temperatures, where the shifts appear to show significant change, limited solubility restricted the range of salt concentrations used and reduced the saturation range; thus the probable errors at these temperatures may be larger than those quoted in the table.

It appears that, to within experimental error, the shieldings of free and complexed methanol both decrease with decreasing temperature, but their differences (the complex shifts) do not.

3.3.1 Association Constants. It is apparent from table 3.1 that, for a given ion, the variation of the association

TABLE 3.4

Shieldings, in ppm vs. TMS, of Substrates, 0.1 M in Acetonitrile, at 35 ± 1°C

Substrate	Shielding (±0.01)
Water	-2.10
Methanol	-2.10
Ethanol	-2.41
n-Butanol	-2.38
i-Propanol	-2.44
t-Butanol	-2.31

TABLE 3.5

Temperature Dependence of Shifts and Shielding of Methanol Cation Complexes

Temp. °C	Complex shifts, ppm Na^+ Δ_c	Na^+ K	Li^+ Δ_c	Li^+ K	Mg^{++} Δ_c	Mg^{++} K	Shielding of Methanol
35.0	-0.75	1.73	-1.54	5.7	-2.99	300	-2.10
21.5	-0.76	1.72	-1.52	6.9	-2.98	-	-2.17
10.0	-0.73	1.90	-1.52	7.7	-2.96	-	-2.23
0.5	-0.71	1.91	-1.51	8.8	-2.95	-	-2.28
-10.5	-0.68	2.1	-1.49	10.6	-2.92	-	-2.33
-21.0	-0.66	2.2	-1.44	13.7	-2.91	large	-2.38

The methanol shielding is for 0.1 M methanol in acetonitrile; it is in ppm vs internal TMS. Standard errors, in temperature, 1°; in complex shifts (Li^+ and Na^+) 0.66 ppm, (Mg^{++}) 0.03 ppm; in methanol shielding, 0.01 ppm; in K (Li^+ and Na^+) *ca* 0.5, (Mg^{++}) > 100.

constant with substrate is in the order, H_2O > (CH_3OH, C_2H_5OH, n-C_4H_9OH) > i-C_3H_7OH > t-C_4H_9OH. This differs from the trend found for anion complexes of alcohols.[41] The anion association constants reflect the inductive properties of substituents on the α-carbon atom; the cation constants do not.

It is possible that the small cation association constants of t-butanol and i-propanol are related to the crowding of methyl groups about the oxygen atom. Formation of the complex with such alcohols may require an exceptional amount of desolvation of the ion. This is not observed in the case of anions, since they associate with the more accessible hydroxyl hydrogen atom, and because anions in carbon tetrachloride are less strongly solvated than cations in acetonitrile.

The cation association constants of water are larger than those of any alcohol. Since acetonitrile is a basic solvent, it will preferentially solvate the hydrogen of a hydroxyl group. Thus, the alcohols will be singly, and water doubly hydrogen bonded to the solvent. This interaction with the solvent should result in the polarisation

$$CH_3CN\cdots H^{\delta+}\text{-}O^{\delta-}\text{-}R \qquad CH_3CN\cdots H^{\delta+}\text{-}O^{\delta-}\text{-}H^{\delta+}\cdots NCCH_3$$

of the O-H bonds and the resulting charge shift should be larger for water than for the alcohols. The charge shift

accompanying hydrogen bonding should enhance the nucleophilicity of the water oxygen, and thus the association constants, relative to those of the alcohols.[81,82]

For all of the substrates except *i*-propanol and *t*-butanol, there is a regular variation of the equilibrium constant across the rows of table 3.1. The substrates are more strongly bound to ions of high surface potential. This was previously observed in the case of the anion complexes.[41,71,77] A less regular variation is observed for *i*-propanol and *t*-butanol, more closely related to ionic size than to ionic charge. It is possible that association with these substrates is sterically controlled.

An attempt was made to study the effect of a strongly electron withdrawing substituent on the complexing ability of an alcohol by conducting the TYPE III experiment for 2,2-2-trifluoroethanol with Mg(II) in dilute acetonitrile solution. For salt concentrations of up to 1 M there was almost no change in the shieldings of the protons in this substrate, nor in the shielding of the CF_3 group fluorine nuclei. Since there is no reason to expect a very small complex shift for this substrate, the explanation of these observations is most probably that the association constant K is close to zero. It appears that 2,2,2-trifluoroethanol acts as a weaker base towards Mg(II) than either ethanol or acetonitrile.

Sherry and Purcell [83] have shown that trifluoroethanol is able to form strong hydrogen-bonded complexes with basic

molecules in methylene chloride. The hydroxyl proton in the complex is deshielded to the extent of 2 to 6 ppm relative to that in the free substrate. The CF_3 group appears to increase the acidity of the hydroxyl proton in trifluoroethanol whilst decreasing the basicity of the hydroxyl oxygen atom, towards cations and basic molecules respectively. It is apparent that whereas the strongly electron withdrawing CF_3 substituent in the substrate is able to affect the cation association constant, any differences in the inductive properties of the alkyl chains of the other substrates studied do not significantly influence the cation association constants for these substrates.

3.3.2 The Complex Shifts. The values of the cation-substrate complex shifts given in table 3.3 show a large regular variation with ionic surface potential. The variation with the substrate is smaller and irregular. For a given cation, all substrates show essentially the same complex shift, with a relative standard deviation of 10% or less. This suggests that, in all cases, the ion complexes have the same structure, which is primarily determined by the properties of the hydroxyl group.

3.3.3 Effect of the Counterion. Perchlorate is a large monovalent anion and may be expected to have low polarising capability. However, its effect on the substrate hydroxyl

proton shielding may be estimated by studying the effects of the addition of increasing amounts of tetrabutylammonium perchlorate to acetonitrile solutions of a substrate. The tetrabutylammonium cation is also weakly polarising. Although the effects of the cation and anion cannot be separated, an upper limit may be placed on the effect of perchlorate. In this system, the shielding moved downfield monotonically and did not exceed -0.2 ppm at 1 M salt concentration. Cogley, et al., [74] reported that the salt induced shifts of water in propylene carbonate were identical for perchlorate, tetrafluoroborate, and tetraphenylborate salts. It is therefore reasonable to propose that the counterion effect is negligible.

3.3.4 Effect of the Solvent. It is possible that the solvation of the substrate by acetonitrile, the "inert" solvent, may affect the complex shift. For the cation complexes, involvement of the solvent S may be represented by the equation

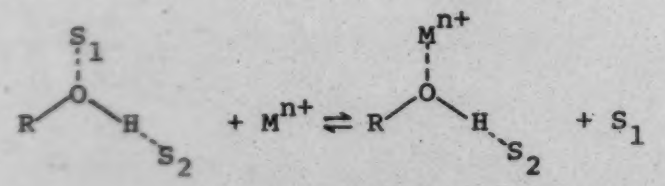

(3.12)

The displacement of the solvent molecule S_1 from the substrate oxygen may affect the hydroxyl proton shielding, but there is evidence that it does not.[72,74] Solvation of the proton by S_2 is significant. Cogley et al. [74] have studied

complexes of water with lithium and sodium ions in propylene carbonate solution. When their data are analyzed by the Scott method,* complex shifts of -1.49 ppm for lithium and -0.96 ppm for sodium are deduced. The corresponding shifts for these ions in acetonitrile are -1.48 ppm and -0.89 ppm. Thus, the cation-water complex shifts are the same in both solvents, even though the shieldings of both the substrate and the complex differ between the two solvents. Apparently the solvent effect on the hydroxyl proton shielding is unaffected by formation of the complex.

The absence of temperature effects on the complex shifts is also consistent with the assertion that all significant substrate-solvent interactions, which would presumably give rise to the temperature effect, occur at a site other than that at which the complex forms.

Similar studies of anion complexes support the postulate that solvation of the substrate oxygen does not affect the shielding of the hydroxyl proton. The significant change of state upon the formation of a methanol-chloride

---

* Cogley et al. (Ref. 74) analyzed their shift vs. concentration curves by an uniterated Benesi-Hildebrand method in which the equilibrium ion concentration was assumed to be the total ion concentration. For reasons state previously, the iterated analysis is considered to be more self-consistent and the complex shifts quoted above were obtained from Cogley's data by the iterative method of analysis.

complex is

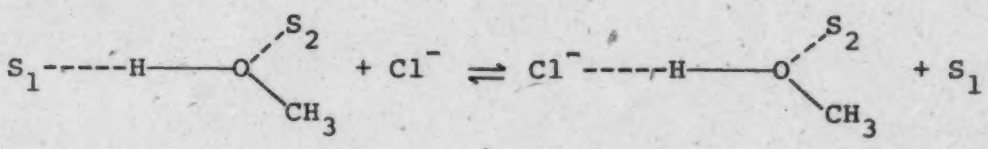

(3.13)

One would expect that since the important solvation is removed on formation of the complex, the complex shift would be solvent dependent, but that the shielding of the complexed substrate would be insensitive to the solvent.

Ormondroyd et al.[72] have shown that the methanol-chloride complex has the same hydroxyl proton shielding in acetonitrile and in carbon tetrachloride. In these solvents, dilute methanol has widely different shieldings. Thus, the anion complex shift is solvent dependent, while the complex shielding is not.

The cation and anion complex shifts thus indicate that the largest contribution to the solvent-induced shielding of hydroxyl protons in dilute solution arises from solvation of the hydrogen, and that solvation at the oxygen does not produce a significant effect. This is consistent with a short-range shielding mechanism. Thus cation induced shifts are dominated by the direct ion-substrate interaction.

3.4 Cation Complexes of Bidentate Substrates.

The substrates discussed in section 3.3 had the common feature of containing only one nucleophilic site: the

hydroxylic oxygen atom. The (approximate) structure of the cation complexes of these substrates can be predicted with confidence from the consideration of the interaction between the ion monopole and the substrate permanent and induced dipoles (see Chapter 4). When a substrate molecule contains two labile groups as in an alkane diol, several questions arise in predicting the stoichiometry and structure of their cation complexes. Are one or both donor sites involved in bonding? If the latter is the case, do the two sites donate to the same or different ions? Will the structure and stoichiometry be the same for all ions? Do two or more of the possible equilibria occur simultaneously? The treatment of the data depends strongly on the answers to these questions.

For example, consider the cases of a 1,2-diol acting in either a monodentate (I) or bidentate (II) fashion.

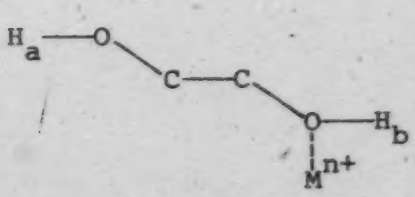

I.

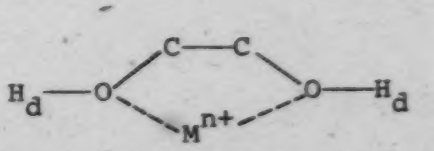

II.

If *one* of these complexes exists in equilibrium with the free substrate, the population averaged shielding (σ_I and σ_{II}) in each case will be

$$\sigma_I = \frac{[S]\sigma_s}{C_s} + \frac{[C]}{C_s}\,\frac{\sigma_a + \sigma_b}{2} \qquad (3.14)$$

$$\sigma_{II} = \frac{[S]\sigma_s}{C_s} + \frac{[C]\sigma_d}{C_s} \qquad (3.15)$$

where a, b, and d label the hydroxyl protons shown in structures I and II. It is likely that $\sigma_a \approx \sigma_s$ and $\sigma_b \approx \sigma_d$, so that $(\sigma_a + \sigma_b)/2 \approx (\sigma_s + \sigma_d)/2$. In this event, the complex shift Δ_c for structure I will be about half of that for the chelate II. It is expected that the complex shift for structure II will be of the order of that found for the complexes of water and the alcohols with the same cations in acetonitrile solution. If 2:1 association (2 ions and 1 substrate) does not occur, then it should be possible to distinguish between species I and II in this way.

The association constant K should also give some indication of the nature of the complex. The equilibrium constant for species I could be larger than that for the corresponding alcohol complex by a maximum factor of 2, simply because the diol has twice as many nucleophilic centres. It is well known [84] that for a bidentate substrate, chelation is energetically favoured over the alternative monodentate donation. Thus, species II should be more stable than species I and chelation should give rise to much larger values of the equilibrium constant than those found

for the alcohols. A complex (III) involving two ions will probably be less stable than either of the others because of coulombic repulsion by the cations and because of competition for the negative charge in the polarisation

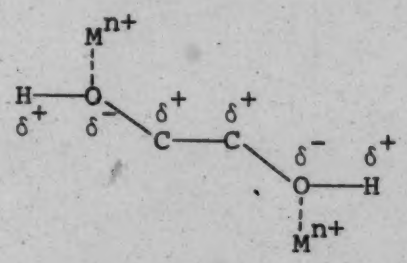

III.

of the substrate molecule. This would predict a lower degree of association than in species I.

The salt concentration dependence of the hydroxyl proton shielding of ethylene glycol and 2-methoxyethanol was analysed by the method outlined in section 3.1, assuming 1:1 association. The limiting shifts and equilibrium constants are listed in table 3.6.

The limiting shifts are in all cases slightly larger than those found for water, methanol and ethanol with these cations. The association constants, which were computed assuming 1:1 association, are larger than those found for water or any alcohol with a given cation. From this data and the prior discussion, it may be inferred that structure II is the one predominantly involved in the complex equilibrium.

TABLE 3.6

Limiting Hydroxyl Proton Shifts and Equilibrium Constants of the Cation Complexes of Bidentate Substrates

Ion	Substrate			
	1,2-ethanediol		2-methoxyethanol	
	Δ_c	K	Δ_c	K
Na^+	-0.84 ± .05	5.8 ± .5	-0.85 ± .05	5.5 ± .3
Ba^{++}	-1.63 ± .04	300 ± 100	-1.73 ± .03	300 ± 100
Ca^{++}	-2.26 ± .03	Large	-2.44 ± .03	Large

The salt dependent proton shifts in the α-CH_2 and CH_3O groups were analysed in the same way. The results are presented in table 3.7. The values of the equilibrium constants are the same, within experimental error, as those found from the hydroxyl proton spectra. For 2-methoxyethanol, both of the CH_2 and CH_3O proton shieldings are affected to the same extent upon addition of the salt. The shieldings of the protons in the CH_2 groups of 1,2-ethanediol are also affected to the same extent by the cations. This would not be expected if the oxygens donated to two different cations unless the equilibrium constants were fortuitously equal, which is an unlikely eventuality. Thus, all of the available data is indicative of the formation of a chelate complex of the type II.

Certain alicyclic compounds, such as cyclopropane and norbornane, have rigid frameworks and their *cis* and *trans* 1,2-diol derivatives should have strong and weak chelating ability respectively. Although not treated here, their cation complex equilibria could be studied in the same way.

3.5 Cation Complexes of Nitrogen Bases.

It is well known that the coordination chemistry of the alkali and alkaline earth metal ions is dominated by coordination to oxygenic compounds. These ions demonstrate little tendency to associate with nitrogen bases in the solid phase.[84] An attempt was made to determine if a cation complex of an amine could be formed to any great extent in acetonitrile solution.

TABLE 3.7

Limiting CH_2 and CH_3O Proton Shifts and Equilibrium Constants of the Cation Complexes of Bidentate Substrates

Ion		Substrate			
		1,2-ethanediol		2-methoxyethanol	
		Δ_c	K	Δ_c	K
Na^+	CH_2	-0.05 ± .01	5 ± 2	-0.06 ± .01	3 ± 2
	CH_3O			-0.06 ± .01	3 ± 2
Ba^{++}	CH_2	-0.14 ± .03	300 ± 100	-0.15 ± .02	300 ± 100
	CH_3O			-0.15 ± .02	300 ± 100
Ca^{++}	CH_2	-0.23 ± .03	Large	-0.22 ± .04	Large
	CH_3O			-0.22 ± .04	Large

Increasing amounts of magnesium perchlorate were added to 0.1 M acetonitrile solutions of diethylamine and the proton NMR spectra were recorded. The CH_2 and CH_3 signals (of diethylamine) moved progressively downfield as the salt concentration was increased. The single peak assigned to the N-H proton resonance appeared in only a few of the spectra of solutions containing the salt. Presumably the signal is (quadrupole and/or exchange) broadened to the extent that it disappears in most spectra. For this reason, its shielding dependence could not be analysed. However, it should still be possible to analyse the equilibrium by resorting to the ethyl group proton shieldings. The dependence of the CH_2 and CH_3 proton shieldings upon the $Mg(ClO_4)_2$ concentration is shown in figure 3.2. Upon analysis of these curves using equation (3.10), the substrate was found to be quite weakly complexed. The parameters K and Δ_c could only be found approximately because of the restricted saturation range. The equilibrium constant is about 1.5 and the complex shifts are about 0.25 ppm for the methyl protons and 0.75 for the methylene protons of diethylamine.

The complex shifts may be compared with those obtained for the ethyl group protons in the association of magnesium with ethanol, for which the equilibrium constant is two orders of magnitude greater. The limiting shifts found for ethanol are 0.13 ppm for the CH_3 and 0.23 for the CH_2. Thus, it appears that Mg(II) is able to induce greater shifts in

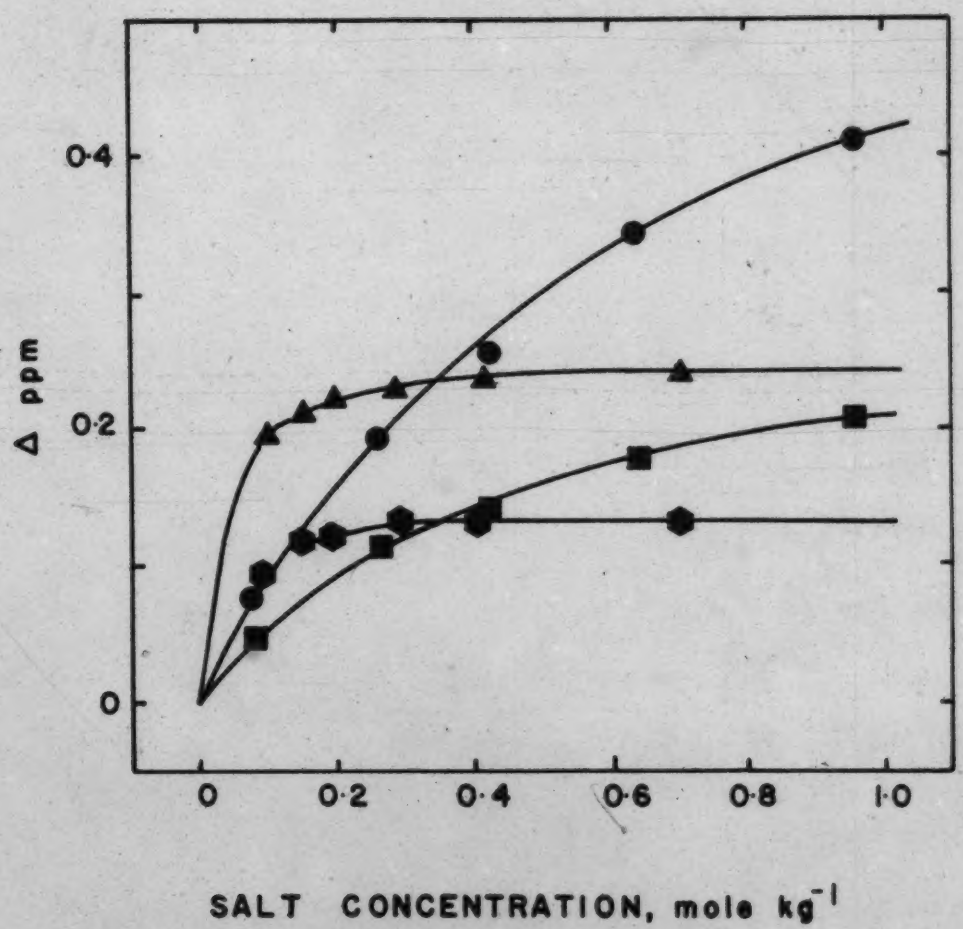

FIGURE 3.2. Dependence of the alkyl proton shieldings on $Mg(ClO_4)_2$ concentration for 0.1 M solutions of ethanol and diethylamine in acetonitrile at 35 . Diethylamine CH_2 (●), CH_3 (■). Ethanol CH_2 (▲), CH_3 (●).

the alkyl protons of an amine than in those of an alcohol, even though the association with the alcohol is much stronger than with the amine. Because the shift decreases with distance from the oxygen or nitrogen atom in the two substrates, it is reasonable to propose that association between the amine and the cation occurs through the nitrogen atom.

$$(CH_3CH_2)_2NH + Mg^{++} \rightleftharpoons (CH_3CH_2)_2\overset{Mg^{++}}{\underset{|}{N}}H$$

However, in the amine complex, the cation is forced to take up a position at the nitrogen lone pair and the structure of this complex may be different from that of the alcohol complex, for which a planar configuration is possible.

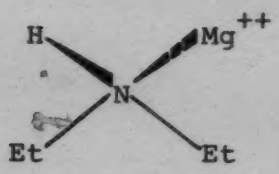

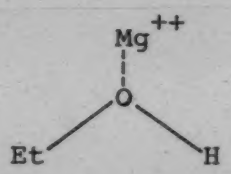

It is not possible to distinguish between the alternative structures for the alcohol complex from the available data. However, the large differences in the alkyl proton complex shifts for the amine and the alcohol complexes of Mg(II) may suggest a structural difference between them, possibly of the kind suggested.

CHAPTER 4

ELECTROSTATIC MODELS FOR THE 1:1 ION-MOLECULE ASSOCIATION

Experimental quantities are generally regarded as being "understood" or "accounted for" when they are successfully calculated on the basis of the elementary laws of physical science. When exact calculation is not possible, attempts are made to show qualitative consistency with theory or with other data which is "understood". For the 1:1 complex equilibria described and tabulated in chapter 3, both the equilibrium constants and complex shifts may be subjected to theoretical treatment.

The exact nature of the bonding in the 1:1 complex is unknown. Because the bonding is weak (ΔH of formation is about an order of magnitude less than a stable chemical bond) it is not unreasonable to proceed with the assumption of an entirely electrostatic interaction. Such a description has been used by others [71] to account for weak ion-molecule interactions. The possibility of a small covalent contribution is of course not ruled out.

4.1 The Equilibrium Constants.

The process involved in the formation of the 1:1 complex is one of selective solvation

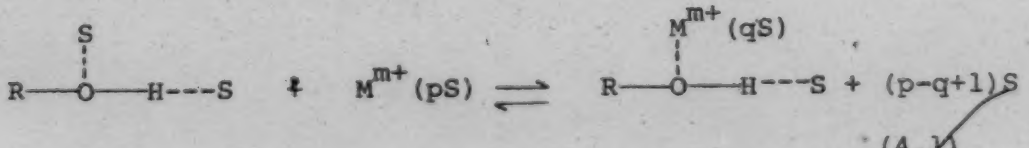

(4.1)

Where S represents a solvating acetonitrile molecule, and p and q are the solvation numbers of the cation in the free and complexed states respectively. The values of p and q are unknown and it must be assumed that the quantity p-q remains constant for all of the ion-molecule complexes studied. The desolvation free energy should then vary in the same way as the energy of the ion-substrate interaction and it may be ignored. The process depicted in equation (4.1) then becomes

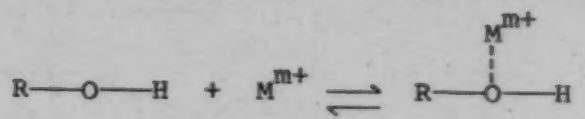

(4.2)

with the free energy change

$$\Delta G^\circ = -RT\ln K_{th} \qquad (4.3)$$

where K_{th} is the thermodynamic equilibrium constant, which was shown to be proportional to the equilibrium constant defined by equation (3.4) and tabulated for the cation complexes of water and the alcohols in table 3.2.

The Gibbs free energy has the contributions $\Delta G^\circ = \Delta H^\circ - T\Delta S^\circ$. The contribution to ΔS° arising from the choice of standard state is constant for both the gas phase and solution phase reactions. According to Searles and Kebarle [85], ΔS° for the complex reaction (depicted by equation (4.2)) in the gas phase may be estimated by standard statistical mechanical methods (Sackur-Tetrode equation). The calculated ΔS depends upon the calculated ion-molecule potential energy U, which is related to the enthalpy change $\Delta H^\bullet$. Thus, ΔS°

is expected to vary in the same way as ΔH° and, from equation (4.3) and the above arguments, ln K_{th} should be proportional to ΔH° and to U.

Green and Martin [71] have estimated the ion-molecule electrostatic potential energy U_e for hydrogen bonded complexes and their procedure is applied here. The electric field due to the ion monopole is regarded as interacting with the permanent and induced dipole moments of the substrate when the ion and the molecule are in Van der Waals contact. The Van der Waals attractive (dispersion) and repulsive forces are disregarded since they are expected to remain approximately constant, in which case the potential energy U_e is given by

$$U_e = -\sum_i \left(\mu_i E_i + \tfrac{1}{2} E_i \alpha_i E_i \right) \qquad (4.4)$$

where E_i is the electric field at the i^{th} bond, μ is the permanent bond dipole moment, and α is the bond polarisability tensor.

The permanent dipole is represented by point charges q, at the atoms, derived from a sum over bond moments. The induced dipole is located at the polarisability centroid of the bond. The potential energy then becomes

$$U_e = 69.13 Ze \sum_i q_i / r_i^2$$

$$-332.1\, Z^2 \sum_{i<j} n_{ij} \left(\alpha_{\perp ij} \sin^2\theta_{ij} + \alpha_{||} \cos^2\theta_{ij} \right) \Big/ 2r_{ij}^4 \qquad (4.5)$$

U_e is in kcal.mol^{-1} if distances are in cm^{-1}, dipole moments in Debyes, and the charges q and Ze are in atomic units (esu x 10^{-10}). $\alpha_{||}$ and $\alpha_{\perp}$ are the components of α along and perpendicular to the bond. $n_{ij} = 1$ when atoms i and j are bonded and zero otherwise. The radii r_{ij} and angles θ_{ij} are defined in figure 4.1. The calculations were made using standard values [86-88] of bond lengths, angles, moments, and polarisabilities, as listed in table 4.1.

Examination of energies calculated with the ion in contact with the envelope of the atomic Van der Walls surfaces showed, as one would expect, a minimum energy of association at the oxygen atom. The minimum was broad, so the energy is not critically dependent on the assumed geometry of the complex. The values presented are for a planar complex in which the cation is on the bisector of the oxygen bond angle.

For complexes of similar structure, one would expect the computed electrostatic potential energy to predict the gross trends in the enthalpy of association. If, as is usually found [89], the entropy changes and desolvation contributions are either constant or proportional to the enthalpy changes, then log(K) should be linear in U_e. Figure 4.2 shows that such a relationship does obtain. It appears that the dependence of the energies on the cation may be accounted for electrostatically.

TABLE 4.1

Quantities Used in the Calculation of the Ion-Molecule Electrostatic Potential Energy for Methanol Complexes of the Cations

Atom	Polarisability	Radius Å
H	4.33×10^{-25}	1.2
O	8.00×10^{-25}	1.4
CH_3	22.0×10^{-25}	2.0

Ion	Charge Ze	Radius Å
Li^+	+1	0.60
Na^+	+1	0.97
Mg^{++}	+2	0.65
Ca^{++}	+2	0.99
Sr^{++}	+2	1.13
Ba^{++}	+2	1.35

Bond	Dipole Moment	Polarisabilities	
		$\alpha_\perp$	$\alpha_{\|\|}$
O-H	-1.51	8.23	6.17
C-O	-2.16	8.40	4.78

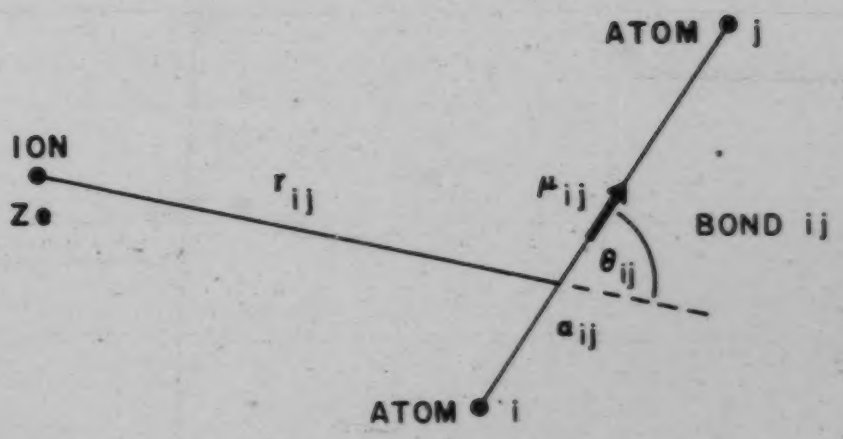

FIGURE 4.1. Interaction of the cation, charge Ze, with bond dipole μ_{ij} and polarisability α_{ij}.

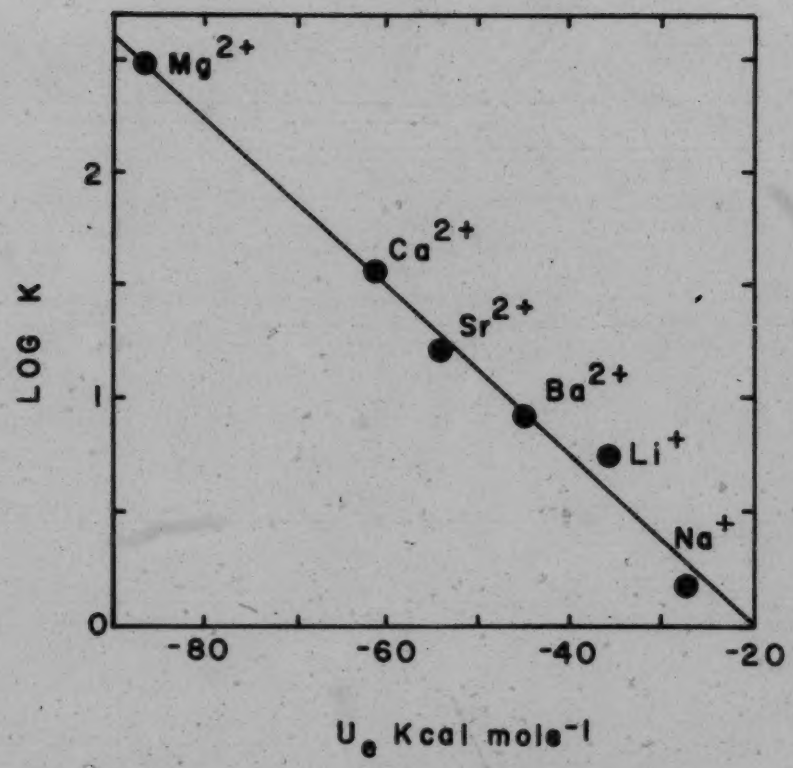

FIGURE 4.2. Relationship between the observed cation-molecule association constant and the calculated electrostatic potential energy.

4.2 The Complex Shieldings

Calculations of the nuclear shielding constant σ have in general been based upon models in which σ is divided into atomic contributions. According to Saika and Slichter [90]

$$\sigma = \sigma_d + \sigma_p + \sigma_o + \sigma_c \qquad (4.6)$$

where σ_d and σ_p are the diamagnetic and paramagnetic contributions, σ_o is the shielding induced by the magnetic moments of other atoms, and σ_c is the contribution from interatomic currents. σ_o is zero in a tumbling molecule if the other atoms have isotropic susceptibilities.

Buckingham [91] has shown that for a molecule in an external electric field E_z, the distortion of the electron cloud about a nucleus will affect σ_d and σ_p. σ_d will be diminished in the x, y and z directions with the greatest effect in the z direction. σ_p is unaffected in the z direction but will be reduced in the x and y directions. For electric field induced shifts in protons attached to carbon, Buckingham arrived at the equation

$$\Delta\sigma_e = 2 \times 10^{-12} E_z - 1 \times 10^{-18} E^2 \qquad (4.7)$$

where higher orders of E are neglected.

Subsequent work [92,93] has shown that an equation of this form may be applied more generally to protons attached

to any heavy atom. In this more general setting, the Buckingham-Musher equation

$$\Delta\sigma_e = A \times 10^{-12} E_z - B \times 10^{-18} E^2 \qquad (4.8)$$

has enjoyed considerable success. The coefficient B is usually assigned the hydrogen atom value [94] 0.738. Since the contribution of the quadratic term is usually small, the value assigned to B is not critical. The coefficient of the linear term A has been evaluated experimentally [81,93] and theoretically [91,92] for protons bonded to various first row atoms. It may be related to the polarisability of the X-H bond.[95]

Green and Martin [41,71] have applied equation (4.8) to shifts induced in proton shieldings by the electric field of the anion in 1:1 ion-molecule complexes. For interactions of the type X-H---Y^-, where Y^- is a halide anion, they obtained values of $A = 3$ when X is a carbon atom and $A = 5.5$ when X is an oxygen atom. It is consequently of interest to apply the Buckingham-Musher equation (4.8) to the 1:1 cation complexes of water and the alcohols.

In order to estimate the electric field due to the cation acting at the hydroxyl proton, it is necessary to assume a particular geometry for the complex. A planar complex was chosen for the calculation, as depicted in figure 4.3. The electric field at the proton is Ze/r^2, in

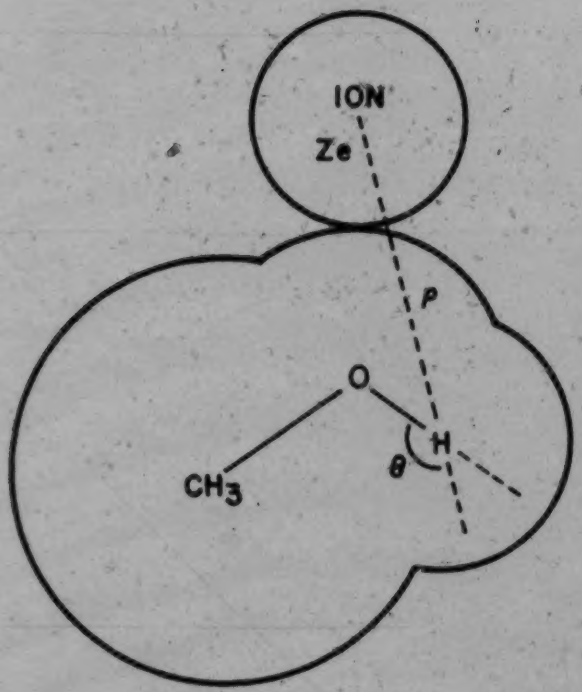

FIGURE 4.3. Planar cation-methanol complex.

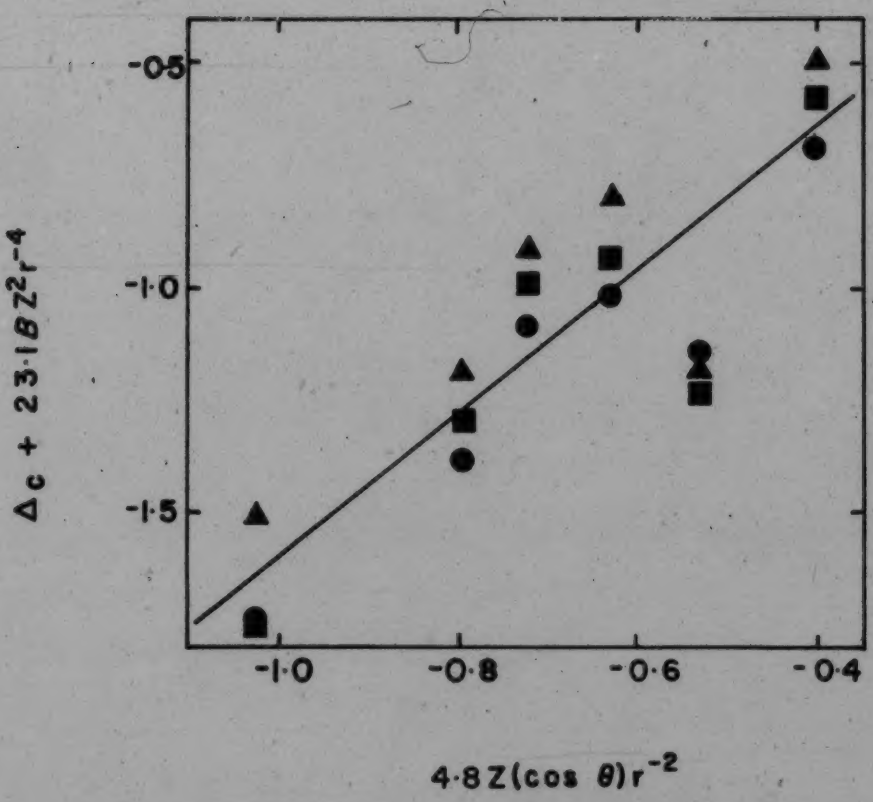

FIGURE 4.4. Derivation of the Buckingham-Musher A coefficient for cation complexes of water (●), methanol (■), and ethanol (▲).

which case the component in the z direction E_z will be $(Ze\cos\theta)/r^2$; Z is the ionic charge, and the radius r (in units of Å) and angle θ are defined in figure 4.3. The Buckingham-Musher equation then becomes

$$\Delta\sigma_e = 4.80AZr^2\cos\theta - 23.1BZ^2r^{-4} \qquad (4.9)$$

in which case $\Delta\sigma_e$ is in ppm.

Assuming van der Waals contact and a planar configuration, r and θ may be computed from the values listed in table 4.1. Equating $\Delta\sigma_e$ with Δ_c, equation (4.9) may be rearranged such that a plot of $y = \Delta_c + 23.1BZ^2r^{-4}$ vs. $x = 4.80Z\cos\theta$ would yield the *A* coefficient as the slope. A least-squares fit in this way was performed for all of the ions with water, methanol and ethanol, as shown in figure 4.4, and a value of $A = 1.6 \pm 0.3$ esu^{-1} was obtained.

It is of course important to estimate the extent to which the value of *A* depends upon the assumed geometry. The fit to equation (4.9) is dominated by the linear term and it turns out that the quantity $r^{-2}\cos\theta$ is quite insensitive to the position of the ion on the oxygen atom. Thus, the calculated value of *A* does not depend strongly upon the assumed geometry.

The observed differences between the complex shifts of the alkyl group protons in the complexes of magnesium(II) with ethanol and diethylamine are difficult to rationalise in terms of this model. The *A* coefficient appropriate to

this discussion is that of the C-H bond, and is usually taken to be 3.0 esu^{-1}. It is a property of the C-H bond and should be independent of the atom in the substrate to which the ion is attached since the Buckingham-Musher equation is concerned only with the through-space interaction between the ion and the alkyl proton in question. The small difference between the Van der Waals radii of O and N is insufficient to account for the large discrepancy found between the shifts for the amine and alcohol complexes (a factor of 3 for the CH_2 and 1.8 for the CH_3). Furthermore, the observation that the differences are not the same for the CH_2 and CH_3 protons implies, according to the model, that the average distances between the alkyl protons and the ion are not the same in the two complexes. This suggests a possible average conformational difference between the diethylamine and ethanol complexes. It is also possible that there exists an important through-bond contribution to the shift which is not allowed for by the Buckingham-Musher model. In view of the limited data, it does not seem profitable to pursue this point any further at the present time.

The A coefficient for the O-H bond of 1.6 esu^{-1}, deduced from the cation complexes of alchols, is substantially smaller than the value previously inferred from the shifts of anion-alcohol complexes.[41] This discrepancy is greatly in excess of experimental error and it cannot be resolved in

terms of the simple electrostatic model.

The counter-ion, perchlorate, may contribute to the field at the proton, but its effect is much less than that of the cation (see section 3.3.3).

The electrostatic model used takes no account of dielectric polarization of solvent and substrate. There is no obvious way to evaluate this effect. However, there appears to be no reason why it should differentiate strongly between cation and anion association.

The discrepancy between the two A values does not arise from saturation of the hydroxyl charge shift by large electric fields. The fields arising from the cations studied can be calculated; they span the range of the anions' electrostatic fields.

4.2.1. The Solvent-Substrate Interaction. It is of interest to evaluate the hydroxyl proton shift arising from solvating acetonitrile. The model of Berkeley and Hanna [96], and their value of the nitrile anisotropy, was used to calculate the shift arising from a collinear O-H---$NCCH_3$ complex in Van der Waals contact. The shift was calculated to be -0.2 ppm if A = 1.6, and -2.1 ppm if A = 5.5. The observed shielding of dilute monomeric methanol is about 2 ppm less in acetonitrile than in hydrocarbon solvents.[99] If the difference arises entirely from acetonitrile association with the hydroxyl proton, then it is more in accord with the

calculation using A = 5.5, as in the case of anion association.

At this point it appears that the most reasonable way to reconcile the two values of A is to postulate that the value 1.6 esu^{-1}, derived from cation association at a point remote from the hydrogen, is representative of purely electrostatic deshielding. The larger effects observed when an ion or molecule associates directly with the proton involve an additional mechanism, possibly a covalent contribution to the hydrogen bond.[98]

CHAPTER 5

TYPE I AND II SOLVATION SPECTRA

The lifetimes of the solvation shells of certain highly polarising cations (Be(II), Al(III) etc.) are so long, at low temperatures, that it is possible to observe separate NMR signals for molecules in the solvation shell and in the bulk solvent in solutions of these ions. Spectra of this kind were designated TYPE II in Chapter 1.

Aqueous electrolyte solutions have relatively high freezing points (0 to -20°C) and TYPE II spectra of water have been observed only for very concentrated solutions of the salts close to their freezing points.[99] Since the NMR shifts which characterise this experiment are defined in the limit of infinite dilution of the salt (see equations (1.10) and (1.11)), the spectra of the concentrated solutions are of limited utility. They have been used primarily to evaluate the cation solvation number.

The lower primary alcohols have freezing points considerably lower than that of water and solutions of electrolytes in alcohols have been studied by NMR down to *ca* -100°C. At the lower temperatures the rate of exchange of the bulk and bound solvent molecules is slow (on the NMR time-scale) and several TYPE II spectra of alcoholic solutions have been reported.

Of the six cations whose 1:1 complex equilibria with

hydroxylic substrates (TYPE III experiments) were discussed in Chapter 3 and 4, TYPE II spectra have been observed only for solutions of magnesium perchlorate in methanol and in ethanol. For these systems, the cation solvation numbers and bulk-bound solvent exchange kinetics have been reported.[36,37] In addition, the dependence on the salt concentration of the hydroxyl proton shielding of molecules in the solvation shell of Mg(II) has been reported for methanolic solutions of magnesium perchlorate.[59] This data allows the evaluation of the infinite dilution solvation shell shift for Mg(II) in methanol, as shown in section 5.1. A similar experiment was performed in the present work for solutions of magnesium perchlorate in ethanol and the results are presented in section 5.2. The infinite dilution solvation shell shifts derived in this Chapter for Mg(II) in methanol is required in the correlation of the TYPE I, II and III experiments which is given in Chapter 6 of this thesis.

5.1 TYPE II Spectra of Mg(II) in Methanol.

Butler and Symons [59] have recorded the proton NMR spectra of methanol containing different amounts of magnesium perchlorate, at -69°C. Separate hydroxyl proton resonances were observed for the solvation shell and bulk solvent molecules and the shielding of each species was found to vary linearly with the salt concentration. The coordinated

solvent NMR shifts and salt concentrations* given in table 1 of reference 59 were plotted and are shown in figure 5.1. Extrapolation of the least-squares straight line through the points to zero salt concentration yields the solvation shell shift Δ_s = -1.69 ppm at infinite dilution.

The average shielding σ_r of the residual solvent appears to be linear in total perchlorate ion concentration and the perchlorate ion molal shift was taken to be $(d\sigma_r/dm)_{m\to 0}$. This was justified by Butler and Symons on the basis that when the cation molal shifts derived from the perchlorate value are plotted against ionic surface potential, a continuous curve is obtained. If some other value for the perchlorate shift is used to derive the cation shifts, a discontinuity occurs between the divalent and monovalent cations. Continuous curves were also obtained from correlations of the derived anion shifts with the pK_a's and NMR shifts of the anion conjugate acids. Individual ion molal shifts derived in this way are expected to closely resemble the absolute values of the molal shifts. Similar correlations have since been made for the molal shifts of water [55] and it appears that absolute scales of individual ion shifts are

---

* Only four high concentration values were given in table 1 of reference 59. Butler and Symons stated that lower concentrations were studied and that the shift is linear in salt concentration from less than 0.1 m up to 1.2 m.

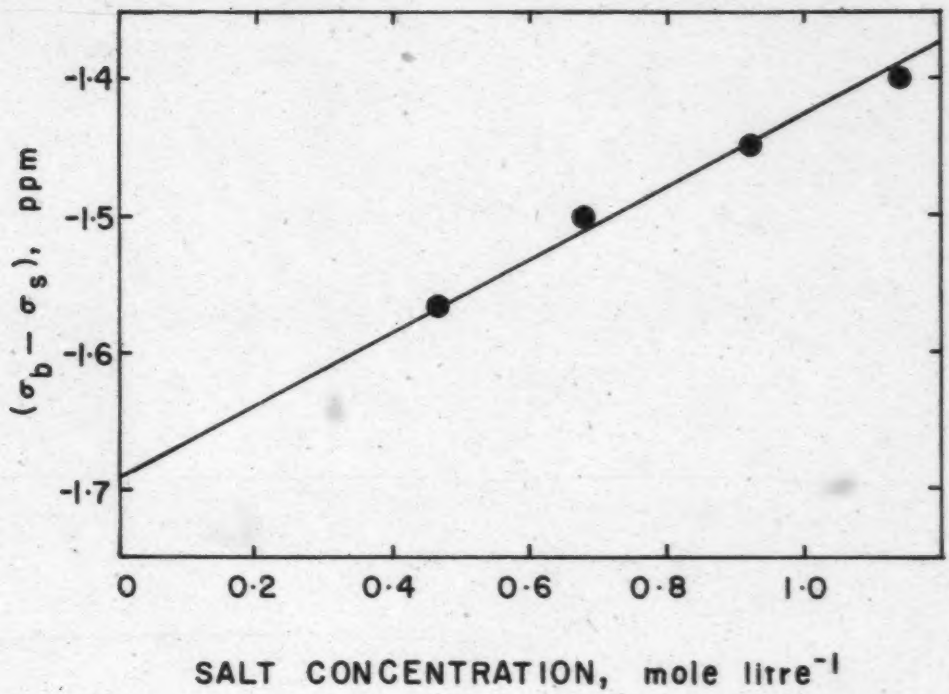

FIGURE 5.1. Deduction of Δ_s for Mg(II) in methanol at -69°.

now available for both solvents.

5.2 TYPE II Spectra of Mg(II) in Ethanol.

Alger [37] has studied the kinetics of the exchange of ethanol coordinated to magnesium(II) with the residual solvent in a 0.25 M solution of magnesium perchlorate in ethanol, using ^{1}H NMR. He has shown that the limit of slow exchange is reached at lower temperatures for this system than for Mg(II) in methanol. Since the concentration dependence of the solvation shell hydroxyl proton shielding is required to evaluate Δ_s, the infinite dilution shift, it is first necessary to establish the temperature regions of slow exchange for the entire concentration range to be studied (a partially coalesced spectrum would not yield the correct value of Δ_s).

The hydroxyl proton shieldings were monitored as a function of temperature for two solutions of magnesium perchlorate (0.22 and 0.81 m) in ethanol*, over the range -93° to +20°. These solutions are representative of the concentration range (0 - 1 m) to be studied. Figure 5.2 shows the plots of the separation (σ_b-σ_r), between the bulk

---

* It is usual to add a trace quantity (*ca* 0.001 M) of perchloric acid to the solvent in order to minimise the base catalysed exchange of the solvation shell hydroxyl protons.[36] This was done for all of the solutions whose spectra are reported in this section.

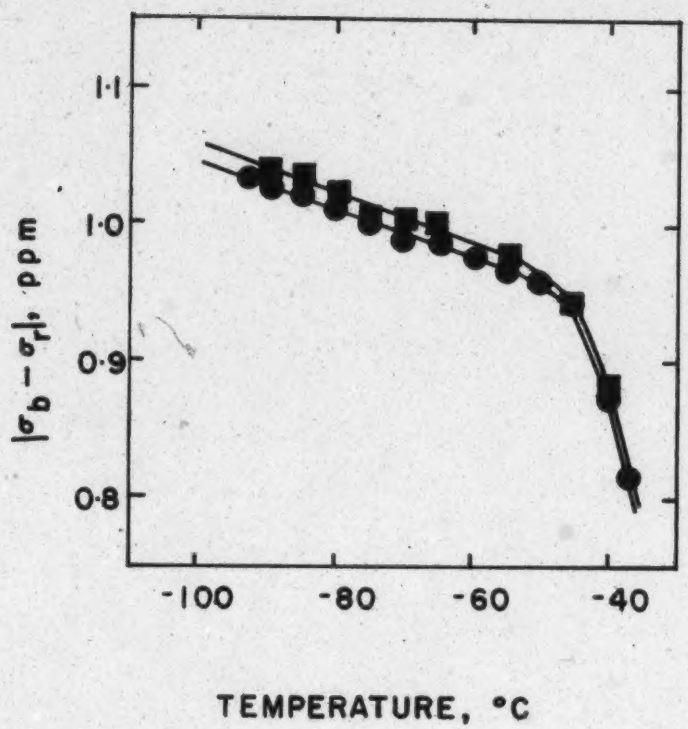

FIGURE 5.2. Effect of temperature on the separation of the bulk and bound solvent hydroxyl proton signals for 0.22 m (●) and 0.81 m (■) magnesium perchlorate in ethanol.

and bound solvent hydroxyl proton shieldings, vs. temperature for the two solutions. The two curves are essentially superimposed and they demonstrate the same coalescence behaviour above *ca* -45° Thus it can reasonably be assumed that "slow exchange" is manifest below -45° for the entire concentration range to be studied. The carbon-13 NMR spectra of this system are presented and discussed in Chapter 7 of this thesis. The coalescence of the bulk and bound solvent signals occurs in the carbon-13 spectrum at about the same temperature as in the proton spectrum. This confirms that the coalescence is due to exchange of the whole molecule and not just to the exchange of the hydroxyl proton.

The dependence of the solvation shell and residual solvent hydroxyl proton shieldings on the salt concentration was determined for solutions of magnesium perchlorate in ethanol. The relative intensities of the two signals were used to deduce the cation solvation number of 6 $\pm$ .5 which remained constant within experimental error over the whole concentration range studied. There was no evidence of contact ion-pairing, which would be manifest in a reduced solvation number at high salt concentrations.[61] The value of the solvation number obtained is consistent with that determined by Alger [37] at a single salt concentration.

The variation of the solvation shell hydroxyl proton shielding with the total perchlorate ion concentration at -70° is shown in figure 5.3. The plot is linear over the

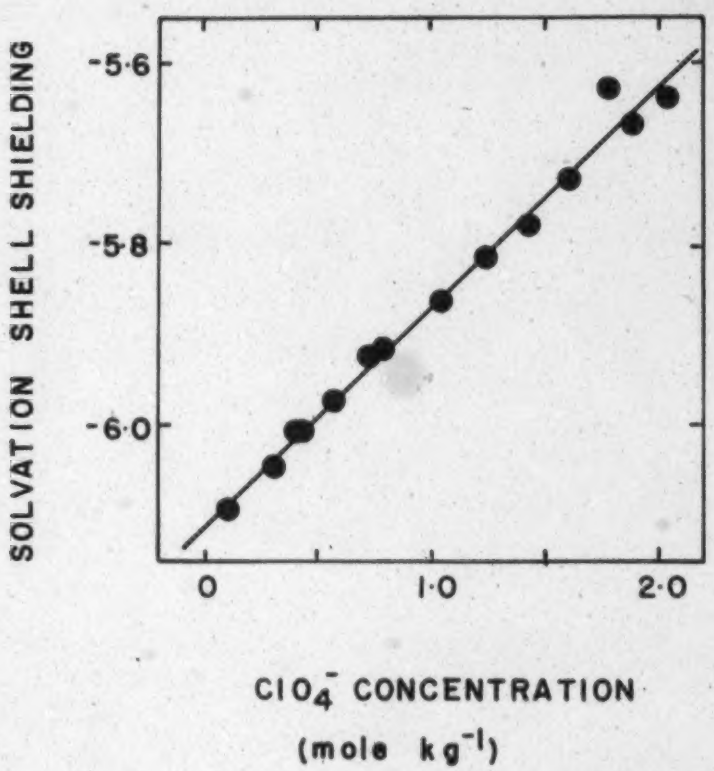

FIGURE 5.3. The dependence of the hydroxyl proton shielding, of ethanol coordinated to Mg(II), on the salt concentration for ethanolic $Mg(ClO_4)_2$ at -70°.

range studied with a slope of +0.05 ppm kg mole^{-1}. The upfield shift with increasing concentration is attributed to the interaction of the solvation shell molecules with the perchlorate ions. This proposal is supported by the observation that if perchlorate is added in another form (in this case as the sodium or calcium salts, whose cation solvation shells are labile) to a magnesium perchlorate solution, the magnesium solvation shell shielding remains linear in *total* perchlorate ion concentration with the same slope as the line in figure 5.3, to within experimental error.

The infinite dilution solvation shell shift was evaluated by extrapolation of the line in figure 5.3 to zero salt concentration and subtracting the shielding from that of pure ethanol at -70°. The value of Δ_s deduced in this way is -1.06 ppm. It is used in Chapter 6 to estimate the molal shift of Mg(II) in ethanol at -70°.

The shielding of the bulk solvent follows the same upfield trend with increasing salt concentration as that of the solvation shell, as shown in figure 5.4, but it is not linear in perchlorate ion molality. In this respect, it differs from the linear correspondence found by others for magnesium perchlorate in methanol.[59] In the absence of solvent separated ion-pairing, the perchlorate ion is expected to sample the available solvent molecules equally, inducing the same shifts in both the solvation shell and residual solvent hydroxyl protons.[100] The broken line super-

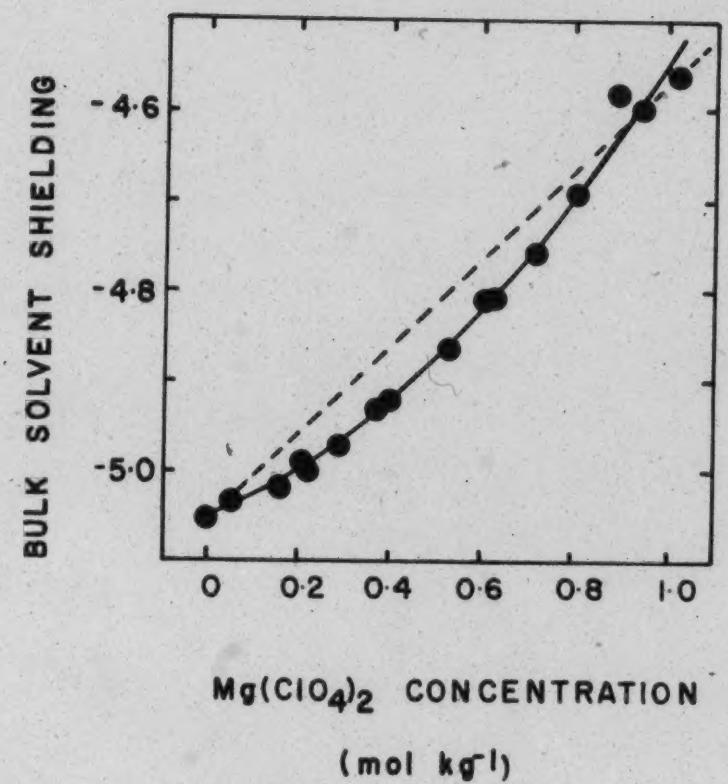

FIGURE 5.4. The dependence of the hydroxyl proton shielding of the residual bulk solvent on the salt concentration for ethanolic $Mg(ClO_4)_2$ at -70°. The broken line has the same slope as the line in figure 5.3.

imposed on the curve in figure 5.4 has the same slope as the line in figure 5.3, and points at intermediate concentrations differ from the broken line by up to 25% of the residual solvent shifts at those concentrations. The discrepancy is quite significant but the reason for it is presently unknown. Solvent separated ion-pairing, of the form

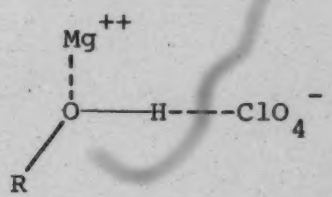

would be expected to induce a non-linear response in the solvation shell hydroxyl proton shielding, as was found for solutions of magnesium acetate in methanol.[100] It also seems unlikely that the direct effect of the cation will extend beyond the first coordination sphere. In view of this, the deviation from linearity is left unexplained. It may indicate additional processes occurring in ethanol solutions that do not occur in methanol.

5.3 The Molal Shift of Barium(II) in Methanol.

Molal shifts in methanol have been published for all of the cations whose 1:1 complex equilibria were studied in Chapter 3, with the exception of barium. Consequently, the molal shift of Ba(II) in methanol was determined, using the method of Butler and Symons.[50] The time-averaged

hydroxyl proton shift, *vs.* the methyl peak, was measured as a function of salt concentration over the range 0.03 to 1 M. The molal shift of $Ba(ClO_4)_2$ in methanol at -69°, evaluated as the slope at zero concentration (see equation (1.8)), was determined to be $+0.28 \pm 0.02$ ppm kg. $mole^{-1}$. The molal shift of perchlorate ion in methanol was estimated by Butler and Symons [59] to be +0.125 ppm kg. $mole^{-1}$. Thus, taking $\Delta_m(Ba(ClO_4)_2) = \Delta_m(Ba^{++}) + 2\Delta_m(ClO_4^-)$, $\Delta_m(Ba^{++}) = 0.28 - 2(0.125) = +0.03$ ppm kg. $mole^{-1}$.

CHAPTER 6

CORRELATION OF THE NMR SOLVATION EXPERIMENTS

Earlier reports [49,50,58,60] of NMR solvation studies have acknowledged that ionic molal shifts in methanol and water contain contributions arising from several solvation phenomena. It appears that at least three processes must be considered, as described below.

(i) The ion is expected to polarise the molecules in its primary solvation shell and induce a shift Δ_p in the hydroxyl proton resonance of these molecules. Cations associate with the negative (oxygen) end of the hydroxyl group and anions associate with the positive (hydrogen) end. In both cases, the ionic field should induce a shift of electrons away from the hydroxyl proton and this process is generally assumed to result in deshielding. In this and previous work [41], it is confirmed that this is the case for all cations and anions studied.

(ii) The formation of a hydrogen bond has been shown empirically to cause deshielding of the proton in the hydrogen atom donor in all known cases.[35,101] The disruption of hydrogen bonding, which occurs when molecules are removed from the bulk solvent into the primary solvation shell of an ion, should lead to increased hydroxyl proton shielding in both the solvation shell and residual solvent molecules. The average shift resulting from this process is designated

by the symbol Δ_h.

(iii) Secondary effects, due to structural solvation, may occur in molecules outside the primary solvation shell. While it is unlikely that the direct effect of the ion will extend beyond the first coordination shell, there is considerable evidence (see Chapter 1) that the structure of water is altered in the neighbourhood of the ions.

6.1 A Solvation Model.

The processes (i), (ii) and (iii) discussed above may be incorporated in an extremely simple model for ion solvation. Cations are discussed first because they appear to have well defined solvation shells.[28] Attention is focussed on a "reference" solvent molecule in its average state of hydrogen bonding, as shown on the left hand side of equation (6.1).

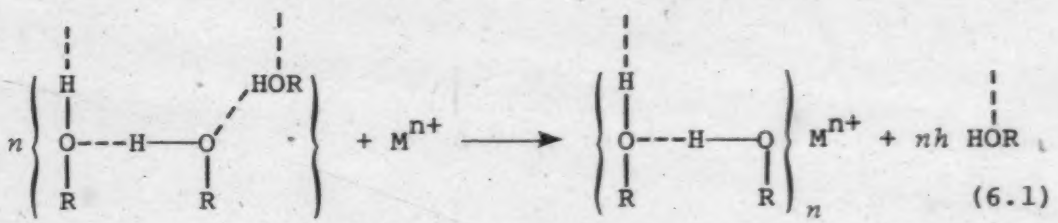

(6.1)

where n is the primary solvation number and h is the number of moles of hydrogen bonds per mole of pure solvent.

The NMR shift resulting from the direct ion-molecule interaction (i) was designated Δ_p. In Chapter 3, it was shown that Δ_c, the 1:1 cation complex shift measured in

acetonitrile, represents the direct effect of the ion on the substrate in the absence of solvent effects. If the molecules in the cation's solvation shell do not affect each other's shielding, Δ_p should be adequately measured as the 1:1 complex shift Δ_c.

Equation (6.1) suggests that, if there are h moles of hydrogen bonds per mole of solvent, then h hydrogen bonds will be broken per molecule removed from the bulk solvent into the cation's solvation shell. The average NMR shift resulting from this process (ii) was designated Δ_h. It is expected to be of the order of the liquid to gas shift for the pure solvent.

The effects of structural solvation (iii) may be interpreted in terms of the proportion of hydrogen bonds in the residual solvent of the electrolyte solution. Structure-making and structure breaking may mean more and fewer hydrogen bonds, and lead to decreased and increased shielding respectively. Consequently, structural solvation may modify the value of Δ_h, the hydrogen bond shift, which is expected to be of the order of the liquid to gas shift in the absence of structural solvation. Thus, the experimental value of Δ_h is expected to characterise structural solvation by the extent of its deviation from the liquid to gas shift.

If a solvent, of $b = 1000/M$ mole $kg.^{-1}$, contains cations of molality m mole $kg.^{-1}$ and solvation number n, its concentration average shielding σ will thus be

$$\sigma = \sigma_p + (nm/b)(\Delta_c + \Delta_h) \qquad (6.2)$$

where σ_p is the shielding in the pure solvent. Using equations (1.8) and (6.3), the molal shift is predicted to be

$$\Delta_m = (n/b)(\Delta_c + \Delta_h) \qquad (6.3)$$

In the absence of secondary effects Δ_h, as well as b, should be characteristic of the solvent alone. Δ_c and n are characteristic of the ion in that solvent. The solvation number n appearing here is the time-average statistical excess of nearest-neighbour molecules which are polarised in the same average orientation as that of the 1:1 complex in acetonitrile. If the ion's field is sufficient to completely orient the inner shell, then n should be determined primarily by close-packing requirements. For ions with radii of about 1 Å in methanol and water, the number of nearest neighbour solvent molecules is of the order of six. An incompletely oriented inner shell would shown an effective solvation number n somewhat less than the number of nearest-neighbour molecules.

6.2 Solvation of Small Cations in Water.

Davies et al.[55] have reported scales of individual ion molal shifts for water at three temperatures, and they have presented evidence that their values are good estimates of the absolute values of the shifts. In Chapter 3 of this

thesis, the 1:1 complex shifts Δ_c of the water complexes of six cations were derived (see table 3.3). If it is assumed that the solvation numbers of these cations in water are equal, then equation (6.3) becomes linear in Δ_m and Δ_c, with intercept Δ_h and slope n/b. Figure 6.1 shows that the complex shifts Δ_c and molal shifts Δ_m are linearly related. A least-squares fit to equation (6.3) yields an average solvation number $n = 5.1 \pm 0.2$, and $\Delta_h = 1.38 \pm .11$ in water at 25°. The standard deviation of fit is 0.007 ppm kg. mole^{-1}. The average hydration number is reasonably close to the value of 6, commonly observed for these ions.[28,102] The model represented by equation (6.3) fits the observed data to well within the probable error of the measured values. The standard deviation is comparable to that observed in similar correlations, for example, that with ionic radii.[55,60] Note that the molal shifts change sign at a point where Δ_c is comparable in magnitude to Δ_h.

The model suggests that the temperature dependence of the molal shifts arises primarily in Δ_h. If the cation shifts [55] in water at 0°, 25° and 40° are analysed according to equation (6.3), there is no significant temperature dependence of the average solvation number. Δ_h changes monotonously with temperature, thus: $1.60 \pm .32$ at 0°, $1.38 \pm .11$ at 25°, and $1.32 \pm .19$ at 40°. The decrease in Δ_h with temperature is expected, if Δ_h is related to the proportion of hydrogen bonding in the liquid.[2]

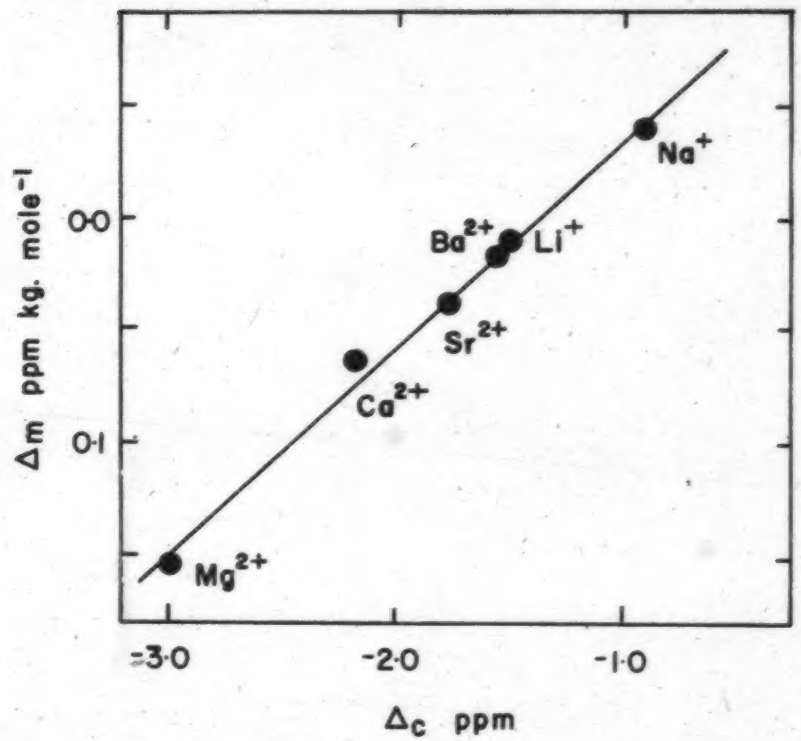

FIGURE 6.1. Correlation of the molal shifts Δ_m and the 1:1 complex shifts Δ_c for water at 25°.

The liquid to gas shift for water at 25° is about +5 ppm.[28] The value of Δ_h = +1.38 ppm is significantly less than the liquid to gas shift, suggesting that the residual solvent in solutions of these ions contains more hydrogen bonds per mole than does pure water at the same temperature. Thus the small value of Δ_h for cations could be interpreted as evidence that these ions are structure-making outside the primary solvation shell, if there is a direct relationship between the proportion of hydrogen bonding and structure.

6.3 Solvation of Small Cations in Methanol.

Butler and Symons [60] have proposed a scale of absolute ionic molal shifts in methanol at -69°. The 1:1 complex shifts of the methanol complexes of six cations are given in table 3.3. If the solvation numbers of these cations in methanol are assumed to be equal, then equation (6.3) may be analysed to yield values of n and Δ_h. Figure 6.2 shows that Δ_m and Δ_c are linearly related. A least-squares fit to equation (6.3) yields average solvation number n = 6.9 $\pm$ .7 and Δ_h = 1.5 ppm. The standard deviation of fit is 0.4 ppm kg. mole^{-1}.

The liquid to gas shift for methanol at -69° is also about +5 ppm, and the small value of Δ_h may again be interpreted in terms of structure-making by these ions in methanol at -69°. This contradicts the findings of Krishnan and

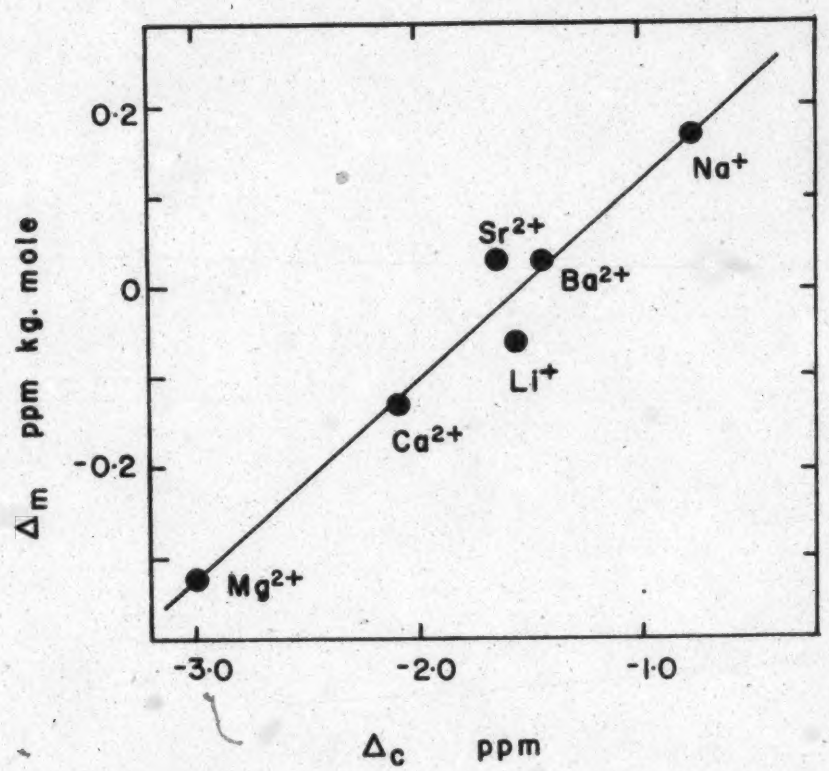

FIGURE 6.2. Correlation of the molal shifts Δ_m and the 1:1 complex shifts Δ_c for methanol at -69°.

Friedman.[33] They have proposed, on the basis of the entropy of solvation of potassium chloride at 25°, that structural solvation is a unique property of water. Note that the entropies of solvation of ions in methanol at -69° would be extremely useful values to have, but they have not yet been measured.

It is apparent that when both solvents are at 25° above their freezing points, all measured characteristics of the solvation process are approximately equal. It is for this reason that the observed molal shifts for these solvents are in the ratio of the solvent molecular weights, a fact which appears to have been overlooked until now.

At -69°, at infinite dilution in methanol, the hydroxyl proton in the solvation shell of Mg(II) appears at -1.69 ppm (see TYPE II spectra, Chapter 5) relative to that in pure methanol. From this value, Butler and Symons [59] calculated the Mg(II) molal shift using the relationship

$$\Delta_m = n/b(\Delta_s) \qquad (6.4)$$

Their value of Δ_m = -0.30 ppm was calculated using their determination of the magnesium solvation number: 5.5 $\pm$ 0.5. Several recent determinations indicate that the solvation number is 6, in which case the molal shift is recalculated to be Δ_m = -0.324 ppm kg. mole^{-1}. This is the value used in figure 6.2.

It is important to notice that equation (6.4) is not in accordance with the solvation model represented by equation (6.1), and yet there is considerable evidence [59,60] that the molal shift of Mg(II) calculated from equation (6.4) is the correct value. The fact that the point for Mg(II) in figure 6.2 falls on the same straight line as the points for the other ions also indicates that the Mg(II) molal shift is correct. The solvation shell shift Δ_s has, according to the model, two components: the polarisation shift Δ_p (measured as Δ_c) and Δ_h^o, the shift in the solvation shell resonance due to the breaking of the hydrogen bond to the *oxygen atom* of the molecule entering the ion's solvation shell.

$$\Delta_s = \Delta_c + \Delta_h^o \qquad (6.5)$$

The Δ_h included in equation (6.3) contains Δ_h^o, and an additional contribution Δ_h^p

$$\Delta_h = \Delta_h^o + \Delta_h^p \qquad (6.6)$$

Δ_h^p is the shift due to breaking the hydrogen bond to the hydroxyl *proton* of a molecule displaced by the cation on formation of the primary solvation shell (the "displaced" molecules are those appearing on the extreme right of equation (6.1)).

A value of Δ_h = +1.30 ppm was deduced by substituting

the experimental value of Δ_s = -1.69 ppm and Δ_c = -2.99 ppm into equation (6.5). It appears that the values of Δ_h = +1.5 ppm and Δ_h^o = +1.3 ppm are very similar, and they can be regarded as being indistinguishable within experimental error. The implications of this observation are quite profound.

It was mentioned above that the value of Δ_h is expected to be of the order of the liquid to gas shift, *ca* 5 ppm for methanol at -69°.* From this value, and the value of Δ_h^o = +1.3 ppm, equation (6.6) predicts $\Delta_h^p \approx +3.7$ ppm. This relatively huge shift of almost 4 ppm apparently does not contribute to the values of the molal shifts of the ions studied, because the value of Δ_h derived from the molal shifts is 1.5 ppm rather than 5 ppm. The simplest way to reconcile the discrepancy of *ca* 3.7 ppm is to postulate that the "displaced" molecules become hydrogen bonded back into the residual bulk solvent in such a way that the net shielding of the residual solvent remains close to that of pure methanol. It is necessary to explore the consequences of this "self-healing" of the solvent structure before the shift discrepancy is accounted for.

The change of state occurring in the postulated self-

---

*This value of the liquid to gas shift was estimated by subtracting the shielding of monomeric methanol in cyclohexane [103] at +25° from that of bulk methanol [104] at -69°.

healing process is

$$R\text{-}O\text{-}H_a \longrightarrow R\text{-}O\text{-}H_a\text{-----}\underset{\displaystyle R}{\overset{\displaystyle |}{O}}\text{-}H_b\text{-----} \qquad (6.7)$$

where the broken lines represent hydrogen bonds to other molecules, as before. The shift in the protons (H_a) of the "displaced" molecules in the self-healing process should be $-\Delta_h^p = -3.7$ ppm. The shift in the protons (H_b) of the other molecules involved in this process should be $-\Delta_h^o = -1.3$ ppm. It is conceivable that the self-healing is not complete and that the net shift of the residual solvent in the process represented by equation (6.7) is fortuitously *ca* -3.7 ppm, to cancel the discrepancy of *ca* +3.7 ppm. For this to occur, approximately 85% self-healing is required. It should be noted that the above arguments neglect changes in the shieldings of molecules further down a hydrogen-bonded chain of solvent molecules. Such changes should be of the order of the experimental error and they are assumed to be insignificant.

The postulated self-healing of the solvent structure would result in the residual solvent of the electrolyte solution containing more hydrogen bonds per mole than in the pure solvent. Thus, the residual solvent would be more highly structured than the pure solvent and the cations may be regarded as structure-makers, even though they do not contribute to the self-healing process directly. This is a novel way of visualising structure-making, since previous descrip-

tions [50,31] of the phenomenon have located the structure enhancement in a narrow sphere just outside the primary solvation shell of the cation, implying that the solvated cation directly affects the structure of the solvent in this region. All of these arguments are quite speculative since there is no way of unambiguously distinguishing between the two pictures of the structure-enhanced solvent. The experiments are incapable of giving a picture of what the solvent *must* be like; they suggest only what the solvent *might* be like.

The correlation of the molal and complex shifts for water and methanol by least-squares fit to equation (6.3) assumes that the solvation number n is constant for all ions. An alternative procedure would be to adopt commonly accepted solvation numbers [28,102] for the ions and use equation (6.3), the 1:1 complex shift Δ_c, and the value of n and Δ_h deduced from the TYPE II magnesium(II) solvation experiment, to calculate the molal shift for each ion. The computed values of the molal shifts for methanol are listed in table 6.1, along with the quantities used in the calculations. The molal shifts deduced from the least-squares values of n and Δ_h are also listed for comparison. It appears that the molal shifts derived using commonly accepted solvation numbers are well represented by equation (6.3), to within the probable error of the measured values. Note that a solvation number of 4 for sodium and lithium does not improve

TABLE 6.1

Prediction of Cation Molal Shifts in Methanol at -69°

Ion	Δ_c ppm	n	Δ_m, ppm. kg. mole^{-1} obs.	calc.[a]	calc.[b]
Na^+	-0.78	4	+0.17[c]	+0.07	-
	-0.78	6	+0.17[c]	+0.10	+0.17
Li^+	-1.57	4	-0.06[c]	-0.04	-0.01
	-1.57	6	-0.06[c]	-0.05	-
Ba^{++}	-1.45	6	+0.03[d]	-0.03	+0.02
Sr^{++}	-1.65	6	+0.03[e]	-0.07	-0.02
Ca^{++}	-2.09	6	-0.13[e]	-0.15	-0.12
Mg^{++}	-2.99	6	-0.32[f]	-0.32	-0.32

[a] Calculated using Δ_h = 1.30 ppm, and n shown in column 3.

[b] Calculated using least squares values: Δ_h = 1.54 ppm, n = 6.9.

[c] Ref. 60

[d] Calculated from our molal shift of $Ba(ClO_4)_2$, using perchlorate molal shift -0.125 (Ref. 69).

[e] Estimated from Fig. 1 of Ref. 105.

[f] Recalculated from data of Ref. 59 using a solvation number of 6.

the agreement with observation. A solvation number of about 6 for all of these ions is consistent with the data, but it should be realised that the results are insensitive to n when the molal shifts are close to zero.

6.4 Solvation of Large Monovalent Cations.

The molal shifts of the six small cations in water and methanol may be interpreted in terms of a primary solvation shell of about 6 completely oriented molecules. This is not surprising since these ions, which have high surface potentials, should be strongly solvated. In fact, it is for this reason that their 1:1 complex shifts could be determined. Only the perchlorate salts of small or multivalent cations are soluble in acetonitrile; $KClO_4$, $RbClO_4$ and $CsClO_4$ are insoluble, and their cation complex shifts are not accessible to direct measurement.

Since cation complex shifts may be adequately calculated by the Buckingham-Musher electrostatic model, it is of interest to use the ionic radii to predict the complex shifts by equation (4.8), use equation (6.3) to predict molal shifts, and compare the results with experimental values. This has been done for four cations in methanol at -69° and water at 25°, using the least-squares values of n and Δ_h derived above. The predicted and observed values are given in table 6.2.

The molal shifts of zinc and potassium are well repre-

TABLE 6.2

Prediction of Cation Complex Shifts and Molal Shifts

Ion	Radius Å	Complex Shift ppm	Molal shifts, ppm. kg. mole^{-1} Methanol, -69° calc.	obs.[a]	Water, +25° calc.	obs.[b]
Zn^{++}	0.74	-2.63	-0.24	-0.32	-0.115	-
K^{+}	1.33	-0.64	+0.20	+0.15	+0.068	+0.050
Rb^{+}	1.48	-0.57	+0.22	+0.17	+0.074	+0.037
Cs^{+}	1.69	-0.50	+0.23	+0.14	+0.081	+0.025

[a] Ref. 60.

[b] Ref. 55.

sented, considering that the predicted values arise from the application of two semi-empirical models involving only the ionic radius. On the other hand, the trend to less positive molal shifts with increasing radius in the series K^+, Rb^+, Cs^+ (a reversal of the normal sequence) is not predicted by the model. The model unambiguously predicts an increasingly positive Δ_m as $|\Delta_c|$ decreases in the order $K^+ > Rb^+ > Cs^+$. All determinations of molal shifts clearly show an inversion of the normal sequence, beginning at K^+ or Rb^+.

Other properties, such as entropy, also show anomalies in the case of large cations.[30] These have been explained in terms of exceptionally great structure breaking in the secondary solvation region beyond the primary solvation shell. It appears that this explanation is inadequate to account for the molal shifts. If the very large cations, Rb^+ and Cs^+, differed from the smaller ones only by the presence of exceptionally great structure breaking, one would expect a positive contribution to Δ_h, reflecting decreased hydrogen bonding in the bulk solvent. This would produce an anomalously *large* positive molal shift, rather than the observed anomalously *small* one.

As an explanation of the anomalously small molal shifts for the large cations, a phenomenon is proposed which has been discussed by Hindman [50] and Butler and Symons [60], and was first suggested by Bernal and Fowler.[14] If the ion-molecule interaction energy exceeds a certain value, of the

order of the solvent intermolecular energy, then solvation shell molecules will be completely oriented during their residence time, as shown in figure 6.3a. The solvation number will be the number of nearest-neighbour molecules, and Δ_c will have the value appropriate to the minimum energy complex. These assumptions are implicit in the model and appear to be valid for small cations.

Bernal and Fowler suggested that when the ion-molecule interaction energy falls below a critical value, which they estimated to occur at ionic radius *ca* 1.5 Å (that of rubidium), the ion cannot maintain order in its primary solvation shell. This situation is illustrated in figure 6.3b. The nearest-neighbour molecules differ from those in the bulk solvent by a statistical bias in favour of the oriented arrangement, oxygen towards the ion. The onset of a disordered primary solvation shell will be manifest in all of the parameters of equation (6.3), but it is most simply envisioned in terms of a decrease in the effective solvation number, n. This will result in a decrease in the magnitude of the molal shift, as the primary solvation shell becomes less ordered, in the series $K^+ > Rb^+ > Cs^+$, as observed.

Using the least-squares values of Δ_h, the observed molal shifts and the calculated complex shifts, equation (6.3) can be solved to yield the effective solvation numbers of K^+, Rb^+ and Cs^+ in methanol: 5.4, 5.7 and 4.4, and in water 3.8, 2.6 and 1.6, respectively. These values clearly show the

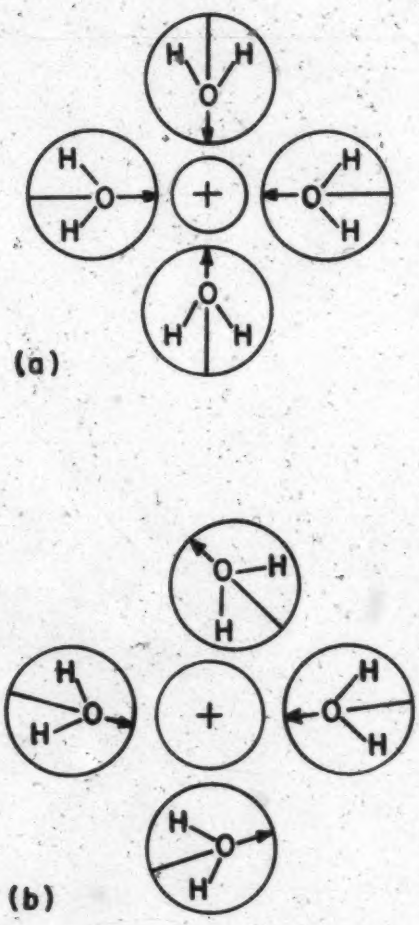

FIGURE 6.3. Primary cation solvation shells.

(a) Ordered (b) Disordered.

onset of the disordered solvation shell for the large cations.

6.5 Solvation of Anions.

The molal shifts of the halide ions in methanol, and the corresponding 1:1 complex shifts measured in carbon tetrachloride solution, are available from the literature.[60,72] A formal analysis of these values according to equation (6.3) yields effective solvation numbers of *ca* 2 and Δ_h of *ca* 6 ppm. The small solvation number suggests a disordered primary solvation shell for the large halide ions, as found for the large cations. In addition, the value of Δ_h, which is larger than the liquid to gas shift for methanol, is consistent with the known structure-breaking properties of the halide ions.[31] Since bulky neutral molecules also exhibit the structure-breaking effect, it has been suggested [50] that structure-breaking by anions is due to the inability of such a bulky (solvated) ion to fit into the normal solvent structure, and that the structure-broken region lies immediately outside the primary solvation sphere of the anion.[31,50] This argument appears to be reasonable and no evidence to the contrary is presented here. However, if the new description of structure-making is accepted, it is shown that structure-making by cations and structure-breaking by anions may be caused by two quite different phenomena and that the effects may occur in different regions of the solvent, relative to the ions.

6.6 Solvation in Ethanol.

All of the data required for the correlation of the TYPE I, II and III experiments for ethanol are not yet available. The TYPE II and III results were obtained in the present work and can be found in Chapters 3 and 5. Franconi and Conti [106] have reported "molal shifts" for a few alkali halide salts in this solvent but they were based on a single NMR measurement at high salt concentration and they are consequently incompatible with the currently accepted definition of the molal shift (see equation (1.8)).

The infinite dilution solvation shell shift Δ_s for Mg(II) in ethanol at -70° is -1.06 ppm, and the 1:1 complex shift measured in acetonitrile is -2.75 ppm. Equation (6.4) may be used to calculate a molal shift for this ion in ethanol and the deduced value is -0.293 ppm kg. $mole^{-1}$. This value is subject to the same reservations (described in section 6.3 above) as the corresponding molal shift for Mg(II) in methanol. It must be regarded as suspect until it can be correlated with the molal shifts for several other ions, which are not presently available.

The values of Δ_s and Δ_c for Mg(II) with ethanol can be used to deduce the value of Δ_h^o for this solvent. According to equation (6.5), Δ_h^o = +1.69 ppm, somewhat larger than the value found for methanol.

The results presented in this section must be regarded as groundwork for a more complete study which may be achieved when a range of molal shifts is available for this solvent.

CHAPTER 7

CARBON-13 SOLVATION SPECTRA

Previous application of carbon-13 NMR spectroscopy to the study of ion solvation has been limited to the single report of Boubel et al.[82] of a TYPE II spectrum of a solution of anhydrous aluminum chloride in dimethylsulphoxide - heavy water mixture (DMSO-D_2O) at 30°. The ^{13}C NMR signal due to DMSO molecules coordinated to the cation appears at 1.94 ppm to high field of the solvent DMSO signal. This observation is interesting because all hydroxyl proton resonances of coordinated molecules appear to low field of the bulk solvent.[24,25]

The object of the present study is to investigate the more general applicability of the ^{13}C method to solvation chemistry through the study of spectra of solutions of electrolytes in single solvents, which serve better as models for quantitative treatment.

7.1 TYPE II Solvation Spectra

The proton NMR spectra of solutions of highly polarising cations in alcohols and other polar solvents have been used to investigate the free and bound solvent exchange kinetics.[36, 37,108,109] It is generally recognised that the coalescence of the bulk and bound hydroxyl proton resonances with rising temperature may be controlled by two kinetic processes:

exchange of the whole solvent molecule and exchange of the hydroxyl proton.[36] The observation of splitting of the hydroxyl proton signal due to coupling with alkyl protons, and the observation of separate resonances for the alkyl group protons in the solvation shell, is usually taken as evidence that the whole molecule exchange controls the line broadening and coalescence phenomena.[36] In cases where neither of these observations were made, the dominance of whole molecule exchange has been assumed.[37] It must be recognised that the rate constants reported in such studies may contain a contribution from or be due entirely to the exchange of the hydroxyl proton.

In principle, the line broadening and coalescence phenomena in carbon-13 spectra may be used to obtain definitive whole molecule exchange rate constants since they are unaffected by the exchange of the hydroxyl proton. However, there are several factors which complicate the measurement of exchange processes using carbon-13 spectroscopy and they are discussed fully in Appendix A. It may also be possible to study, by the carbon-13 method, the solvation of cations in organic solvents such as ketones, ethers and nitriles, whose proton resonances are shifted only slightly and do not yield separate solvation shell signals. The carbon-13 data is potentially of great value to the theory of ^{13}C shieldings, which is generally less well understood than that of the proton shieldings.[110]

The present work should be regarded as a preliminary

investigation with these ultimate goals in mind. The carbon-13 NMR spectra of solutions of $Mg(ClO_4)_2$ in methanol and ethanol, $AlCl_3$ in ethanol and n-propanol, and $Al(ClO_4)_3$ and $GaCl_3$ in ethanol were recorded over a wide range of temperatures. In some cases, separate solvation shell and bulk solvent resonances were observed.

7.1.1 ^{13}C Spectra of Ethanolic $Mg(ClO_4)_2$ Solutions.

The Fourier transform carbon-13 NMR spectra of solutions of magnesium perchlorate in ethanol were recorded over the temperature range -90° to +30°, both with and without proton decoupling, using natural abundance samples. The methyl and methylene carbon resonances of pure ethanol are separated by *ca* 40 ppm. The fully proton decoupled spectrum of ethanolic magnesium perchlorate below -50° contains two additional small signals, one at about 1.5 ppm to low field of the methylene and one 0.8 ppm to high field of the methyl, as shown in figure 7.1a. At higher temperatures these signals broaden and coalesce with the bulk solvent signals. Assignment of the small signals to the methylene and methyl carbons of molecules in the cation solvation shell was confirmed by the observation of the appropriate proton splittings in the absence of decoupling, as illustrated by the spectrum in figure 7.1b. The coupling constants were unchanged in the solvation shell compared with the bulk solvent, to within the limits of experimental accuracy (*ca* 2%).

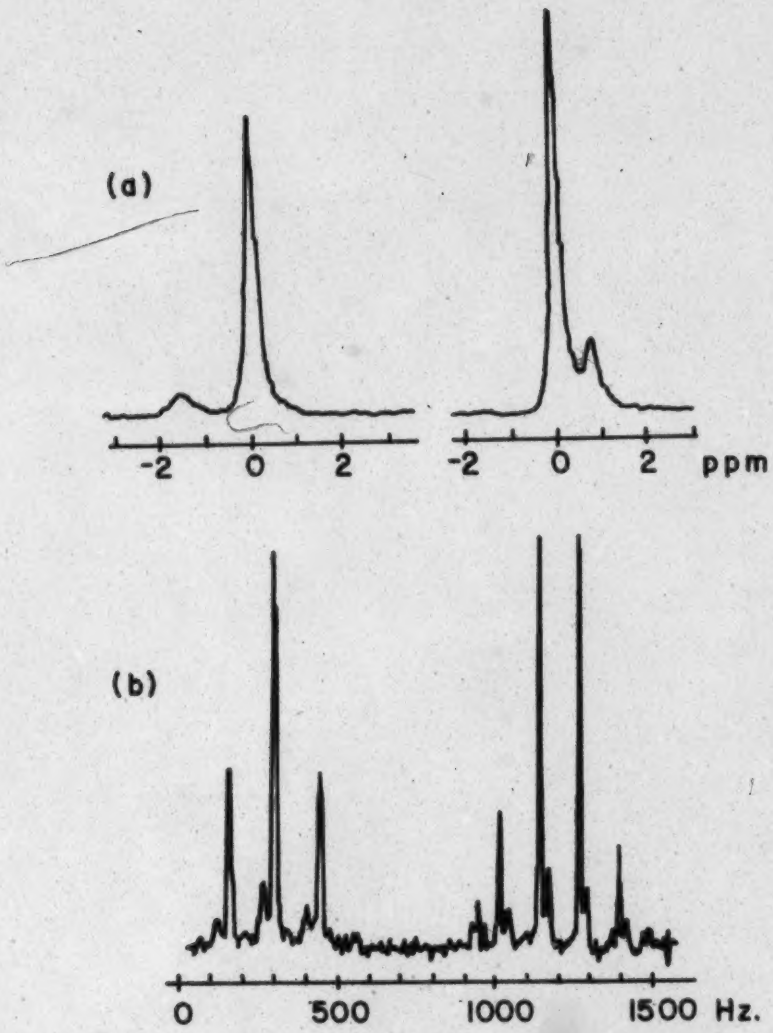

FIGURE 7.1. Carbon-13 NMR spectra of 0.72 m solution of $Mg(ClO_4)_2$ in ethanol at -70°. (a) Proton-decoupled spectrum; (b) Proton coupled spectrum.

The temperature dependence of the bulk and bound solvent chemical shift separations is shown in figure 7.2, and that of the bulk solvent line width in figure 7.3. The shifts are independent of temperature, within experimental error, up to the coalescence temperature of about 45°. Thus the low-temperature shifts represent the exchange-independent values.

No attempt was made to study the concentration dependence of the shieldings and the chemical shifts in the region of slow exchange are taken to approximate Δ_s, the solvation shell shift, for each nucleus. This assumes that σ_r, the residual solvent shieldings are about the same as σ_p, the pure solvent shieldings. This assumption is reasonable because the separation of the bulk solvent signals in the solution is only slightly different from that in the pure solvent. Since the residual shift is attributed to interaction between the hydroxyl proton in the bulk solvent with perchlorate ion, and to disruption of hydrogen bonding at the hydroxyl proton (a site remote from the carbon atoms considered), this observation might be expected. The values of Δ_s obtained here for both carbons are used in section 7.2. The bulk-bound solvent relative signal intensities gave a solvation number of 5.5 ± 1, (i.e. about 6) consistent with the proton result.[25]

The lowest temperature ^{13}C spectra of this system demonstrated an unusual feature which turned out to be character-

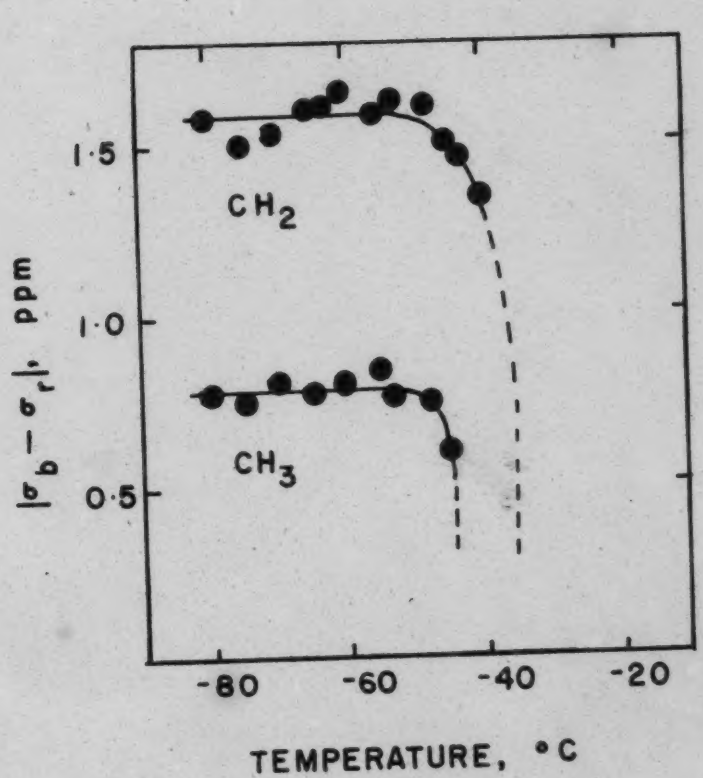

FIGURE 7.2. Temperature dependence of the CH_2 and CH_3 carbon-13 bulk-bound chemical shift for 0.716 m $Mg(ClO_4)_2$ in ethanol.

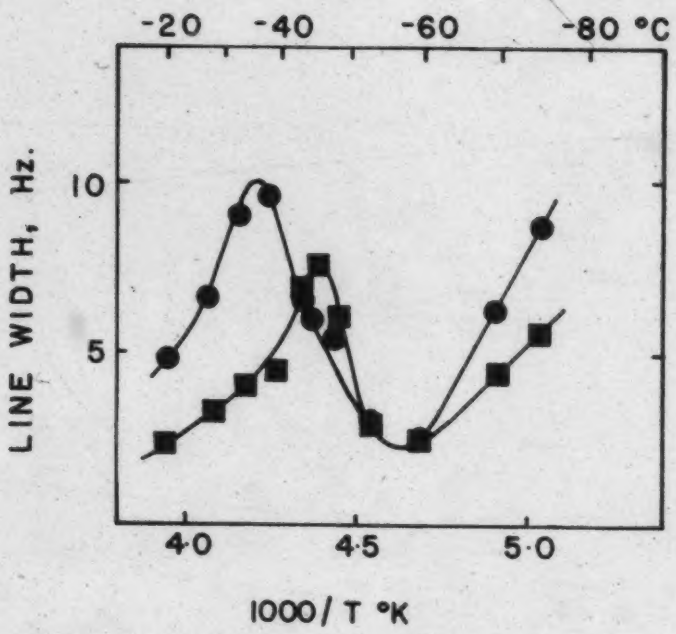

FIGURE 7.3. Temperature dependence of the ^{13}C CH_2 (●), and CH_3 (■) bulk solvent linewidths for 0.716 m $Mg(ClO_4)_2$ in ethanol.

istic of all of the salt solutions studied. As the temperature of the solution was lowered, the signal due to the carbon atom directly bonded to the oxygen became selectively broadened to the extent that it disappeared into the baseline noise whilst the other solvation shell signals remained relatively sharp. A tentative explanation of this phenomenon is given in section 7.4.

7.1.2 ^{13}C and ^{1}H Spectra of Al(III) Solvation Shells.

Grasdalen [108,109] has reported the ^{1}H NMR spectra of solutions of aluminum chloride in ethanol and n-propanol at several temperatures and concentrations. He discovered that these solutions show at least three hydroxyl proton solvation shell signals at low temperatures. Some of his hydroxyl proton spectra for ethanol coordinated to Al(III) are shown in figure 7.4. He assigned peak A, which persists to highest temperature, to a normal single ion solvation shell. From the temperature and concentration dependence of peaks B and C, he suggested that they may be due to polymeric species involving hydrogen bonds between the solvation shells of two or more different cations, as illustrated for the dimer in figure 7.5.

The natural abundance carbon-13 spectra were recorded for solutions of $AlCl_3$ in ethanol and n-propanol at several temperatures. For ethanolic $AlCl_3$ solutions, the solvation shell signals appeared to low field of the methylene and to

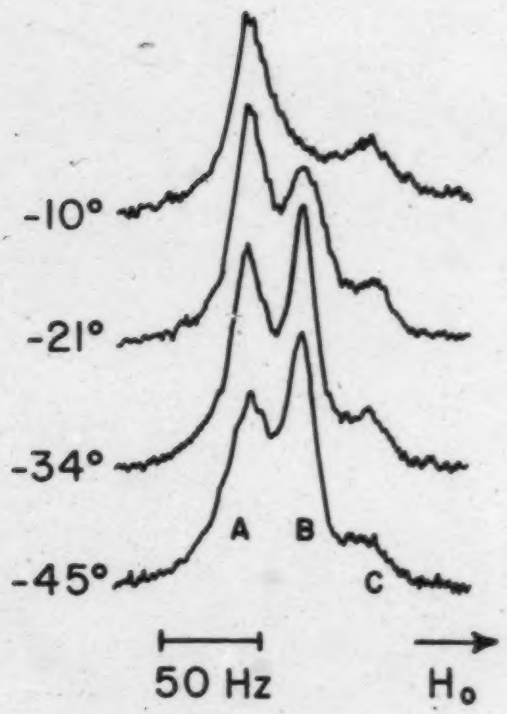

FIGURE 7.4. The effect of temperature on the hydroxyl proton signals of ethanol coordinated to Al(III). Taken from reference 108.

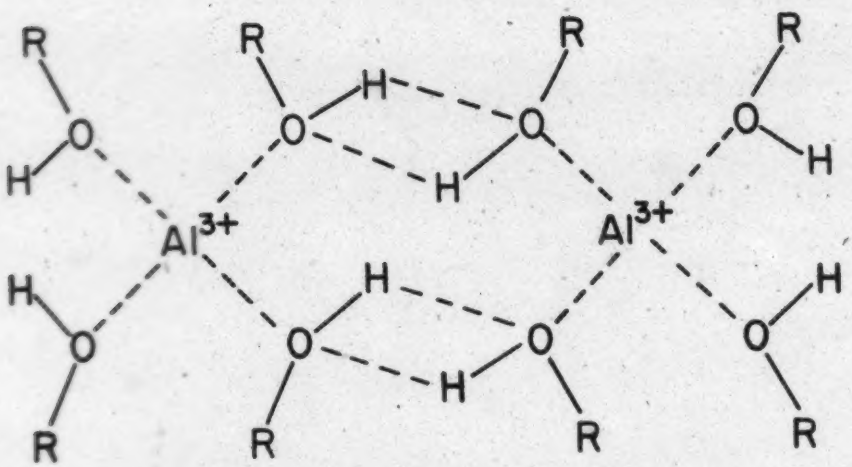

FIGURE 7.5. Hydrogen-bonded solvated-cation dimer in alcohol $AlCl_3$ solutions, as proposed by Grasdalen, reference 108.

high field of the methyl resonances of the bulk solvent. One to three solvation shell methylene signals were observed, consistent with the proton results, but only two methyl signals appeared at the lower temperatures, as shown in figure 7.6. It is likely that the third methyl signal, which corresponds to the lowest intensity methylene signal (peak C), was masked by the larger CH_3 peaks. The intensities and temperature variation of the carbon-13 signals resemble those of the proton signals so closely that is is reasonable to make a corresponding assignment of the peaks in the methylene carbon spectrum. Thus, peak A is assigned to the monomer solvation shell and peaks B and C to as yet unidentified polymeric species. Integration of the intensities of all solvation shell signals gave a solvation number of 3.6 ± 1, consistent with the value of about 4 obtained by Grasdalen from the proton spectra.

Solutions of $AlCl_3$ in n-propanol show separate solvation shell resonances for all three carbon atoms. The carbon bonded to oxygen is deshielded and the other two are shielded relative to the bulk solvent signals. In contrast to the proton results of Grasdalen [109], no multiplicity of the solvation shell signals was observed at low temperatures. However, the solvation shell signals were so broad at temperatures where multiplicity was expected that the splitting may have been masked. The methylene carbon bonded to oxygen was selectively broadened and its shielding in the absence

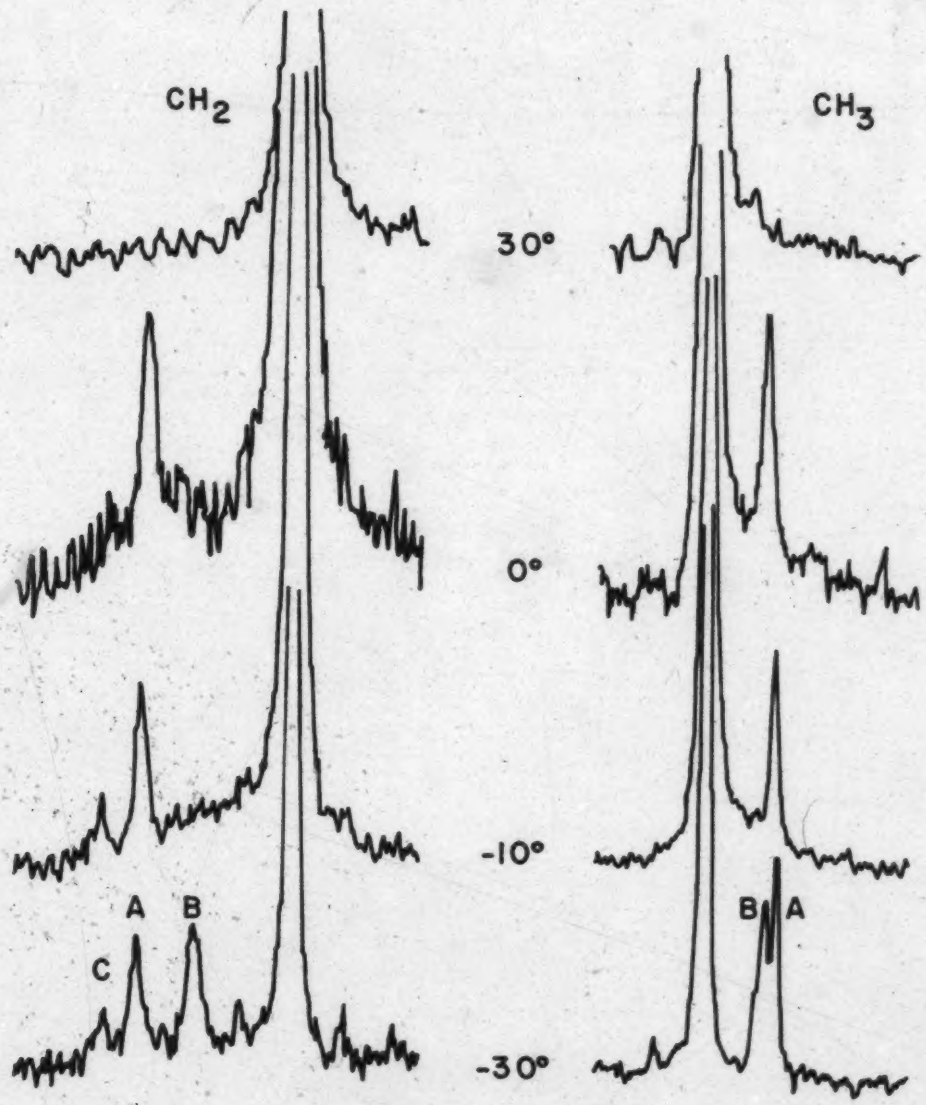

FIGURE 7.6. Carbon-13 spectra of ethanolic $AlCl_3$ at several temperatures.

of exchange could not be measured. From the higher temperature, partially coalesced spectra, it is known to be more than 3 ppm downfield.

The interpretation of spectra of solutions containing two relatively highly polarising ions (in this case Al(III) and Cl^-) is always subject to satisfactory separation of the cation and anion effects. It is known that chloride ion associates strongly with the hydroxyl protons of alcohols in carbon tetrachloride solutions,[41] and Cl^- has substantial molal shifts in bulk hydroylic solvents.[55,60] This leads one to suspect that the chloride ion might have something to do with the peculiarities of the aluminum solvation shell.

This possibility was investigated by replacing the chloride ion with perchlorate, an ion which is known to associate only weakly with alcohols. Solutions of aluminum chloride in ethanol were treated with ethanolic silver perchlorate and the precipitated silver chloride was removed with the centrifuge. The experiment was performed in such a way that the Al(III) concentration remained the same (0.62 m) in all solutions, but the ratio of Cl^- to ClO_4^- varied between 3:0 and 0:3. The carbon-13 NMR spectra of these solutions are shown in figure 7.7. The chemical shifts are given in table 7.1. There is no question that the multiplicity of the solvation shell spectra is associated with the chloride ion, since only peak A remains (though somewhat shifted) for the aluminum perchlorate solution. This sup-

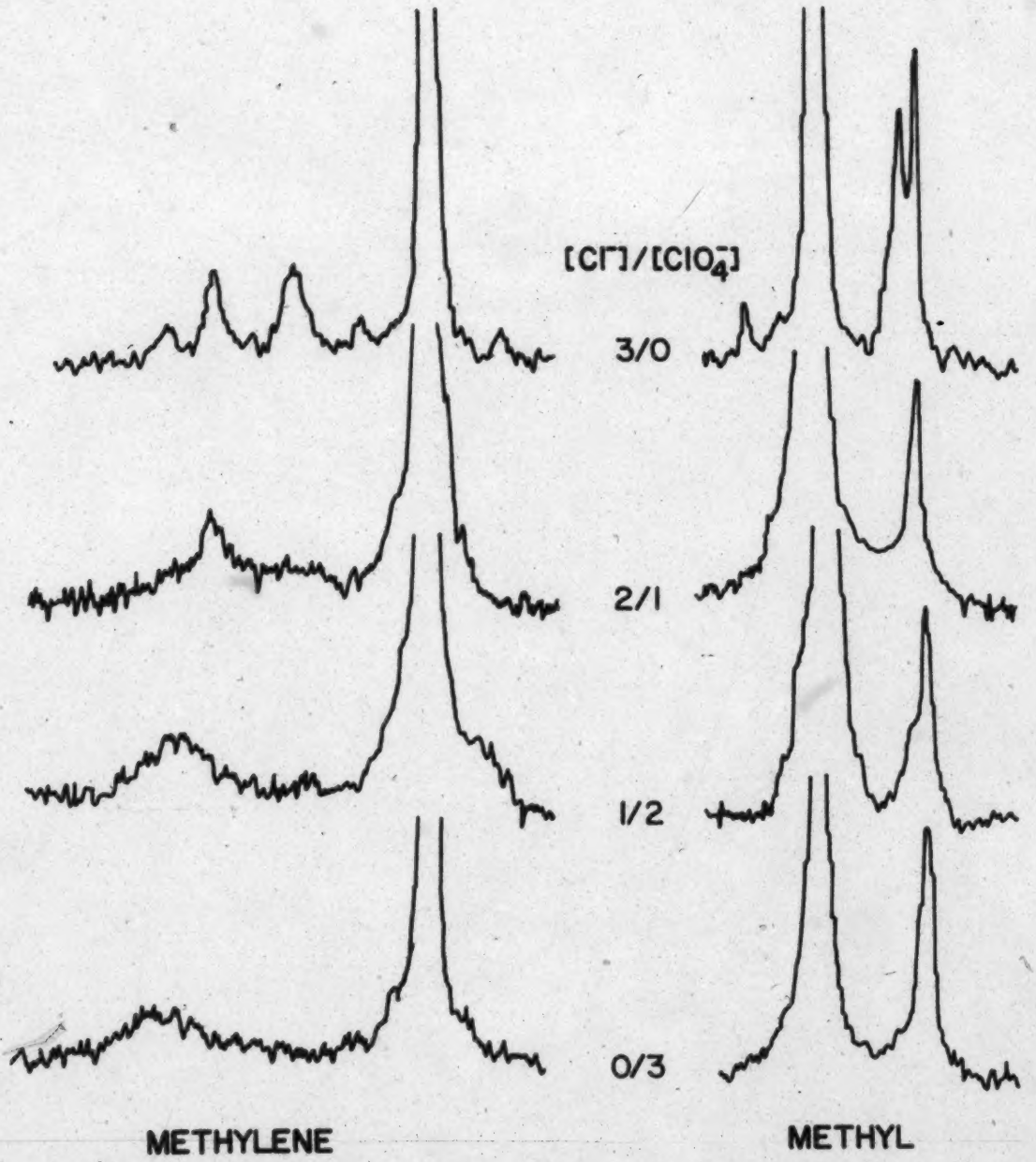

FIGURE 7.7 22.63 MHz NMR spectra of the solvation shell carbon-13 nuclei of ethanolic solutions of $AlCl_3$, as the chloride ion is replaced by perchlorate, at -30°.

TABLE 7.1

^{13}C Solvation Shell Shifts* for Ethanolic $AlCl_3$ Titrated with $AgClO_4$

System	Methylene (β) ^{13}C			Methyl (γ) ^{13}C		
	C	A	B	C	A	B
1.24m $AlCl_3$ in ethanol at -50°	-5.5	-4.6	-2.8	?	+2.0	+1.7
1/3 titrated with $AgClO_4$		-4.4			+2.0	
2/3 titrated with $AgClO_4$		-5.0			+2.1	
Fully titrated with $AgClO_4$		-5.6			+2.2	

* Uncertainty of measurement is ± 0.05 ppm.

ports Grasdalen's conclusion that peak A may represent a normal solvation shell.

The titration of chloride ion with silver perchlorate was also followed by proton NMR, and the solvation shell spectra at -30° are shown in figure 7.8 and the shifts are listed in table 7.2. The use of less concentrated, and hence less viscous, solutions and the use of a 100 MHz spectrometer gives better resolved spectra than those obtained by Grasdalen. These spectra confirm that peak A is not influenced by the anion. The changes in B and C are linearly dependent on the anion ratio. Whatever the structure of the solvation shells giving these signals may be, they certainly involve the chloride ion. Even perchlorate yields some complexity: the broad signal remaining to highfield of peak A in the spectrum of the aluminum perchlorate solution at -30° sharpens to give a distinct signal at lower temperatures.

The information presently available does not allow definite identification of the extra solvated species. It is possible that direct-contact ion-pairs such as $AlCl^{++}$ and $AlCl_2^{+}$ may exist in the solution but there is evidence to suggest that they do not. Haraguchi and Fujiwara [111] have studied the ^{27}Al NMR spectra of solutions of Al(III) salts and complexes in water and the alcohols. The concluded that Al(III) is octahedrally solvated (n = 6) in water, ethanol and n-propanol on the basis of the narrow line width (which is determined largely by quadrupole interactions) and chemi-

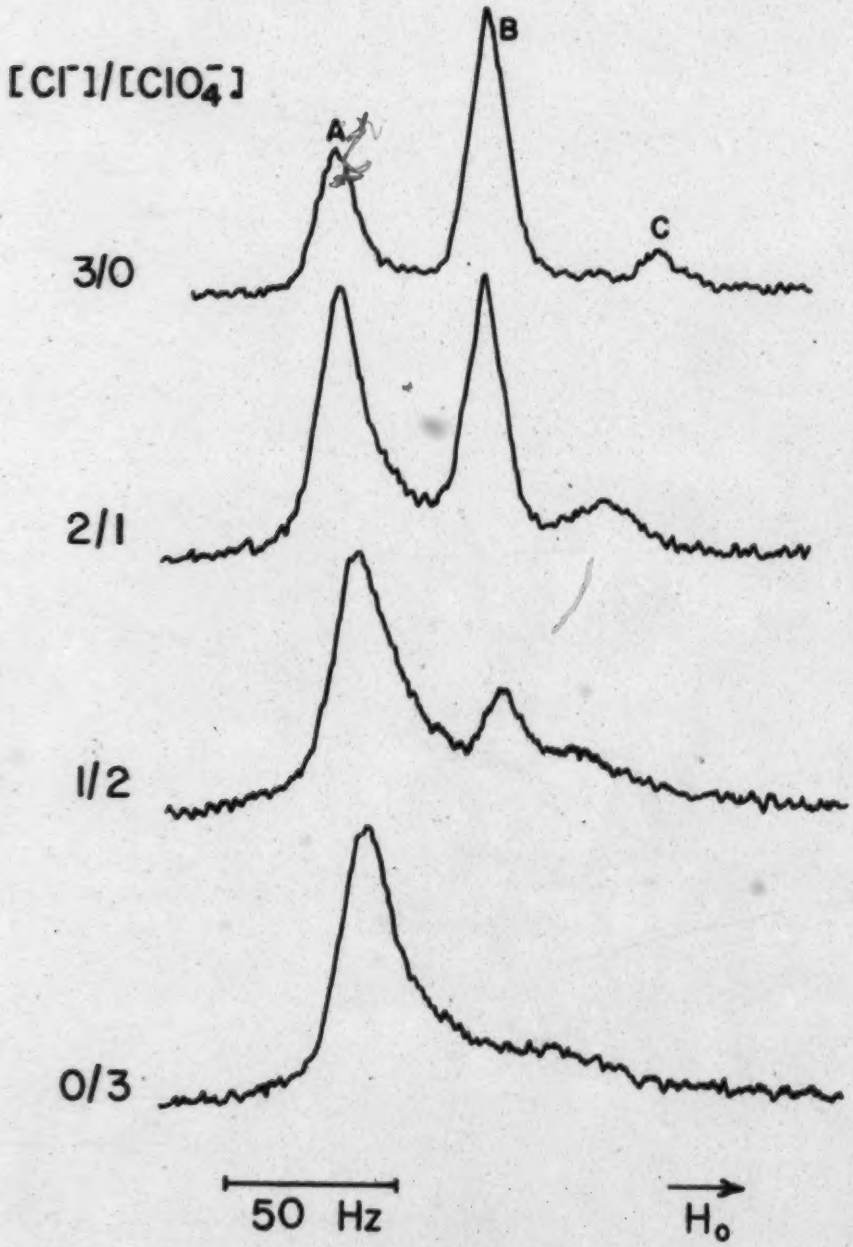

FIGURE 7.8 100 MHz NMR spectra of the solvation shell hydroxyl proton of ethanolic solutions of $AlCl_3$, as the chloride ion is replaced by perchlorate, at -30°.

TABLE 7.2

Hydroxyl Proton Shifts* for Ethanolic $AlCl_3$ Titrated with $AgClO_4$

$[Cl^-]/[ClO_4^-]$	Solvation Shell			Bulk Solvent
	A	B	C	
3/0	-6.70	-6.25	-5.76	-2.25
2/1	-6.61	-6.20	-5.84	-2.22
1/2	-6.58	-6.16	-5.96	-2.46
0/3	-6.54	-	*ca* -6	-2.46

* In ppm, relative to the bulk solvent CH_2 resonance.

cal shift measurements. The narrow lines indicate an absence of ion pairing with Cl^- or ClO_4^- in these solvents. Note the difference in solvation numbers obtained from the ^{27}Al spectra (n = 6) and those from the ^{1}H and ^{13}C spectra (n = 4). The aluminum-27 results may not be conclusive. It is possible that the presence of very broad lines due to contact ion pairs may have been overlooked and that the narrow line observed may correspond only to normally solvated (n = 6) Al(III). This point could be settled by following the *intensity* of the ^{27}Al resonance through a titration with silver perchlorate.

There remains the possibility of solvent-separated ion-pairs or ion-clusters involving such interactions as

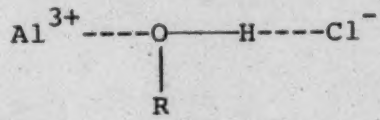

There appears to be no way of unambiguously distinguishing between the large number of possible structures on the basis of the avilable information. It is possible that further ^{27}Al and ^{35}Cl NMR studies could throw light on the structures of the various solvating species in alcoholic aluminum chloride solutions.

7.2 TYPE III Carbon-13 Solvation Spectra

In chapter 3 of this work, it was shown that magnesium-(II) is able to form a strong (K = 140) 1:1 complex in dilute

acetonitrile solution at ordinary temperatures. The substrate is completely complexed when the salt/substrate ratio becomes greater than about 4:1. Thus it should be possible to observe the carbon-13 complex shielding directly by choosing suitable concentrations.

It was not at first possible to observe the carbon-13 NMR spectrum of ethanol at about 1/10 molar in acetonitrile. By monitoring the dilution of ethanol with acetonitrile over a wide concentration range and the use of extensive averaging (8000-24000 pulses), it was possible to pick out the ethanol signals from the baseline noise at concentrations as low as 0.2 M and to observe the shifts upon addition of $Mg(ClO_4)_2$. The limiting shifts found in this way are $\Delta_c(CH_2) = -2.01$ and $\Delta_c(CH_3) = +1.43$ ppm.

These values are somewhat larger than the solvation shell shifts found in the previous section for Mg(II) in ethanol. The solvation model applied in Chapter 6 to the hydroxyl proton resonance may be used here to illustrate that the same general considerations describe the carbon-13 shifts. If the hydrogen bond shift is estimated by use of equation (6.5), the deduced values are $\Delta_h^o(CH_2) = +0.5$ and $\Delta_h^o(CH_3) = -0.6$ ppm. The uncertainty in measurement of the shieldings is about 0.05 ppm (1 Hz). The values of Δ_h are not especially useful to solvation chemistry at the present time because the carbon-13 gas to liquid shifts are not known. However, they are extremely significant in the dis-

cussion of carbon-13 shieldings in the next section.

7.3 The ^{13}C NMR Shieldings in Coordinated Molecules.

Table 7.3 lists all of the presently known carbon-13 NMR shieldings in molecules coordinated to diamagnetic cations, relative to the bulk solvent or free substrate shielding according to the system studied. It is immediately apparent that the carbon (C_β) closest to the site of attachment (the oxygen atom) is always deshielded and the next carbon down the chain (C_γ) is always shielded. The single measurement on a molecule containing a third carbon (C_δ) indicates that its nucleus is very slightly shielded.

One may draw a comparison between the solvation shell shifts listed in table 7.3 and those observed in a straight chain alkane when a hydrogen atom on the end carbon is substituted by an electronegative group.[112] It is necessary to consider the oxygen atom to which the ion is attached in the same way as the substituted carbon in the alkane (the α carbon). For this reason, the carbon atom attached to the oxygen in the coordinated molecule is regarded as the β carbon.

In the substituted alkane, it is almost universally observed that the α carbon is deshielded, the β carbon is deshielded but to a lesser extent, the γ carbon is shielded and the δ carbon exhibits a very small shielding or deshielding.[112]

TABLE 7.3

The Carbon-13 Shieldings, in ppm, of Coordinated Molecules Relative to those in the Bulk Solvent or Free Substrate.

System	Nucleus[a]		
	C_β	C_γ	C_δ
0.72m $Mg(ClO_4)_2$ in ethanol at -70°	-1.54	+0.79	
$Mg(ClO_4)_2$ + ethanol in acetonitrile at +30°	-2.01[b]	-1.43[b]	
1.24m $AlCl_3$ in ethanol at -50°	-5.5 -4.6 -2.8	c +2.0 +1.7	
1.24m $Al(ClO_4)_3$ in ethanol	-5.6	+2.2	
1.15m $AlCl_3$ in n-propanol at -30°	See Text	+1.95	+0.07
$AlCl_3$ in DMSO/D_2O at +30°		+1.94[d]	

a. The carbon bonded to oxygen is designated C_β for reasons given in the text.

b. 1:1 complex.

c. A third methyl signal was not observed.

d. Taken from reference 82.

The anomalous shielding of the third carbon in alkanes and other molecules has become known as the "γ-effect" and is known to be transmitted through hetero atoms.[113] It is thought to be caused by a non-bonded interaction between the substituent and the hydrogens on the γ carbon.[114] The effect appears to be manifest in the solvation shell shieldings: the β carbon is deshielded and the γ carbon is shielded.

The solvation shell shift decreases in magnitude with distance from the perturbation and increases with ionic surface potential at both the β and γ positions. The observation that the 1:1 complex shifts Δ_c are larger than the solvation shell shifts Δ_s for both the β and γ carbon atoms provides a further clue as to the origin of the γ-effect. The difference between Δ_c and Δ_s arises from the shift Δ_h^o due to desolvation of the oxygen atom in the alcohols (see section 6.3). It seems highly probable that both the β and γ carbon shifts arise from the direct interaction at the alcohol oxygen atom. Hence, it appears that the γ-effect in these systems arises from the perturbation at the oxygen atom and not through a non-bonded interaction between the γ carbon protons and the ion, which would presumably result in deshielding of the carbon nucleus rather than the observed increased shielding.

Any theoretical treatment of the γ-effect will have to account for the appearance of the γ-effect in carbon-13 solvation spectra. In view of the alternative interpretation of

the γ-effect offered above, conformational studies based upon the observation of a positive γ carbon shielding may be subject to reconsideration.

7.4 The Selective Broadening of the C_1 Resonance.

In section 7.1 it was mentioned that the resonance of the carbon atom (C_1) directly bonded to the oxygen in all of the solvation shell molecules studied becomes selectively broadened at low temperatures. Figure 7.9 illustrates this phenomenon for the $AlCl_3$ in ethanol system. It is apparent that the C_1 (methylene) resonance disappears at low temperatures. A tentative explanation is now offered.

The parameters which influence the intensity and line width of the FFT spectra are the longitudinal and transverse relaxation times T_1 and T_2. The spin-lattice relaxation time T_1 determines the degree of saturation and T_2 determines the unsaturated line width. Both T_1 and T_2 are inversely proportional to the correlation time τ_c, the characteristic time of molecular tumbling motions, for $\tau_c < \omega_o^{-1}$.[115] The correlation time is directly proportional to the solution viscosity η and inversely proportional to the temperature. Thus, for a spherical molecule [116] of radius r,

$$\tau_c = \frac{4\pi\eta r^3}{3kT} \qquad (7.1)$$

At lower temperatures, the viscosity of the solution increases and hence the relaxation rates decrease.

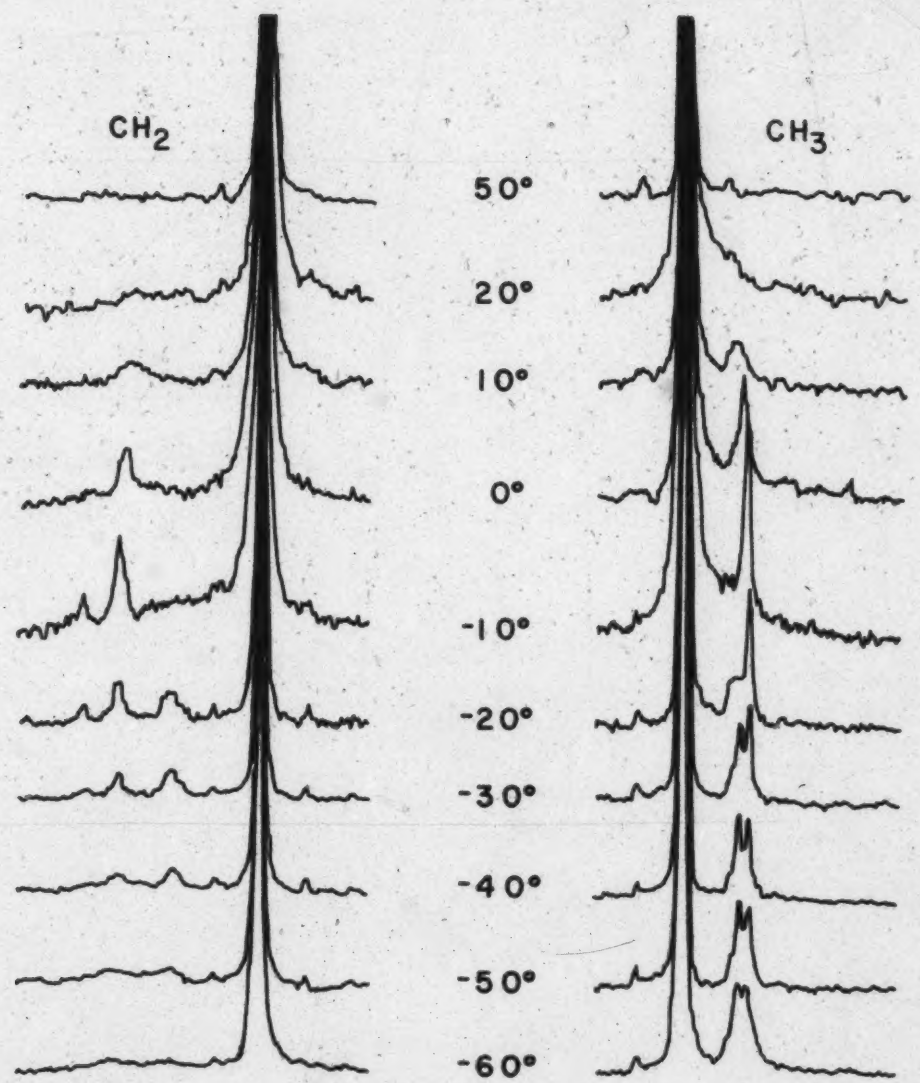

FIGURE 7.9. Selective broadening of the C_1 resonance at low temperatures.

There are three processes which may contribute to the anomalous disappearance of the C_1 resonance in alcoholic salt solutions. When T_2 becomes smaller, the natural line width $1/\pi T_2$ increases. When T_1 becomes very short, the lifetimes of the spin states are short and a broadening occurs which can be explained by the Heisenberg uncertainty principle.[43] The nuclear Overhauser enhancement of the proton-decoupled ^{13}C signals is controlled by the relaxation rates and it may be reduced, resulting in a loss of intensity. This latter mechanism could only account in part for the disappearance of the methylene carbon signal. It is not possible to determine the relative importance of the three contributions from the available data, but it is known that T_1 is usually much longer than T_2 for ^{13}C nuclei and the increased natural line width is probably the dominant effect. The three contributions are combined in the correlation time τ_c for the C_1 nucleus and an anomalously large increase in τ_c for C_1 relative to those of other nuclei in the molecule could be attributed to restricted motion of the methylene group in the crowded region close to the ion.

This phenomenon may account for the failure to observe a separate carbon-13 solvation shell resonance for methanolic magnesium perchlorate solutions, even though the separate hydroxyl proton resonance is readily observed. At temperatures below the coalescence point, the correlation time for the methanol carbon nucleus may be so long that its spectrum is

broadened to the extent that it is totally obscured by the baseline noise.

CHAPTER 8

CONCLUSION

8.1 Cation Complexes in Acetonitrile.

The association constants and hydroxyl proton complex shifts of 1:1 cation complexes of water and several alcohols were measured and they all show the dependence upon ionic charge and radius to be expected of an electrostatic interaction. The shifts are negative, consistent with cation association in the neighbourhood of the oxygen lone pairs. Solvation of the substrate at the oxygen atom by acetonitrile does not significantly alter the hydroxyl proton shielding and the desolvation shift accompanying the formation of the complex is therefore negligible. Consequently, the complex shift is attributed entirely to the polarisation of the substrate by the cation in the 1:1 complex.

The 1:1 cation complexes of 1,2-ethanediol and 2-methoxyethanol were shown to have a chelate structure involving the association of both oxygen atoms in the substrate with the cation.

The complex shifts for the alkyl protons of diethylamine in its 1:1 complex with Mg(II) are much larger than those occurring in the complexes of the monodentate or bidentate oxygenic substrates. This may imply that the structure of the amine complex is different from that of the alcohol or diol complexes. It is possible that the amine

complex is formed with the cation at the nitrogen lone pair and that the oxygenic complexes are centrosymmetric with the cation between the oxygen lone pairs.

The hydroxyl proton complex shifts for water, methanol and ethanol suggest a Buckingham-Musher *A* coefficient of about 1.6 esu^{-1} for the O-H bond, in contrast to the value of 5.5 esu^{-1} found for hydrogen-bonded 1:1 complexes between the halide ions and alcohol substrates. The hydrogen-bonded interaction between the hydroxyl proton in methanol and the nitrogen lone pair in acetonitrile results in a hydroxyl proton shift whose value is consistent with the higher value of the *A* coefficient. It appears that one of the interactions, most probably the hydrogen bond, cannot be accounted for by the Buckingham-Musher electrostatic model. The value of $A = 1.6\ esu^{-1}$ may be representative of a purely electrostatic interaction and the larger value of 5.5 esu^{-1} may imply an additional effect due to a covalent contribution to the hydrogen bond.

8.2 The Solvation Model.

The molal shifts Δ_m of cations in water at +25° and methanol at -69° appear to be related to the 1:1 complex shifts Δ_c by a simple solvation model which takes explicit account of nearest-neighbour interactions only. The solvation shell shifts Δ_s for magnesium(II) in methanol at -69° and ethanol at -70° are also correlated with the molal and

complex shifts by this model. The implications of the model are best explained in terms of the parameters used.

The direct ion-molecule interaction shift is assumed to be Δ_c, the complex shift measured in acetonitrile. It is a quantity which characterises individual ions and it may be estimated with reasonable accuracy by an electrostatic model. It is, to within experimental error, independent of temperature, which is reasonable for an interaction of energy in excess of 15 kcal. per mol. of solvate.[117]

The solvation number, n, determined by this correlation is to be regarded as a measure of the average number of oriented nearest-neighbour solvent molecules. For small and/or highly charged cations, this number is about 6, which is a reasonable value for the total number of nearest neighbours. These ions, therefore, have completely oriented solvation shells, consistent with their large negative contributions to the entropy of solution. Large monovalent cations and anions appear to have small effective solvation numbers. This suggests that they do not have fully oriented solvation shells but rather a slight statistical excess of nearest neighbours in the lower energy orientation. The absence of a structured solvation shell is consistent with the anomalously high entropies of solutions containing these ions.

The quantity Δ_h, which evaluates the net disruption of the solvent per solvating molecule, is related to the amount

of hydrogen bonding in the residual bulk solvent of an electrolyte solution. It decreases with increasing temperature as expected. It is the only measured quantity that is sensitive to structural solvation and it is the first NMR shielding parameter of this kind to be reported. Since the nearest-neighbour-interaction model predicts that Δ_h should be about 5 ppm for both cations and anions in water and methanol, the observed values of *ca* 1.5 ppm for cations and *ca* 6 ppm for anions indicate that the residual solvent in the solution contains more and fewer hydrogen bonds per mole, respectively, than in pure solvent. The observed values of Δ_h may be interpreted as representing structure-making by cations and structure-breaking by anions, if there is a direct relationship between the proportion of hydrogen bonding and structure.

All measured characteristics of the solvation process are essentially equal in water at -25° and methanol at -69°, when each solvent is roughly 25° above its freezing point. As a consequence of this, the molal shifts of cations in water and methanol are observed to be in the ratio of the solvent molecular weights, an intriguing fact which appears to have been overlooked until now.

8.3 Carbon-13 Solvation Spectra.

In spite of the sophistication of the Fourier transform method, natural abundance carbon-13 NMR is still a consider-

ably more time-consuming technique than continuous-wave proton NMR. Nevertheless, this inconvenience must be overlooked because carbon-13 NMR promises to be more useful in the study of ionic solvation by organic solvents than conventional proton NMR. The TYPE II ^{13}C spectra of solutions of highly polarising cations in alcohols have exhibited separate solvation shell resonances for carbon atoms as much as three bonds removed from the site of attachment of the ion. The inherently larger ^{13}C shifts allow the observation of the solvation shell molecules in cases where this would not be possible with ^{1}H NMR. The use of very high field spectrometers (greater than 60 kgauss) and ^{13}C enriched samples would give even larger chemical shift separations and much improved sensitivity.

The TYPE II and III carbon spectra of solutions of magnesium perchlorate in ethanol yield values of Δ_s and Δ_c which can be used to deduce the hydrogen-bond shift Δ_h^o for each carbon nucleus. The deduced hydrogen-bond shifts have the signs to be expected from a knowledge of the signs of the shifts Δ_s and Δ_c induced by the ion. This demonstrates that the general considerations of the solvation model used to interpret the proton shifts also apply to the carbon-13 shifts of coordinated molecules. A knowledge of the gas to liquid carbon-13 shifts is required before the solvation spectra can be fully interpreted.

The carbon-13 shielding changes (relative to the bulk solvent) in all of the coordinated molecules studied are downfield at C_1 and upfield at C_2. They resemble the β and γ carbon shifts induced in an alkane by an electronegative substituent at the γ-carbon. The usual explanation of the upfield γ-carbon shift in terms of a non-bonded interaction between the hydrogen atoms on the γ-carbon and the substituent appears to be insufficient to account for the shifts in coordinated molecules. Any explanation of the γ-effect must account for all observations. The appearance of the γ-effect in the coordinated molecules raises some doubts of the validity of conformation studies of organic molecules which are based on the observation of the γ-effect.

8.4 Aluminum(III) Solvation Shells.

The ^1H and ^{13}C TYPE II NMR spectra of solutions of $AlCl_3$ in ethanol and n-propanol exhibit signals which are attributed to the presence of at least three solvated species. The ^1H spectra were previously explained by postulating the presence of a normal cation solvation shell and additional polymeric species involving long-lived hydrogen bonds between the solvation shells of two or more cations.[108, 109] Comparison of the ^1H and ^{13}C spectra of ethanolic aluminum chloride and ethanolic aluminum perchlorate solutions demonstrates quite unambiguously that the chloride ion is involved specifically in the extra solvating species. At

the present time, the most reasonable explanation of the spectra seems to be that of the presence of a normal solvation shell and additional species involving solvent-separated ion-pairs or ion-clusters between Al^{3+}, Cl^{-} and solvent molecules.

8.5 Suggestions for Future Work.

It is possible that the data presented in this thesis could be applied in other areas of chemistry. In several instances, the techniques used here could be applied to other systems of current interest. A number of observations were made which deserve further investigation, and the following is a list of suggestions for possible future work.

(i) The ionic molal shifts from TYPE I spectra should be measured for ethanol and the higher alcohols. It would be interesting to compare the solvation properties of the higher alcohols with those of water and methanol.

(ii) The TYPE II carbon-13 spectra of solutions of highly polarising cations in organic solvents such as ethers, ketones and nitriles should be investigated. It may be possible with the use of this technique to gain information about many organic reactions which are catalysed by aluminum chloride.

(iii) The cation complexes of primary, secondary and tertiary amines should be studied by proton NMR. In con-

junction with the complex shifts for the alcohol and diol complexes, these would provide the necessary background for the study of cation complexes of nucleotides, which are currently of great interest.

(iv) Much more work is needed before the proton and carbon-13 shifts induced in solvent molecules by ions are properly understood. The Buckingham-Musher model seems to be able to correlate the shifts induced in the protons of one particular substrate by a range of ions. In this respect it accounts for the dependence on ionic surface potential. It does not account for the effects of a particular ion on different substrates or for the different effects of cations and anions on a given substrate. In view of this, further theoretical study of ion-induced shifts is strongly urged. Some effort should also be directed towards explaining the origin of the γ-effect in the carbon-13 spectra of coordinated molecules.

(v) Further ^{27}Al and ^{35}Cl NMR studies of ethanolic solutions of aluminum chloride and perchlorate are required, with a view to determining the role of chloride ion in the complex solvation shells of aluminum(III).

(vi) The kinetics of the exchange of the solvation shell and bulk solvent molecules in ethanolic magnesium perchlorate solutions should be determined by both proton and carbon-13 NMR. The coupled spectra should be analysed

by the correct (density matrix) method, and the effect of the Overhauser enhancement in the decoupled spectra should be evaluated.

REFERENCES

1. W. H. Bragg, Proc. Phys. Soc. Lond., 34, 98 (1922).
2. D. Eisenberg and W. Kauzmann, "The Structure and Properties of Water", Oxford Clarendon Press (1969).
3. "Water, A Comprehensive Treatise", Felix Franks (ed.) Plenum Press, New York, (1972).
4. W. K. Röntgen, Ann. Phys., 45, 91 (1892).
5. H. S. Frank and W. Y. Wen, Discuss. Faraday Soc., 24, 133 (1957).
6. D. P. Stephenson in "Structural Chemistry and Molecular Biology", A. Rich and N. Davidson (eds.) Freeman, San Francisco (1968).
7. G. E. Walrafen, J. Chem. Phys., 48, 244 (1968).
8. H. J. Bernstein, Raman Newsletter 1968 (Nov.) No. 1.
9. G. E. Walrafen in reference 3, pp.201-203.
10. G. E. Walrafen, J. Chem. Phys., 52, 4176 (1970).
11. J. B. Hasted, Prog. Dielect., 3, 103 (1961).
12. S. K. Garg and C. P. Smyth, J. Phys. Chem., 69, 1294 (1965).
13. M. Forte and S. Menardi, Nuovo Cimento XLVIB, 7 (1966).
14. J. D. Bernal and R. H. Fowler, J. Chem. Phys., 1, 515 (1933).
15. J. A. Pople, Proc. Roy. Soc., A205, 163 (1951).
16. O. Ya. Samoilov, Zh. Fiz. Khim., 20, 12 (1946).
17. E. Forsling, Acta. Polytech. Scand., 115, 9 (1952).

18. M. D. Danford and H. A. Levy, J. Amer. Chem. Soc., 84, 3965 (1962).

19. L. Pauling in "Hydrogen Bonding" (D. Hadzi, ed.), Pergamon Press, New York (1959).

20. C. M.David and J. Jarzynski, Final Report of Office of Saline Water, Grant No. 14-01-0001-684 (1968).

21. F. Franks and D. J. G. Ives, Quart. Revs., 20, 1 (1966).

22. W. H. Zachariasen, J. Chem. Phys., 3, 158 (1935).

23. G. G. Harvey, J. Chem. Phys., 6, 111 (1936).

24. M. Born, Z. Phys. 1, 45 (1920).

25. W. M. Latimer, K. S. Pitzer and C. M. Slansky, J. Chem. Phys., 7, 108 (1939).

26. R. E. Powel and W. M. Latimer, J. Chem. Phys., 1139 (1951).

27. S. Goldman and R. G. Bates, J. Amer. Chem. Soc., 94, 1476 (1972).

28. J. F. Hinton and E. S. Amis, Chem. Revs., 71, 628 (1971).

29. J. F. Hinton and E. S. Amis, Chem. Revs., 67, 367 (1967).

30. H. S. Frank and M. W. Evans, J. Chem. Phys., 13, 507 (1945).

31. J. E. Desnoyers, XV^{eme} Conseil International de Chimie Solvay. Brussels, June 1972.

32. G. E. Walrafen, J. Chem. Phys., 55, 768 (1971).

33. C. V. Krishnan and H. I. Friedman, J. Phys. Chem., 75, 388 (1971).

34. J. A. Pople, W. G. Schneider and H. J. Bernstein, "High-Resolution Nuclear Magnetic Resonance", McGraw-Hill, New York, (1959).

35. H. M. McConnell, J. Chem. Phys., 28, 430 (1958).

36. S. Nakamura and S. Meiboom, J. Amer. Chem. Soc., 89, 1765 (1967).

37. T. D. Alger, J. Amer. Chem. Soc., 91, 2220 (1969).

38. V. M. Vdovenko and V. A. Scherbakov, J. Struct. Chem., 2, 55 (1961).

39. H.G. Hertz, Ber. der Bunsens, 67, 311 (1963)

40. R.D. Green, Can. J. Chem., 47, 2407 (1969)

41. R. D. Green, J. S. Martin, W. B. Cassie and J. B. Hyne, Can. J. Chem., 47, 1639 (1969).

42. D. F. Evans, J. Chem. Soc., 5575 (1963).

43. J. Burgess and M. C. R. Symons, Quart. Revs., 22, 276 (1968).

44. C. Deverell, Prog. Nuclear Mag. Resonance, 2, 235 (1969).

45. J. J. Delpuech, A. Peguy, M. R. Khaddar, J. Electroanal. Chem., 29, 31 (1971).

46. M. H. Cohen and F. Reif, Solid State Physics, 5, 321 (1957).

47. H. G. Hertz, Z. Elektrochem., 65, 36 (1961).

48. C. Deverell, D. J. Frost and R. E. Richards, Mol. Phys., 9, 565 (1965).

49. J. N. Shoolery and B. J. Alder, J. Chem. Phys., 23, 805

(1955).

50. J. C. Hindman, J. Chem. Phys., 36, 1000 (1962).

51. H. G. Hertz and W. Spalthoff, Zeit. fur Electrochem., 63, 1096 (1959).

52. C. Franconi and F. Conti, in "Nuclear Magnetic Resonance in Chemistry", B. Pesce (ed.), Academic Press, New York, 349 (1965).

53. J. E. Gordon and R. L. Thorne, J. Phys. Chem., 73, 3643 (1969).

54. J. E. Gordon and R. L. Thorne, J. Phys. Chem., 73, 3652 (1969).

55. J. Davies, S. Ormondroyd and M. C. R. Symons, Trans. Faraday Soc., 67, 3465 (1971).

56. J. Davies, S. Ormondroyd and M. C. R. Symons, J.C.S. Faraday II, 68, 686 (1972).

57. B. S. Krumgal'z, K. P. Mishchenko and B. I. Ionin. Russ. J. Phys. Chem., 41, 1045 (1967).

58. R. M. Hammaker and R. M. Clegg, J. Mol. Spectroscop., 22, 109 (1967).

59. R. N. Butler and M. C. R. Symons, Trans. Faraday Soc., 65, 2559 (1969).

60. R. N. Butler and M. C. R. Symons, Trans. Faraday Soc., 65, 945 (1969).

61. S. A. Al-Baldawi and T. E. Gough, Can. J. Chem., 47, 1417 (1968).

62. R. E. Connick and D. N. Fiat, J. Chem. Phys., 39, 1349 (1963).

63. D. Fiat and R. E. Connick, J. Amer. Chem. Soc., 88, 4754 (1966).

64. A. Fratiello, R. E. Lee, M. Nishida and R. E. Schuster, Chem. Comms., 173 (1968).

65. A. Fratiello, R. E. Lee, V. M. Nishida and R. E. Schuster, J. Chem. Phys., 47, 4951 (1967); Inorg. Chem., 8, 69 (1969).

66. S. Thomas and W. L. Reynolds, Inorg. Chem., 9, 78 (1970).

67. L. D. Supran and N. Sheppard, Chem. Comms., 832, (1967).

68. J. J. Delpuech, A. Peguy, and M. R. Khaddar, J. Mag. Res., 6, 325 (1972).

69. R. D. Green and N. Sheppard, J.C.S., Faraday Transactions II, 68, 1077 (1972).

70. R. D. Green and J. S. Martin Can. J. Chem., in press.

71. R. D. Green and J. S. Martin, J. Amer. Chem. Soc., 90, 3659 (1968).

72. S. Ormondroyd, E. A. Phillpot and M. C. R. Symons, Trans. Faraday Soc., 68, 1253 (1971).

73. F. Y. Fujiwara and J. S. Martin, J. Chem. Phys., 56, 4091 (1972).

74. D. R. Cogley, J. N. Butler and E. Grunwald, J. Phys Chem., 75, 1477 (1971).

75. C. W. Haigh in "Annual Reports on NMR Spectroscopy" Vol. 4, E. F. Mooney (ed.) Academic Press, 1971.

76. F. Daniels and R. A. Alberty, "Physical Chemistry", John Wiley & Sons, Inc., 1966.

77. H. A. Benesi and J. H. Hildebrand, J. Amer. Chem. Soc., 71, 2703 (1949).

78. R. L. Scott, Recl. Trav. Chim. Pays-Bas., 75, 787 (1956).

79. D. A. Deranleau, J. Amer. Chem. Soc., 91, 4044 (1969).

80. D. A. Deranleau, J. Amer. Chem. Soc., 91, 4050 (1969).

81. R. U. Lemieux and A. A. Pavia, Can. J. Chem., 47, 4441 (1969).

82. P. A. Kollman and L. C. Allen, J. Amer. Chem. Soc., 93, 4991 (1971).

83. A. D. Sherry and K. F. Purcell, J. Phys. Chem., 74, 3535 (1970).

84. F. A. Cotton and G. Wilkinson, "Advanced Inorganic Chemistry", Interscience 1966.

85. S. K. Searles and P. Kebarle, Can. J. Chem., 47, 2619 (1969).

86. "Handbook of Chemistry and Physics", 48th ed., Chemical Rubber Co., Cleveland, Ohio, 1967.

87. L. G. Groves and S. Sugden, J. Chem. Soc., 1992 (1937).

88. K. G. Denbigh, Trans. Faraday Soc., 36, 936 (1940).

89. G. C. Pimentel and A. L. McClellan, Annu. Rev. Phys. Chem., 22, 347 (1971).

90. A. Saika and C. P. Slichter, J. Chem. Phys., 22, 26 (1954).

91. A. D. Buckingham, Can. J. Chem., 38, 300 (1960).

92. J. I. Musher, J. Chem. Phys., 37, 34 (1962).

93. W. T. Raynes and B. P. Chadburn, Mol. Phys., 17, 543 (1969).

94. T. W. Marshall and J. A. Pople, Mol. Phys., 1, 199 (1958).

95. R. D. Green, Ph.D. Thesis, University of Alberta, (1968).

96. P. J. Berkeley and M. W. Hanna, J. Amer. Chem. Soc., 86, 2990 (1964).

97. W. B. Dixon, J. Phys. Chem., 74, 1396 (1970).

98. S. Bratoz, Adv. Quantum Chem., 3, 209 (1967).

99. N. A. Matwiyoff and H. Taube, J. Amer. Chem. Soc., 90, 2796 (1968).

100. R. N. Butler, J. Davies and M. C. R. Symons, Trans. Faraday Soc., 66, 2426 (1970).

101. J. N. Murrel, Chemistry in Britain, 5, 107 (1969).

102. S. F. Lincoln, Coord. Chem. Revs., 6, 309 (1971).

103. W. B. Dixon, J. Phys. Chem., 74, 1396 (1970).

104. A. L. Van Geet, Anal. Chem., 40, 2227 (1968).

105. J. Davies, S. Ormondroyd and M. C. R. Symons, Chem. Comms., 1426 (1970).

106. C. Franconi, C. Dejak, and F. Conti, "Nuclear Magnetic Resonance in Chemistry", Academic Press, New York, 363 (1965).

107. J. C. Boubel, J. J. Delpuech, M. R. Khaddar and A. Peguy, Chem. Comms., 1265 (1971).

108. H. Grasdalen, J. Mag. Res., 5, 84 (1971).

109. H. Grasdalen, J. Mag. Res., 6, 336 (1972).

110. R. Ditchfield, D. P. Miller and J. A. Pople, J. Chem. Phys., 54, 4186 (1971).

111. H. Haraguchi and S. Fujiwara, J. Phys. Chem., 73, 3467 (1969).

112. J. B. Stothers, Applied Spectroscopy, 26, 1 (1972).

113. A. J. Jones and M. M. Hassan, J. Org. Chem., 37, 2332 (1972).

114. D. M. Grant and B. V. Cheney, J. Amer. Chem. Soc., 89, 5315 (1967).

115. N. Bloembergen, E. M. Purcell, and R. V. Pound, Phys. Rev., 73, 679 (1948).

116. A. Carrington and A. D. McLachlan, "Introduction to Magnetic Resonance", Harper and Row, 1967.

117. N. Muller and R. C. Reiter, J. Chem. Phys., 42, 3265 (1965).

118. C. S. Johnson, Adv. Mag. Res., 1, 33 (1965).

APPENDIX A

CHEMICAL EXCHANGE AND SOLVATION SPECTRA

Although this thesis does not deal explicitly with rate processes, the discussions presented in earlier chapters require a statement of the effects of chemical exchange in solvation spectra. Furthermore, they suggest possible kinetic studies which should be performed. Several theories of the effect of chemical exchange in NMR spectra have appeared in recent reviews.[118] In the general case of multi-site exchange between coupled nuclei, the analysis of the spectrum is extremely complicated and can only be achieved by use of the density matrix formalism and a high-speed computer. In the absence of spin-spin interactions, the modified Bloch equations may be used to extract the kinetic information contained in the NMR spectrum.

A-1. Two-site exchange. It is convenient to describe the effects of chemical exchange in the simplest possible case of two uncoupled spin-1/2 nuclei with the same T_2 exchanging between equally populated sites, and then to discuss the TYPE II solvation spectra in terms of this simple model system. If the residence time τ in each site is reduced from infinity, the NMR spectrum changes through three distinct stages.

(i) *Slow exchange, initial broadening.* When the exchange rate constant ($k = 1/\tau$) increases to the point where the NMR signals begin to broaden, then for each site

$$\frac{1}{\tau} = \frac{1}{T_2^e} - \frac{1}{T_2} \qquad \text{(A-1)}$$

where $1/\pi T_2$ is the natural line width in the absence of exchange and $1/\pi T_2^e$ is the exchange broadened line width.

(ii) *Coalescence.* When the exchange rate increases further the lines continue to broaden and the frequency separation between them decreases. In this region

$$\frac{1}{\tau} = \frac{1}{2\sqrt{2}} \left[(\delta\omega_o)^2 - (\delta\omega_e)^2 \right]^{\frac{1}{2}} \qquad \text{(A-2)}$$

where $\delta\omega_o$ is the angular frequency separation in the absence of exchange and $\delta\omega_e$ is the separation in the partially coalesced spectrum. Equation (A-1) is a good approximation in this region if the signals do not significantly overlap. At the coalescence point

$$\frac{1}{\tau} = \frac{\delta\omega_o}{2\sqrt{2}} \qquad \text{(A-3)}$$

(iii) *Fast exchange.* When the coalescence is complete, a single broad line remains at a position intermediate between those of the two initial lines. As the exchange rate continues to increase, this broad line begins to narrow, and

$\tau << T_2$

$$\frac{1}{\tau} = \frac{(\delta\omega_o)^2}{8}\left[\frac{1}{T_2^e} - \frac{1}{T_2}\right]^{-1} \qquad \text{(A-4)}$$

In the limit of very fast exchange, the line width is simply the natural line width $1/\pi T_2$.

A-2. TYPE II ^{1}H solvation spectra. The exchange processes which can occur in ionic solutions complicate this simple picture considerably. For the alcohols or water coordinated to a cation, several simultaneous exchange processes could occur. (a) The whole solvent molelcule may exchange between the solvation shell and the bulk solvent. (b) The hydroxyl protons may exchange between the molecules in the solvation shell, or between those in the solvation shell and those in the bulk solvent. (c) The hydroxyl protons in the bulk solvent may exchange with each other.

It is possible to suppress the process (c) by the addition of a trace amount of acid to the solution.[36] The process (b) may also be affected by the addition of acid, since the base catalysed exchange of the hydroxyl proton in coordinated molecules should be suppressed.[36]

Assuming that the process (a) is the only one influencing the NMR spectrum of an acidified solution and that there are no spin-spin interactions, in the limit of very slow exchange separate solvation shell and bulk solvent signals will be observed. Although the populations P_a and

P_b and residence times τ_a and τ_b are unequal, equations of the form of (A-1) and (A-2) may still be applied, since $1/\tau_a = (P_a/P_b)\tau_b$.[36] For each site (a or b), the $1/T_2^e$ may be obtained directly from the observed line widths. The natural line widths $1/\pi T_2$ are not equal at the two sites and it is impossible to measure them directly from the spectrum. In previous studies, T_{2a} and T_{2b} have been estimated by extrapolation of the low temperature, viscosity-broadened line widths to higher temperatures.[36,37]

When the hydroxyl protons in coordinated alcohols are not exchanging rapidly, they are coupled to the alkyl-group protons and splittings occur in the solvation shell resonance. This complicates the analysis considerably and the spin-spin interactions must be taken into account in the treatment of the line width data. In the kinetic study of the exchange of methanol coordinated to Mg(II), due allowance was made for the observed scaler coupling.[36] In a similar study of the exchange of ethanol coordinated to Mg(II), spin-spin splitting was not observed in the solvation shell signal.[37] The signal multiplicity was described as being "masked by broadening effects" and it appears to have been ignored. The width of the broad "hump" in the spectrum attributed to solvation shell protons was used directly to deduce T_2^e. This "hump" is in fact composed of three overlapping broad signals, the triplet structure due to coupling between the hydroxyl-group and

methylene-group protons. In some of the spectra obtained for the work discussed in Chapter 5 of this thesis, a partially resolved triplet was observed for ethanol molecules coordinated to Mg(II). When allowance is made for the coupling, the linewidths estimated from these spectra are considerably smaller than those quoted in the previous study.[37] Thus the previously reported rate constants must be incorrect.

A-3. TYPE II ^{13}C Solvation Spectra. The difficulty of estimating the natural line width over a range of temperatures and the complications of spin-spin interactions in ^{1}H solvation spectra also arise in ^{13}C spectra. In addition, several other problems arise in ^{13}C NMR. For natural abundance spectra, the signal to noise ratio is usually inadequate and ^{13}C enriched samples should be used to obtain accurate linewidths. The long periods of time required to accumulate several thousand free induction decays create difficulties in maintaining good field homogeneity, and hence a constant natural line width. At temperatures other than ambient, temperature control over long periods of time may also be a problem since the chemical shifts are temperature dependent. It is usual to truncate the accumulated F.I.D. by multiplication with exponential and/or trapezoidal functions. This greatly improves the signal to noise ratio, at the expense of the linewidth: the linewidth is increased and the lineshape may be non-Lorentzian. Thus, care must be

taken in using this procedure when the linewidths are important.

The ^{13}C spin system is greatly simplified by proton noise decoupling since the signal multiplicities are removed. The kinetic analysis would be correspondingly simplified since equations similar to (A-1) to (A-4) could be used directly. However, there is one disadvantage to heteronuclear decoupling. The decoupling may affect the lineshapes of the solvation shell and bulk solvent nuclei differently and render them difficult to interpret. An additional practical difficulty is that the spectra recorded at 22.63 MHz exhibited partially overlapping solvation shell and bulk solvent signals. Unless a higher field spectrometer is used to separate the signals, a lineshape fitting technique would have to be used to deduce the rate constants. Several computer programs exist for this purpose.

Each of the above-mentioned difficulties must be thoroughly investigated and overcome before meaningful rate constants can be obtained for the exchange of ethanol (or other alcohols) coordinated to Mg(II) (or other ions), and agreement between the ^{1}H and ^{13}C results must be obtained. This would constitute a rather lengthy project and it is suggested as a possible future study.